



HAL
open science

Effect of condensable materials during the gas phase polymerization of ethylene on supported catalysts

Fabiana Nascimento de Andrade

► **To cite this version:**

Fabiana Nascimento de Andrade. Effect of condensable materials during the gas phase polymerization of ethylene on supported catalysts. Chemical and Process Engineering. Université de Lyon, 2019. English. NNT : 2019LYSE1016 . tel-02091507

HAL Id: tel-02091507

<https://theses.hal.science/tel-02091507>

Submitted on 5 Apr 2019

HAL is a multi-disciplinary open access archive for the deposit and dissemination of scientific research documents, whether they are published or not. The documents may come from teaching and research institutions in France or abroad, or from public or private research centers.

L'archive ouverte pluridisciplinaire **HAL**, est destinée au dépôt et à la diffusion de documents scientifiques de niveau recherche, publiés ou non, émanant des établissements d'enseignement et de recherche français ou étrangers, des laboratoires publics ou privés.



N°d'ordre NNT : 2019LYSE1016

THESE de DOCTORAT DE L'UNIVERSITE DE LYON

opérée au sein de

l'Université Claude Bernard Lyon 1

**Ecole Doctorale 206
Ecole Doctorale de Chimie**

Spécialité de doctorat : Polyoléfines Réaction Engineering

Discipline : Génie de Procédés

Soutenue publiquement/à huis clos le 01/02/2019, par :

Fabiana Nascimento de Andrade

Effect of condensable materials during the gas phase polymerization of ethylene on supported catalysts

Devant le jury composé de :

Fulchiron, René	Professeur - Université Lyon 1	Président
Silva, Fabricio M.	Professeur - Université de Brasilia (Brésil)	Rapporteur
Soares, Joao B.P.	Professeur - Université de Alberta (Canada)	Rapporteur
Deghedi, Layane	Ingénieur R&D en catalyse - INEOS	Examinatrice
Le Sauze, Nathalie	Professeur - Université Toulouse III	Examinatrice
McKenna, Timothy F.L.	Directeur de recherche - Université Lyon 1	Directeur de thèse

UNIVERSITE CLAUDE BERNARD - LYON 1

Président de l'Université

Président du Conseil Académique

Vice-président du Conseil d'Administration

Vice-président du Conseil Formation et Vie
Universitaire

Vice-président de la Commission Recherche

Directrice Générale des Services

M. le Professeur Frédéric FLEURY

M. le Professeur Hamda BEN HADID

M. le Professeur Didier REVEL

M. le Professeur Philippe CHEVALIER

M. Fabrice VALLÉE

Mme Dominique MARCHAND

COMPOSANTES SANTE

Faculté de Médecine Lyon Est – Claude Bernard

Directeur : M. le Professeur G.RODE

Faculté de Médecine et de Maïeutique Lyon Sud –
Charles Mérieux

Directeur : Mme la Professeure C. BURILLON

Faculté d'Odontologie

Directeur : M. le Professeur D. BOURGEOIS

Institut des Sciences Pharmaceutiques et Biologiques

Directeur : Mme la Professeure C. VINCIGUERRA

Institut des Sciences et Techniques de la Réadaptation

Directeur : M. X. PERROT

Département de formation et Centre de Recherche en
Biologie Humaine

Directeur : Mme la Professeure A-M. SCHOTT

COMPOSANTES ET DEPARTEMENTS DE SCIENCES ET TECHNOLOGIE

Faculté des Sciences et Technologies

Directeur : M. F. DE MARCHI

Département Biologie

Directeur : M. le Professeur F. THEVENARD

Département Chimie Biochimie

Directeur : Mme C. FELIX

Département GEP

Directeur : M. Hassan HAMMOURI

Département Informatique

Directeur : M. le Professeur S. AKKOUCHE

Département Mathématiques

Directeur : M. le Professeur G. TOMANOV

Département Mécanique

Directeur : M. le Professeur H. BEN HADID

Département Physique

Directeur : M. le Professeur J-C PLENET

UFR Sciences et Techniques des Activités Physiques et
Sportives

Directeur : M. Y.VANPOULLE

Observatoire des Sciences de l'Univers de Lyon
Polytech Lyon

Directeur : M. B. GUIDERDONI

Ecole Supérieure de Chimie Physique Electronique

Directeur : M. le Professeur E.PERRIN

Institut Universitaire de Technologie de Lyon 1

Directeur : M. G. PIGNAULT

Ecole Supérieure du Professorat et de l'Education

Directeur : M. le Professeur C. VITON

Institut de Science Financière et d'Assurances

Directeur : M. le Professeur A. MOUGNIOTTE

Directeur : M. N. LEBOISNE



This work has financial support from the National Council of Scientific and Technological Development (CNPq), branch of the Ministry of Science, Technology, Innovation and Communications (MCTIC) of Brazil. Program Ciência sem Fronteiras, nº 659/2014-0.



ACKNOWLEDGEMENTS

Many people deserve my thanks. First, I would like to express my sincere gratitude to my mentor and teacher Dr. *Timothy Mc Kenna*, who has always been present, clarifying my doubts, having patience, competence, knowledge, motivation, and confidence in my work. I needed help and guidance in this new field of Polyolefin Reactor Engineering: thank you for all the opportunities you have given me!

In particular, Dr. *Rene Fulchiron*, Dr. *Fabricio Machado* e Dr. *João Soares* who contributed with their knowledge and are participating in the examining board of this work together with Ms. *Nathalie La Souze* e Ms. *Layne Deghedi*: my sincere thanks.

Thank you very much to the C2P2 team, not only for everything that was taught but also for helping me to learn. In particular, I thank Dr. *Sébastien Norsic* for the very efficient management and support in the laboratory; Ms. *Manel Taam*, Mr. *Olivier Boyron* e Dr. *Franck Collas* for the support and expertise in the analysis and Ms. *Natalie Jouglard* for all support and welcome. It was great to work in a group with such standards.

Thanks to the support of LCOMS, represented by Dr. Mostafa Taoufik and support in the rheology analysis in the IMP represented by Dr. René Fulchiron.

To the Group of Applied Macromolecular Engineering of prof. Dr. *Joao Soares*, along with his doctoral students and laboratory staff, especially Dra. *Fernanda Motta*, Dr. *Saeid Mehdiabadi*, e Dr. *Marco Antônio*, thank you for the paid attention and all the lessons I obtained during the internship at the University of Alberta - Canada.

To *CNPq*, for the maintenance of financial support during the development of this work.

To the great team created by McKenna, thank you for the scientific exchanges that were fundamental to completion of this dissertation and for sharing an environment so full of wisdom (share such a wise environment). *Ana Carolina*, for sharing her beautiful friendship and camaraderie; *Aaronzito*, who gave his dedicated contribution to my activities with the reactor and becoming a great friend; *Yashmin*, whose *fofa* friendship giving me comfort because her

sincerity and originality; *Rita*, for her delicacy, a special friend who contributed a lot in the thermodynamic calculations and thanks to very fruitful discussions; *Amel*, a special comrade who arrived to contribute to the solubility data of the species; *Barbara*, who arrived at the catalyze team *agraciando* with her competence; the partnership of *Yue Yu* who I divided the activities in the reactor, *Nida* by the company and conversations in the last period and *Fabricio* the no less professor than friend, for introducing me to Fortran: it was very helpful to work with you! I also thank the new members of the team *Roberta*, *Estela*, and *Niyi*.

Je remercie les amis que j'ai fait à Lyon comme "belissima" le professeur *Cecile* et l'équipe de *Connect* dirigée par *Roxane* et *Henoc* qui ont passé un bon moment.

Aos amigos, "meu pedaço Brasil" na França que permitiu ter momentos especiais com festas bem tradicionais – Bora Baêa!! Além de todos brasileiros (portuguesa, espanhol, francês e alemão) do time do laboratório tem *Eleninha*, *Thiago*, *Thaissa*, *Arne*, *Anderson*, *Gigi*, *Cedric*, *Juliete*, *Igor Paulo*, *Abilio* e *Ana*.

Ao meu berço profissional, que me incentivou a parar minhas atividades no Brasil e ir estudar na França. Principalmente Dr. *Alan*, amigo que foi a semente de tudo e eternos professores e amigos Dr. *Sergio Bello*, Dr. *George Mustafa*, Dra *Ana Claudia Gondim* e Dra *Luciene Carvalho*.

Aos meus pais *Orlando* e *Dora* e meus irmãos *Carine* e *Thiago*, que com muito esforço e dedicação puderam me proporcionar tudo que estava aos seus alcances, além de formarem os fundamentos do meu caráter. Obrigado por serem a minha referência de tantas maneiras e estarem sempre presentes na minha vida de uma forma indispensável, mesmo separados por tantos quilômetros. Saudades!

Al mio amore *Carlo*, meu cúmplice, por todo apoio, amor e respeito durante todo este tempo que passou e que ainda virá. Obrigado pela paciência e pela compreensão em todos momentos, por tonar a minha vida cada dia mais feliz. Grazie per i giorni insieme!

À toda minha família e amigos que estão no Brasil, que de perto ou de longe demonstraram carinho e preocupação, vocês que aliviaram minhas horas difíceis, me alimentando de certezas, força e alegria. Desculpa, o papel não coube nomeá-los!

ABSTRACT

Fluidized bed reactors (FBR) are the only commercially viable technology for the production of polyethylene in the gas phase since the polymerization is highly exothermic and the FBR is the only type of gas phase reactor that offers adequate possibilities of heat transfer. The highly exothermic nature of this polymerization effectively poses many problems for gas phase operation and can limit the production of a certain process. However, in recent years the fluidized bed processes have been improved with new technologies. In particular, the addition of inert (usually liquefied) hydrocarbons allows one to increase the amount of heat removed from the reactor. These compounds increase the heat capacity of the gas phase and, if injected in liquid form, also evaporate and thus absorb even more heat from the reaction medium efficiently. This is known as a condensed mode operation. In it, one uses compounds that can be liquefied in the recycle condenser, and which are called Induced Condensing Agents (ICA). The use of ICA is extremely important from an industrial point of view.

The injection of ICA can have many different physical effects at the level of the growing polymer particles. For instance, adding these compounds can cause changes in solubility and other physical properties, which can facilitate the transport of ethylene and hydrogen to the active sites of the catalysts. It is thus very important that the physical phenomena related to the sorption equilibrium of the monomer(s) and other species from the gas phase to the polymer phase, and their diffusion on the polymer matrix at the active sites should be accounted for. In addition to having an effect on the kinetics, these phenomena can also impact the structure of the polymer molecules and consequently qualify the characteristics of the polymer. Identifying the behavior of these phenomena under process conditions and control variables of the hydrogen/ethylene ratio and the comonomer/ethylene ratio with ICA are central objectives of this study.

A series of ethylene homo- and co-polymerizations in the gas phase were carried out using a commercial Ziegler-Natta catalyst in the presence of ICA (propane, n-pentane, and n-hexane). We investigated the effect of temperatures, the partial pressure of ICA, hydrogen, and comonomers on the behavior of the polymerization. It was found that adding ICA significantly increased the reaction rate and average molecular weights at a given temperature. It was also unexpectedly observed that increasing the reactor temperature in the presence of an ICA actually led to a decrease in the overall reaction rate. These results were attributed to the so-called cosolubility effect. In reactions in the presence of different hydrogen concentrations, for an ICA/C₂ ratio much larger than the H₂/C₂ ratio, the effect of ICA on ethylene solubility can counteract the decrease in average molecular weight caused by the presence of hydrogen. The impact of ICA on the rates of copolymerization reactions is more pronounced in the initial stages, losing strength due to the effect of the comonomer. Finally, an evaluation of the kinetics of crystallization under isothermal conditions for mixtures of different ICA:HDPE concentrations showed that the crystallization time is significantly higher for systems rich in ICA than for dry polymer.

Key Words: Polyethylene in the gas phase, Condensed Mode, Induced Condensing Agents.

RÉSUMÉ

Les réacteurs à lit fluidisé (FBR) constituent la seule technologie viable sur le plan commercial pour la production de polyéthylène en phase gaz, car la polymérisation est hautement exothermique et le FBR est le seul type de réacteur en phase gaz offrant des possibilités suffisantes de transfert de chaleur. La nature hautement exothermique de cette polymérisation pose effectivement de nombreux problèmes pour le fonctionnement en phase gaz et peut limiter la production de certains procédés. Au cours des dernières années, les procédés en lit fluidisé ont été améliorés par de nouvelles technologies. En particulier, l'ajout d'hydrocarbures inertes (généralement liquides) permet d'augmenter la quantité de chaleur évacuée du réacteur. Ces composés augmentent la capacité calorifique de la phase gazeuse et, s'ils sont injectés sous forme liquide, s'évaporent également et absorbent ainsi encore plus efficacement la chaleur du milieu réactionnel. C'est ce qu'on appelle le fonctionnement en mode condensé. On y utilise des composés qui peuvent être liquéfiés dans le condenseur de recyclage et qui sont appelés agents de condensation induits (en anglais : *Induced Condensing Agents - ICA*). L'utilisation de l'ICA est extrêmement importante d'un point de vue industriel.

L'injection d'ICA peut avoir de nombreux effets physiques différents au niveau des particules de polymère en croissance. Par exemple, l'ajout de ces composés peut entraîner des modifications de la solubilité et d'autres propriétés physiques, ce qui peut faciliter le transport de l'éthylène et de l'hydrogène vers les sites actifs des catalyseurs. Il est donc très important que les phénomènes physiques liés à l'équilibre de sorption entre la phase gaz et la phase polymère du ou des monomères et d'autres espèces, ainsi que leur diffusion dans la matrice polymère au niveau des sites actifs, soient pris en compte. En plus d'avoir un effet sur la cinétique, ces phénomènes peuvent également impacter la structure des molécules de polymère et par conséquent changer les caractéristiques du polymère. Identifier le comportement de ces phénomènes dans les conditions de la procédé et les variables de contrôle du rapport hydrogène / éthylène et du rapport comonomère / éthylène avec l'ICA sont les objectifs centraux de cette étude.

Une série d'homo- et co-polymérisations d'éthylène en phase gazeuse a été réalisée en utilisant un catalyseur commercial Ziegler-Natta en présence de l'ICA (propane, n-pentane et n-hexane). Nous avons étudié l'effet des températures, de la pression partielle de l'ICA, de l'hydrogène et des comonomères sur le comportement de la polymérisation. Il a été constaté que l'ajout de l'ICA augmentait significativement la vitesse de réaction ainsi que les poids moléculaires moyens à une température donnée. De manière inattendue, il a également été observé que l'augmentation de la température du réacteur en présence d'ICA entraînait en réalité une diminution de la vitesse de réaction globale. Ces résultats ont été attribués à l'effet de cosolubilité. Dans les réactions en présence de différentes concentrations en hydrogène, pour un rapport ICA/C₂ beaucoup plus grand que le rapport H₂/C₂, l'effet de l'ICA sur la solubilité de l'éthylène peut compenser la diminution en taille des molécules provoquée par la présence d'hydrogène. L'impact de l'ICA sur les taux de réaction de copolymérisation est plus prononcé aux stades initiaux, perdant de son efficacité en raison de l'effet de comonomère. Enfin, une évaluation de la cinétique de cristallisation dans des conditions isothermes pour des mélanges de différentes concentrations ICA: HDPE a montré que le temps de cristallisation est significativement plus long pour les systèmes riches en ICA que pour les polymères secs.

Mots clés : Polyéthylène en phase gazeuse, mode condensé, agents de condensation induits.

CONTENTS

CHAPTER I - GENERAL INTRODUCTION.....	11
1.1. POLYMERIZATION OF ETHYLENE	11
1.1.1. <i>Characteristics of polyethylene</i>	12
1.1.2. <i>Polyethylene catalysts</i>	14
1.1.3. <i>Polyethylene process</i>	15
1.2. IMPACT OF CONDENSABLE MATERIALS	19
1.2.1. <i>Introduction</i>	19
1.2.2. <i>Overview of particle growth and polymer formation.</i>	22
1.2.3. <i>Transport phenomena in the polymer matrix</i>	23
1.2.4. <i>Sorption of ICA in amorphous phase polymer</i>	25
1.2.5. <i>Impact of ICA on other properties.</i>	29
1.3. RESEARCH STATEMENT	30
REFERENCE.....	32

CHAPTER 2 - THE EFFECT OF TEMPERATURE IN THE PRESENCE OF INDUCED CONDENSING AGENTS.....38

2. INTRODUCTION	38
2.1. EXPERIMENTAL SECTION.....	41
2.1.1. <i>Materials</i>	41
2.1.2. <i>Polymerization and characterization of polymer</i>	41
2.1.3. <i>Activity</i>	43
2.2. RESULTS AND DISCUSSION	43
2.2.1. <i>Rate of polymerization</i>	43
2.2.2. <i>Characterization</i>	52
2.3. CONCLUSIONS.....	55
REFERENCES.....	56

CHAPTER 3 – THE IMPACT OF INDUCED CONDENSING AGENTS IN THE PRESENCE OF HYDROGEN58

3. INTRODUCTION	58
3.1. EXPERIMENTAL SECTION.....	60
3.1.1. <i>Materials</i>	60

3.1.2. Homopolymerization and characterization of the polymer.....	61
3.1.3. Experimental design.....	61
3.2. RESULTS AND DISCUSSION	63
3.3. CONCLUSION.....	75
REFERENCE.....	77

CHAPTER IV - THE IMPACT OF INDUCED CONDENSING AGENTS IN THE PRESENCE OF A COMONOMER79

4. INTRODUCTION.....	79
4.1. EXPERIMENTAL SECTION.....	81
4.1.1. Materials.....	81
4.1.2. Copolymerization and copolymer characterization	82
4.1.3. Experimental design.....	82
4.2. RESULTS AND DISCUSSION	84
4.2.1. Ethylene / 1-butene copolymerizations in the presence of n-pentane	84
4.2.2. Combinations of light ICA with heavier comonomer.....	95
4.2.3. Solubility of comonomer in polymer.....	100
4.3. CONCLUSION.....	102
REFERENCE.....	103

CHAPTER V – - REDUCTION OF CRYSTALLIZATION RATE IN THE PRESENCE OF INDUCED CONDENSING AGENTS.....107

5. INTRODUCTION.....	107
5.1. EXPERIMENTAL SECTION.....	111
5.1.1. Materials.....	111
5.1.2. Preparation of sample blends	112
5.1.3. Differential Scanning Calorimetry (DSC).....	113
5.2. RESULTS AND DISCUSSION	114
5.2.1. Non-isothermal analyses	114
5.2.2. Isothermal analyses.....	117
5.3. CONCLUSION.....	123
REFERENCE.....	123

CHAPTER 6 – CONCLUSION & PERSPECTIVES127

1. CONCLUSION & PERSPECTIVES	127
1.1. CONCLUSION.....	127

1.2. PERSPECTIVES.....	130
APPENDIX I – REACTION PROTOCOL AND ANALYSES	133
1. POLYETHYLENE GAS PHASE PROCESS IN THE LABORATORY	134
2. SIZE EXCLUSION CHROMATOGRAPHY (SEC).....	139
3. DIFFERENTIAL SCANNING CALORIMETRY (DSC)	139
4. CRYSTALLIZATION ELUTION FRACTIONATION (CEF).....	140
APPENDIX II – SANCHEZ LACOMBE MODEL	142
1. INTRODUCTION.....	142
2. MODELING POLYMERIC SYSTEMS	144
APPENDIX III – STATITICAL ANALYSIS	153

Chapter 1

General introduction

1.1. Polymerization of ethylene

The polymerization of ethylene has produced one of the most widely used polymers the world has ever seen. Polyethylene (PE) is a macromolecule containing simple (and very inexpensive) repeating units (monomers: ethylene ($-C_2H_4-$), and small amounts of different α -olefin comonomers). Despite the very simple chemical nature of this polymer, PE is the most widely used polymer in the world because it combines useful structural features and properties at a low price. The global PE market was about 78 million tonnes (mmt) in the year 2012, and it is expected to be 100 mmt in 2018. [1]–[3]. The demand for PE is also expected to continue to rise substantially, with consumption of PE growing at around 4 - 5% p.a. [4]. Thus, despite the fact that some people might consider PE to be a mature technology, there is clearly a need for continual optimization of the chemistry and the processes used for its manufacture.

In the following thesis, we will focus on the implications of adding chemical inert compounds, referred to as Induced Condensing Agents (ICA) that help increase heat removal (and thus increase process productivity), during gas phase polymerization of ethylene. For this reason, the bibliographic review presented here will focus on PE made with supported catalysts in gas phase reactors. There are of course other types of chemistries (e.g. free radical) and processes (slurry, solution, supercritical) that are commercially important, but they will not be the focus of the following discussion.

1.1.1. Characteristics of polyethylene

Polyethylene is used for products such as films, blow moldings, injection moldings, and pressure pipes in major economic sectors such as packaging, building & construction, automotive, electrical & electronic, agriculture, textile, and pharmaceuticals. As been said earlier, the wide-spread use of polyethylene is due to its excellent solid state properties, the fact that it is chemically inert, inexpensive and relatively easy to process.

Figure 1.1 shows the structure of a molecule of polyethylene (here linear low density polyethylene – LLDPE). It is a very simple structure, composed of a long main chain upon which one finds pendant groups. It is composed only of H and C molecules yet can be constructed in a myriad of different manners that provide the physical properties required for the applications cited above. These chains assemble in such a way that PE is, in fact, a semi-crystalline material, with both crystalline and amorphous phase.

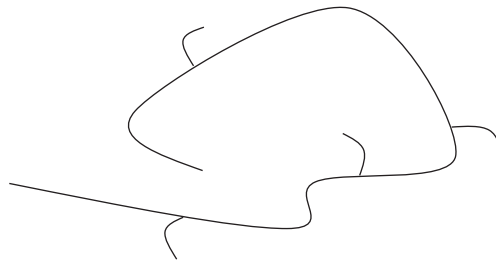


Figure 1.1 Structure of a molecule of polyethylene of type (LLDPE).

When PE molecules crystallize, they form *lamellae*. The *lamellae* are interconnected by linking molecules, which form interlamellar bridges constituting the amorphous regions. The lamellae, in turn, are grouped into spherulites. The degree of crystallinity describes the thermodynamics and statistical mechanics between the macroscopic properties and the atomic or molecular structure. This semi-crystalline nature, its relative proportions and its degree of connectivity with the other elements determine the density and certain properties of a polyethylene sample [5], [6].

The end-use properties will reflect how the elements of PE chains are put together. One can control physical properties such as the density, mechanical, thermal, permeability or optical properties, etc., through the correct choice of chemistry and process. The choice of catalyst,

monomer, hydrogen, and comonomer will, of course, influence the chain architecture and microstructure. However, it is also important to note that the type of process used to make the PE, and in particular the operating conditions used, will also have a strong influence on the material (as we will see in this thesis).

In theory, PE can be formed with only ethylene. However, a large fraction of commercial PE are copolymers of ethylene with different amounts of at least one comonomer. Common comonomers for commodity PE include propylene, 1-butene, 1-pentene, 1-hexene, and 1-octene. Hydrogen is also important because is used as a chain transfer agent to control molecular weight. The amount of hydrogen and comonomer, as well as the type of comonomer, can be used to influence the architecture and properties in different ways. For instance, the more comonomer one adds, the lower the density becomes since pendant side chains (e.g. butyl groups if the comonomer is hexene) perturb the formation of crystals. Since the crystalline phase is denser than the amorphous one, the density of the final product will depend on the relative amounts of both phases [5], [7]–[10]. Architecture basically refers to the size and shape of the chain. In principle polymer chains can be linear, branched, or even star shaped. However, PE made from supported catalysts is essentially linear. It is possible to observe a small amount of long chain branching, but the mechanism by which this occurs is not yet clear. [11].

Table 1.1 shows the main characteristics of different types of polyethylene. Generally speaking, the types or families of products are differentiated by their densities. For instance, if we consider products made using coordination catalysts there are High Density PE (HDPE), Linear Low-Density PE (LLDPE). The product LDPE is low density PE and is made with free radical chemistry. The different chemistry and reaction conditions used for LDPE give it a highly branched structure, which is why it is differentiated from LLDPE (which, as the name suggests in highly linear). The study of the properties of the structure and its relations in the polymer depends on the microstructure of the polymer, but also on the molecular weight and its distribution.

Table 1.1 Standard characteristics of different types of polyethylene [8]–[10].

Type of polyethylene	Architecture	Density [g.cm ⁻³]	Crystallinity [%]	Melt point [°C]
LDPE	Various branches on branches (branched homopolymer)	0.915 – 0.940	22 – 55	98 – 115
LLDPE	Many equal short branches (random copolymer)	0.915 – 0.940	30 – 54	100 – 125
HDPE	Few short or no branches (Linear homopolymer)	0.945 – 0.960	55 – 77	125 – 135

1.1.2. Polyethylene catalysts

The synthesis of PE that is of interest in this thesis (HDPE, LLDPE) occurs by coordination polymerization of ethylene and comonomers in the presence of transition metal compounds. The catalysts used in the modern industry for polyethylene synthesis are:

- i) Chromium oxide catalysts that, based on Cr^{VI} and supported on an inert porous substrate;
- ii) Ziegler Natta using TiCl₄-AlEt₂Cl system. This is the most widely used catalyst from the commercial point of view;
- iii) Metallocenes which refers to an organometallic compound formed by a transition metal (titanium, zirconium or hafnium) attached to at least one aromatic ring of the cyclopentadienyl (Cp), indenyl (Ind) or fluorenyl (Flu) type.

Chromium oxide catalysts do not incorporate comonomers as well as the others but are quite inexpensive. The range of densities available from this type of catalyst is therefore limited. On the other hand, they offer very wide MWD, which can be preferred for some products. Furthermore, they can be activated directly at the production site by thermal treatment. The producers can, therefore, tailor the catalyst properties to the requirements in real time. Chromium oxide catalysts are only used in the supported form.

Ziegler-Natta (ZN) catalysts are the most widely used of the three main groups because of their high activity and selectivity, which allow a wide range of polymer microstructures (molar mass

and molar weight distributions - MWD) and macrostructural properties (particle size distribution, morphology and porosity), at a very low cost with respect to metallocenes. The polymers thus produced have a wide range of applications. [5–7]. They can be used as molecular catalysts in solution processes, but are more commonly found in the supported form. Because of the way in which they are made, both Cr and supported ZN catalysts have many different types of active sites - meaning that at any time, many different kinds of polymer chains are produced on the same supported catalysts.

Finally, metallocenes are quite interesting catalysts. Like ZN catalysts, they can be used in both molecular and supported form. When catalysts are used in the molecular (unsupported) form, they are referred to as single site catalysts. In this case, there is no interaction with the support, and all the metal atoms (i.e. active sites) are identical. However, unlike ZN catalysts, when metallocenes are used in the supported form they are tethered to the support (usually silica) in such a way that there is no support-site interaction, and they can be (mostly) treated as single site catalysts as well. This is useful if one needs very fine control over comonomer incorporation, or over the MWD. However, metallocenes are much more expensive than Cr or ZN catalysts.

In this current thesis, all the data were obtained using a titanium tetrachloride (TiCl_4) Ziegler Natta catalyst, supported on magnesium dichloride (MgCl_2) and activated with triethylaluminum (AlEt_3), because it is the most commonly used catalyst from an industrial standpoint.

1.1.3. Polyethylene process

Polyethylene can be produced by high-pressure free radical, and low-pressure catalyst polymerization. The high-pressure process operates at 1200 - 3500 bar and high temperatures in the range 150 - 350 °C. Here, several initiators (such as organic peroxides) can be used to initiate the polymerization reaction. The combination of extreme operating conditions and free radical chemistry means that the final product is highly branched (with branches upon branches in most cases). The high-pressure process is used to make LDPE homopolymers and is the only means by which ethylene can be commercially polymerized with polar comonomers such as

acetates and acrylates. While commercially important, we will not consider this polymer in the current thesis.

All other types of ethylene polymers can be produced in low pressure processes if a catalyst is used. Low-pressure processes can produce many different polymer grades and can be divided into three categories, depending on the reaction medium: solution, slurry and gas phase. In all processes, hydrogen is used for molecular weight control.

Solution processes take place in the liquid phase (solvents such as isopar or cyclohexane), and use continuous stirred tank reactors (CSTR) or loop reactors [9]. As the name implies, all components are dissolved in the solvent, including the catalyst. This means the catalysts are not supported. Depending on the solvent used and the desired polymer properties, solution processes are run at higher temperatures, typically 100 - 250 °C, and pressures (from 40 to 100 bars) than slurry or gas phase process.

In slurry processes, supported catalysts and growing (solid) polymer particles are dispersed in an inert diluent (typically isobutane, but one also finds hexane or supercritical propane used as diluents). The temperature is between 80 - 110 °C, and pressure around 5 - 40 bar (the exact value depends on the diluent; the heavier the diluent, the lower the ethylene pressure needs to be).

In the gas phase process, the polymer is once again formed from supported catalysts, but the growing particles are dispersed in a gas phase. The gas phase maintains the reaction by supplying monomer, mixing the particles and withdrawing heat from the system. [9], [10], [15]. This Ph.D. dissertation focuses on some of the key issues related to gas phase reactors. Gas phase polyethylene processes have certain advantages over other means of PE production. The operating conditions are more moderate than solution processes, and the absence of diluents offers a number of economic and environmental strengths. In addition, they offer a much wider product range than slurry processes as it is not possible to make polymers with a high content of amorphous material (i.e. LLDPE, or very low molecular weight polymers – $d \leq 915$ typically) in the latter.

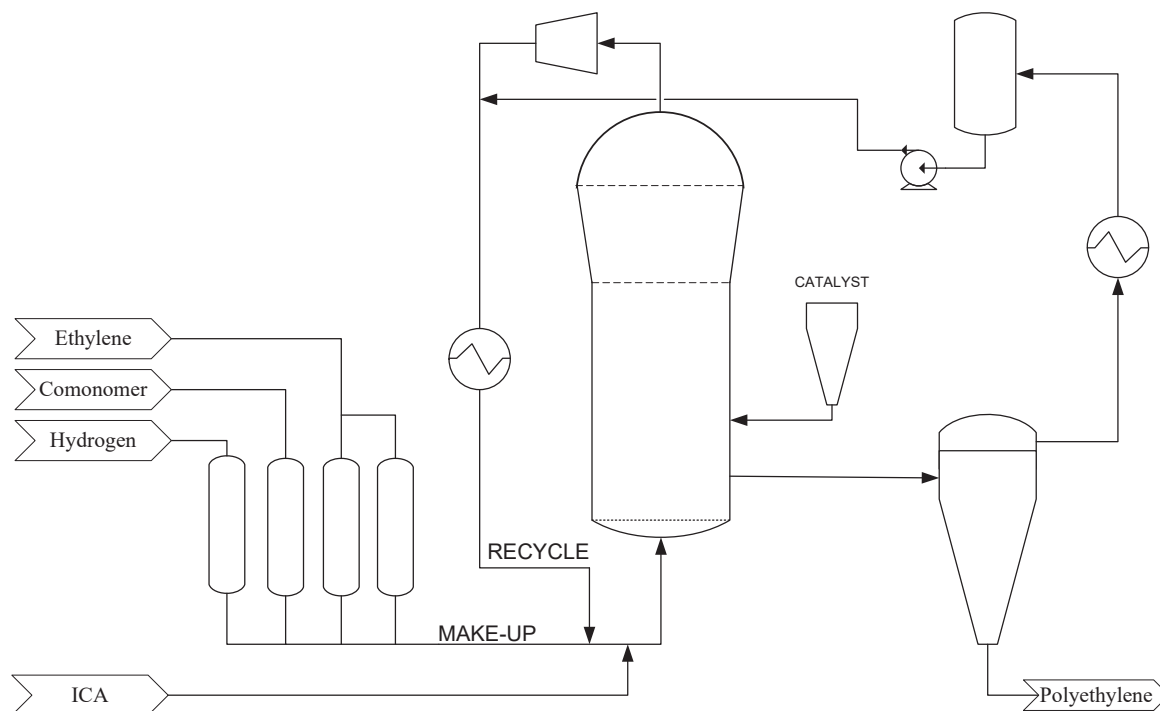


Figure 1.2 Flow diagram of a Unipol PE process with one FBR. Adapted from reference [16].

Polyethylene produced in the gas phase uses only Fluidized Bed Reactors (FBR) as the polymerization is highly exothermic and FBR is the only type of gas phase reactors that offer adequate possibilities for heat transfer [9]. The processes typically operate at temperatures of 75 -110 °C, and at pressures of 20 - 30 bar [9]. A typical gas phase process design is illustrated in Figure 1.2 [16]. The raw feed (monomers, hydrogen, and inert) passes through purification columns, is mixed with the recycle stream, and enters the reactor through distributor plate, while catalyst particles (or pre-polymerized catalyst particles) are fed continuously to the reactor at a point above the gas distribution. The purified components plus recycle stream can equally be mixed with an additional stream containing a purified induced condensing agent (ICA). The gas phase components react to produce a wide distribution of polymer particles. Unreacted gases at the top of the reactor are recovered and compressed, cooled and recycled to the reactor base. The polymer produced is continuously withdrawn from the reactor at a certain point, preferably near the bed base. Unreacted raw materials are separated from the product, cooled, liquefied, and recycled.

In the process, the reactant gas is fed at a rate of 3 - 6 times the minimum fluidization rate. The distributor plate has an important role in guiding the fluidization flow of the reactor bed. Polymerization occurs on the surface of the pores of the catalyst, causing the particles to grow

in granules 15 - 20 times the size of the original catalyst. Fluidization in the bed of the reactor depends on the size of the particles in formation. The per pass ethylene conversion is low (typically on the order of 10%), but high recycle ratios are used, meaning the overall conversion of monomer entering the process can be quite high.

Perhaps the most challenging feature of ethylene polymerization (from a process engineering point of view) is that the reaction is highly exothermic, producing approximately 3600 kJ/kg of converted ethylene [9], [17]. Solutions to overcoming this aspect of ethylene polymerization are central to this thesis and will be discussed in detail below. There are of course additional process challenges, but in general, in order to ensure operational stabilization and product quality, it is imperative to resolve the problems that are associated with the control of temperature and gas composition. The main issues that need to be addressed are: i) formation of hot spots that can arise and lead to particle fusion and agglomeration in equipment; ii) instabilities caused by impurities in the reactor feed and variations in the properties of the polymer; iii) control variables of the hydrogen/ethylene ratio and co-monomer / ethylene ratio, avoiding unreacted stock in the reactor, which may imply low productivity and off-spec. [18], [19].

These factors make it challenging to operate in the gas phase, but in recent years fluidized bed processes have been improved with new technologies. One of the most significant advances, beginning in the 1980s was the addition of inert (often liquefied) hydrocarbons in the polymerization bed to increase the amount of heat removed from the reactor. These compounds increase the heat capacity of the gas phase, and, if sent in in liquid form, also evaporate and absorb the heat from the reaction medium effectively. Compounds that can be liquefied in the recycle condenser shown above are called condensable materials (even if they are in vapor form).

1.2. Impact of Condensable Materials

1.2.1. Introduction

Condensable materials are usually linear hydrocarbons, C3 – C6 alkanes, which, as explained above, are added to a reactor to prevent overheating. Comonomers can also be condensed and then evaporated to remove heat, but we will treat them differently from the chemically inert ICA. Note that even if they are not sent into the reactor in liquid form, ICA still improves the heat transfer coefficient (N.B. occasionally even ethane; which is obviously not condensable under normal circumstances, is added to this effect). For this reason, even if the condensable materials are fed in vapor form, we will still refer to them as induced condensing agents (ICA).

Basically, if the reactor feed stream containing ICA (Figure 1.2) is at a temperature below the dew point, at least a portion of the ICA will be liquefied. If the feed is hotter than the dew point, it will be entirely vaporized. In order to differentiate between different modes of operation we will define different terms: i) dry mode refers to operation without any added ICA; ii) super dry mode refers to operation when the ICA is present but only in the vapor phase; iii) condensed mode of operation refers to a partially liquefied feed stream containing up to 20 %wt of ICA in the liquid phase; iv) super condensed mode refers to operation with a feed stream containing more than 20 %wt of ICA in the liquid phase [19]–[23].

The different roles played by the ICA (in terms of heat transfer) can be understood from the following simplified heat balance around a reactor where all of the reactor contents are assumed to be at a uniform bed temperature (T_R):

$$\dot{m}_{g,in}Cp_{g,in}(T_{g,in} - T_{ref}) - \dot{m}_{g,out}Cp_{g,out}(T_{g,out} - T_{ref}) - \dot{m}_{s,out}Cp_{s,out}(T_{s,out} - T_{ref}) - UA(T_R - T_w) - Q_{vap} + R_pV_R(-\Delta H_p) = 0 \quad (1.1)$$

Where $\dot{m}_{g,in}Cp_{g,in}$ is the thermal capacity of the reactor feeds; $\dot{m}_{g,out}Cp_{g,out}$ is the thermal capacity of the outgoing gas current feeds and $\dot{m}_{s,out}Cp_{s,out}$ that of the solids leaving the reactor. $T_{g,in}$ and $T_{g,out}$ are the inlet and outlet gas stream temperatures, and $T_{s,out}$ that of the leaving solids stream.

T_{ref} is a reference temperature for the calculation of the enthalpy. U is the overall heat transfer coefficient, A is the surface area of contact between the reactor wall and the powder bed, T_w is the average wall temperature, R_p is the total rate of reaction per unit volume of reactor bed, V_R the volume of the reactive bed, $-\Delta H_p$ is the overall enthalpy of polymerization, and is the total enthalpy change due to evaporation of any liquid in the reactor. Adding different ICA can increase the heat capacity of the gas phase (super dry, condensed and super condensed modes) and the value of Q_{vap} is the total enthalpy change due to evaporation of any liquid in the reactor (condensed and super condensed modes). In the event that these terms increase, one can keep the same reactor temperature for a higher value of R_p .

Table 1.2 Hypothetical situations for thermal capacity.

Composition	Mol fractions					
	A	B	C	D	E	F
Ethylene	0.5	0.5	0.5	0.5	0.5	0.55
Hydrogen	0.3	0.3	0.3	0.3	0.3	0.35
Nitrogen	0.2					
Ethane		0.2				
Butane			0.2		0.1	0.09
Pentane				0.2		0.01
Thermal capacity [kJ/kgmole C]	40.0	46.7	58.4	64.7	49.1	50.4

As an example, we have some hypothetical situations in Table 1.2 for the composition of a gas mixture containing 20% of different types of inerts, operating at 20 bar and 80 °C. We can observe a 46% increase in thermal capacity if we replace the nitrogen (condition A) with butane (condition C). Even with only 10% butane in the composition (condition E), there is an increase of approximately 23%. When we increase the molecular weight of these inert alkanes the effect is more pronounced.

Nevertheless, it appears that the situation is far more complex than simply modifying the energy balance of the reactor. A recent review [23] shows that there are many operational challenges caused by the presence of an ICA, not the least of which is the need to maintain bed stability. Figure 1.3 demonstrates the major factors that impact reactor behavior in the presence of ICAs. In addition to the heat transfer effects, it has been observed that ICA contributes to the softening

and increase stickiness of the particles. This can cause agglomeration and sheeting, loss of bed stability, and some of the other problems shown in Figure 1.3. While these problems are important from an operational point of view, they are beyond the scope of the current thesis, so will not be discussed further.

Rather, the scope of the thesis focuses on the impact of ICA on the formation of polyethylene, i.e., a better understanding of the impact on intrinsic properties of the polymer, reactor temperature and partial pressure of components (compositions). For this, we need to understand, the cause and effect relationships of the operation of the condensed mode in the polymerization of ethylene. Several of these challenges, also seen in Figure 1.3 turn around the greater mobility of the chains (known as polymer plasticization) and swelling of the particle in the presence of ICA [23].

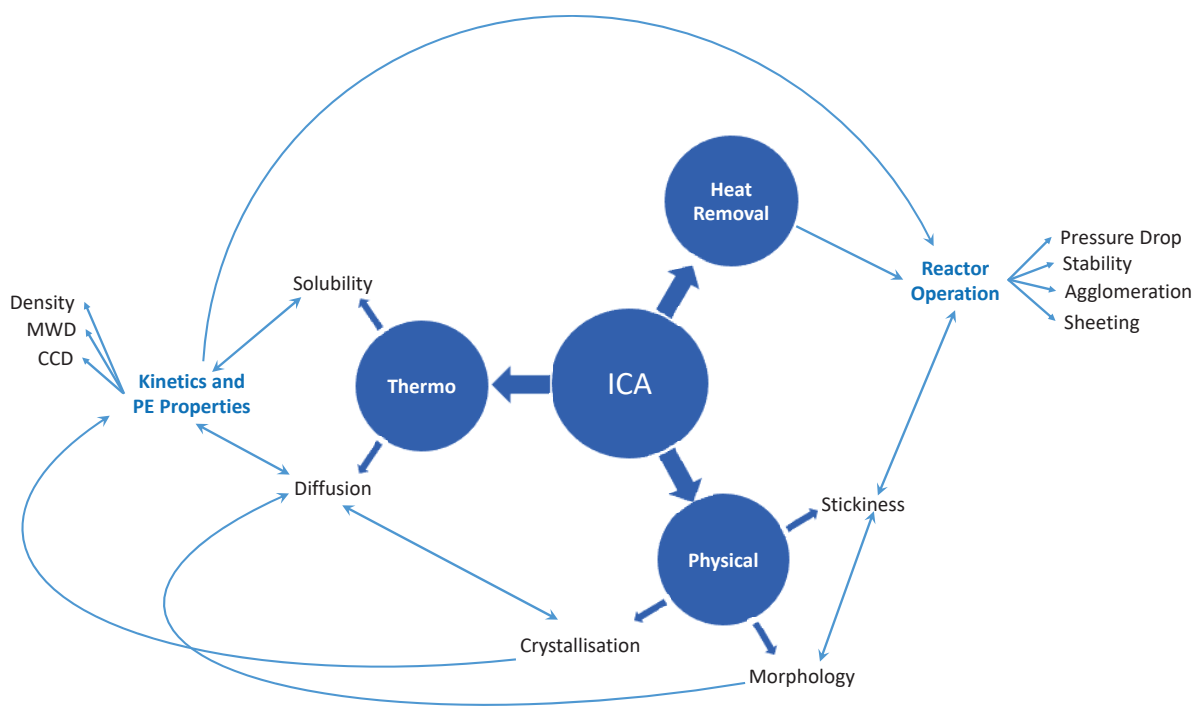


Figure 1.3 Interaction diagram: operation with ICA.

Operation with ICA increases the free volume of the amorphous phase of the polymer and promotes greater mobility of the chains. This contributes to the swelling of the particles. The interaction of these factors can cause different effects on the operation in condensed mode, such as increasing (or decreasing) the diffusivity and solubility of a penetrant in the polymer. These changes will in turn influence (usually increase) the rate of chain growth, and eventually

properties like the molecular weight of the polymer, comonomer incorporation or beginning of crystal formation. In order to understand why these points are important, and how they can impact the polymerization, it is important to understand first how polymer particles are produced in the reactor.

1.2.2. Overview of particle growth and polymer formation.

The general steps that explain how a solid catalyst particle is transformed into a particle polymer have been discussed extensively in the literature, so the reader is referred to other sources for a more detailed discussion [24]–[28]. Briefly, a solid catalyst is accepted to be a 2-tier structure: a larger, macroparticle, that is made up of an assembly of smaller, microparticles. Once it is injected into the reactor, monomer diffuses from the continuous phase of the reactor, through the boundary layer around the catalyst, into the pores, where it begins to polymerize at the active sites on the pore surface (or surface of the microparticles). As polymer begins to form there is an additional step of sorption in the polymer layer above the active sites, and diffusion through this layer. The accumulation of polymer in the pores creates hydraulic pressure that causes the initial support structure to rupture so that we have a growing polymer particle in which are dispersed the numerous micrograins that made up the original catalyst particle. As the polymerization continues, the particles grow by the expansion of the polymer phase, always with the micrograins dispersed therein. The fragmentation process occurs in fractions of seconds and is very important for the evolution of particle morphology [26], [29], as well as the crystallization process [30], [31].

If we assume fragmentation is more or less instantaneous, Figure 1.4 illustrates; in a simplified way, the different transport processes in the growing particles, and how ICA might eventually alter how the polymerization occurs.

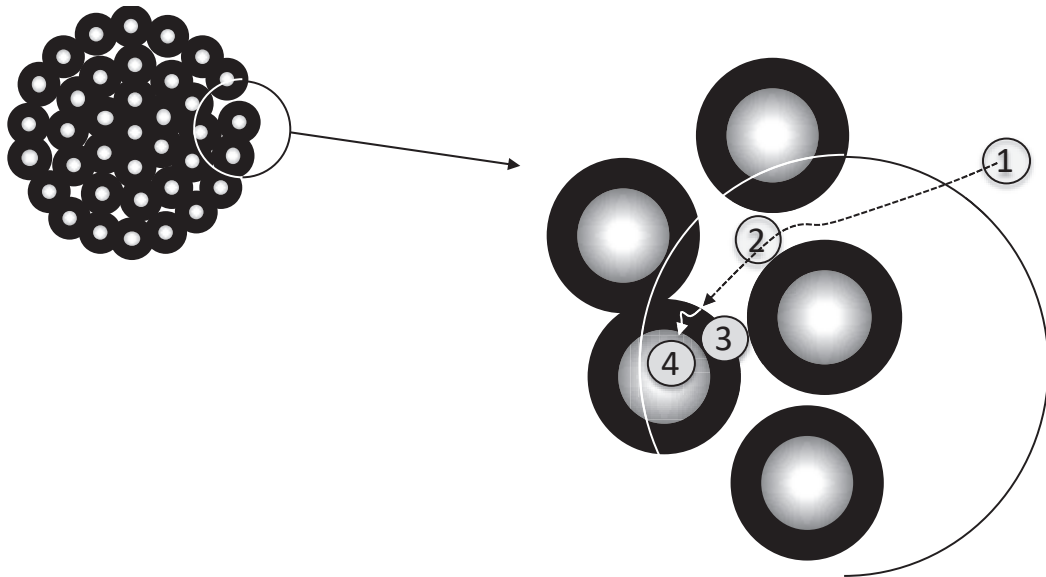


Figure 1.4 Route of the molecule between the bulk fluid to the active sites at the particle level.
Adapted from McKenna presentation and Theodore [32].

The associated resistances promote control steps in the reaction, Figure 1.4 explicitly explains, since this physical trajectory is reversible and dynamic. The description of the gas trajectory in the polymer matrix is:

1 ↔ 2: Transport transfer of the reacting molecules or inerts from the bulk fluid to the outer surface of the catalyst or growing polymer chain vice-versa

2 ↔ 3: Molecular diffusion of the reacting molecule or inerts to the pore surface within the catalyst or growing polymer chain vice-versa

3 ↔ 4: Sorption of the reacting molecule on the pore surface and desorption of the non-reacting molecule or inerts vice-versa

4: Reaction on the active site

While the presence of ICA will have an impact on both heat and mass transfer at the particle level, the impact on mass transfer and sorption is more profound. Aspects related to heat transfer will be treated directly in Chapter 2.

1.2.3. Transport phenomena in the polymer matrix

Heat and mass transfer resistances lead to the creation of temperature and concentration gradients in the particle. In the center of the particle, the temperature is assumed to be highest, and component concentrations lowest (although this might not be the case for inerts and slowly

reacting components [33] in some specific cases). [34], [35]. Since the observed rate of polymerization will depend on the importance of these gradients, we need to briefly discuss how ICA may affect these.

The influence of ICA on the temperature gradients depend on their heat capacity. The amount of heat removed by the circulating gas can determine the reactor productivity. An increase in polymer production can be made possible as a result of increased cooling capacity [36].

The diffusion coefficient represents the mobility of the gas molecules through the polymer layer to the active sites. The factors that influence the diffusion coefficient are the species that diffuses, the properties of the medium in which the diffusion occurs and the temperature. The diffusion coefficient is expected to increase with temperature and be larger for lighter (i.e. smaller) compounds. Also, the mobility depends on the glass transition temperature (T_g) of the polymer [37]. The impact of ICA on monomer diffusivity is quite complex and difficult to predict priority as experimental results and modeling efforts are scarce in this field. However, some studies that do exist suggest that the presence of ICA increases the diffusion of ethylene in the polymer matrix [38], [39].

One model that describes the transport of a gas through a polymer is the free-volume theory [38], [40]. In this theory, the total volume occupied by a polymer is divided into three components: i) volume occupied by the macromolecule; ii) free interstitial volume (the mean distance between the polymer chains) and iii) excess free volume. The free interstitial volume has small dimensions, while the excess free volume has dimensions that allow the transport of the gas molecule. For diffusion to occur in this medium, said theory requires that there is a hole (free volume) in the polymer of a large enough size adjacent to the penetrant molecule, and that same molecule has enough energy to overcome the attractive forces between the polymer chains. In this sense, the free volume in the polymer matrix influences the diffusivity, but also the sorption. The higher the free volume (stationary and/or transient) the greater the gas mobility in the polymer matrix and the higher the sorption capacity of the gas in the polymer matrix [41].

1.2.4. Sorption of ICA in amorphous phase polymer

Solubility: impact on reaction rate and properties

The sorption is related to the coefficient of solubility which is defined as the concentration of gas that a given polymeric membrane can accommodate in equilibrium. By now it should be clear that it is necessary to understand how the sorption of ICA in the polymer phase influences monomer and H₂ solubility, diffusivity and related parameters. A large number of experimental studies concerning gases solubilities in polyethylene has been reported in the literature. Studies on binary systems are quite common (monomer-PE, comonomer-PE, one penetrant-PE) and demonstrate that the solubility of alkanes and alkenes in polyethylene increases with the carbon number of molecules at identical conditions. The solubility of a given component in the polymer increases with increasing pressure and decreasing temperature [42]–[49].

However, it is also well-known that the thermodynamics of penetrant-polymer systems is highly non-ideal, so the use of simple models such as Henry's Law to describe solubilities under reaction conditions is not accurate, even for binary systems. Furthermore, it is also known that the presence of multiple penetrants will make it difficult to quantify the solubilities of the different species present in the reactor [49], [50].

Despite the importance of this aspect of olefin polymerizations, few experimental studies are found in multi-penetrant systems, since it is difficult to evaluate the consistency of the experimental data in phase equilibrium with the method of analysis. Myers et al. [51] have shown that when two penetrants are solubilized in polyethylene, the heavier penetrant increases the solubility of the lighter. W.Yao et al. [52] studied ternary ethylene-penetrant-PE systems by varying partial pressures of n-hexane and iso-pentane as a penetrant. They showed that the ethylene solubility is higher in these ternary systems than in the binary system. Other authors showed the same effect in the presence of comonomers such as 1-hexene (ethylene-comonomer-PE) [45], [49], [50], [53].

This has been demonstrated under polymerization conditions by a recent series of papers presents an analysis of the impact of ICA on different interest groups and on the properties of the formed polymer [45], [50], [52]. Namkajorn et al. [54] evaluated the impact of n-hexane

on the polymerization of ethylene for two hours at a reaction temperature of 80 °C and observed an increase in the instantaneous rate of ethylene polymerization as the partial pressure of hexane increased. In addition, the polymer particles have a smoother surface with less formation of fiber-like substructures as the n-hexane concentration increases.

Alizadeh et al. [55] extended this study to look at the impact of different alkanes on the reaction rate and showed that for equivalent pressures of alkane, the heavier the ICA, the greater the increase observed in the reaction rate. Alizadeh et al. [56] also evaluated the impact of different compositions of comonomers (1-pentene and 1-hexene) and ICA (n-pentane and n-hexane) on the observed polymerization under the same ethylene pressure and reactor temperature conditions, as well as that of the combination of 1-hexene and n-hexane. The study showed that a small amount of 1-hexene (equivalent 0.3 bar) increases the polymerization rate, as it does in the reaction with only n-hexane: the concentration of both the comonomer and the ICA increases the concentration of ethylene in the polymer phase. The combination of two heavy components (1-hexene and n-hexane) was also evaluated and found that 0.6 bar each produced a total rate much higher than the observed rate for each component alone. The study also includes a comparison in the presence of 0.6 bar of n-hexane with 1 bar of hydrogen. Clearly, a mechanistic study of the influence of these compounds on ethylene polymerization is warranted.

As for hydrogen, its solubility in polyethylene (binary system) is very low, ranging in the range of $10^{-4} - 10^{-3} \text{ g}_{\text{H}_2} / \text{g}_{\text{amPE}}$ for partial pressures of 1 - 10 atm of hydrogen. This solubility is thought to increase with increasing temperature [53]. Solubility data for ternary hydrogen-ethylene-PE systems are not found in the literature. However, some studies in solution, using hexane, cyclohexane, and benzene, the solubility of ethylene in these solvents decreases in the presence of hydrogen. This implies that the presence of hydrogen, under polymerization conditions could lower the ethylene concentration in the amorphous phase, and thus lower the polymerization rate [53], [57]. N.B. This is in addition to the fact that it is known that increasing the hydrogen concentration in this polymerization process also decreases the rate of reaction in and of itself [17], [58].

Finally, the available data demonstrates that lighter components (e.g. ethylene) act as anti-solvents for heavier penetrants (e.g. hexane or hexene) [49], [50], [53]. For instance, Cancelas

et al. [59] studied the solubility of ethylene-propylene mixtures in different polypropylenes and also observed a slight cosolubility effect in the sense that propylene seems to enhance the solubility of ethylene. However, they also saw ethylene decreases the solubility of propylene in PP with respect to the solubility in the equivalent propylene PP binary system.

Solubility: modeling

Given the results presented in the previous section, it is clear that being able to quantify these effects is important. The availability of a validated thermodynamic model is quite desirable and essential for the design and development of such kind of processes [60], [61]. In fact, the need for a good thermodynamic description of the impact of ICA on the polymerization rate was shown by Alves et al. [62], who demonstrated that a poor estimation of the cosolubility effect can lead to overprediction of reactor residence times by as much as 100%.

Since thermodynamic behavior of these systems is non-ideal, one needs to use equations of state, rather than simple representations like Henry's Law to describe the sorption process. A review [63] on the equation of state (EoS) approach to modeling vapor-liquid (VLE), vapor-liquid-liquid(VLLE), vapor-solid (VSE) equilibria shows that the EoS approach allows one to describe higher degrees of non-ideality than is possible with mathematically simpler approaches. The main EoS approaches are:

- Cubic EOS based on mixing rules and excess Gibbs free energy models;
- Lattice models (basically Sanchez Lacombe EoS);
- Perturbation Models (e.g. Statistical Associating Fluid Theory -SAFT - and related)

Guerrieri et al. [63] point out that Cubic EoS are not practical for polymer systems on many occasions as they rely on the use of critical temperatures and pressures that do not exist for polymers. Generally speaking, lattice and perturbation models seem to be preferred for modeling the type of systems we are interested in here [27].

In lattice models, it is assumed that molecules have one or more segments, and the partition function of the system can be obtained by counting the possible configurations when these segments are arranged in hypothetical cells that are like the lattice in the solid material. The

Sanchez Lacombe equation of state (SL-EoS) treats polymer chains as a set of interacting beads on a lattice and, as with the Flory-Huggins model, polymer chains are mixed randomly with penetrant molecules [64], [65]. These models permit the existence of some empty sites in the lattice, so that volume changes upon mixing penetrant and polymer molecules are allowed [66]. The Perturbed Chain – Statistical Associating Fluid Theory equation of state (PC-SAFT), developed by Gross and Sadowski [67], is also widely used in industry and academia for its versatile applications. Using concepts of statistical mechanics, the model can determine the properties of substances in both phases (liquid and vapor). The PC-SAFT model is also based on the perturbation theory that represents the potential of the segments of a chain of relevant structure, with respect to the attractive interactions. Thus, the model takes account for the effects of molecular size, molecular shape, dispersion forces and association of molecules. It requires three pure component parameters: segment number, interaction energy and segment diameter [67]–[69]. Both equations also require the use of adjustable interaction parameters between the components.

Alizadeh et al. [70] used both SL-EOS and PC-SAFT models to analyze the impact of vaporized n-hexane on the rate of gas phase ethylene polymerizations in the supported catalyst. The two models were satisfactory in terms of describing the co-solubility effect for the ethylene-n-hexane-PE system once thermodynamic equilibrium is reached. However, when comparing the predicted rate enhancement effect to experimental polymerizations, they noted that the initial rate is much higher than can be accounted for by the cosolubility effect alone. This work suggests that the co-solubility phenomenon may not be the only reason for the observed increase in ethylene polymerization rate.

However, it is important to point out that none of these models take into account the semi-crystalline nature of PE, and that this can also pose a certain number of problems. For instance, Moebus et al. [71] demonstrated that conventional thermodynamic methods, which accurately predict the behavior of the polymer phase in fluid systems, do not take into account a critical concept associated with semicrystalline polymers, the elastic constraint. Using a simple thermodynamic model that addresses this effect, the solubility of ethylene, 1-butene, isobutene, 1-hexene, isopentane, and n-hexane were well estimated using the fraction of elastically affected chains as an adjustable parameter. In addition to using the model to evaluate gas phase polyethylene production with high ICA levels, Moebus et al. [71] argued that the presence of

ICA did not affect the solubility of hydrogen, ethylene, and 1-hexene, suggested that a substitution of nitrogen for isopentane would not modify properties such as molecular weight and density of polyethylene. However, it has been demonstrated clearly that this is not at all the case [56]. However as extensive data for ternary semicrystalline systems as not currently available.

Studies show that SL-EoS represents well interaction parameters for binary and ternary systems [61], [70]. In this work, the SL-EoS was used to model the experimental data found in the literature. Iteration parameters are shown in the chapters corresponding to binary systems and some ternary systems such as hexane-ethylene-PE and n-pentane-ethylene-PE systems and the calculation methodology is described in Appendix II.

1.2.5. Impact of ICA on other properties.

In addition to influencing the solubility of ethylene (and eventually other compounds), the addition of ICA to the polymerization reactor can have other less expected consequences. For instance, Alizadeh et al showed that HDPE produced in the presence of ICA (n-pentane and n-hexane) had a much higher molecular weight and different raw powder crystallinity than did powders produced without ICA [72]. They measured the crystallinity by Differential Scanning Calorimetry (DSC), and the molecular weight was measured by two methods: high-temperature Size Exclusion Chromatography and rheology.

This increase in the average MW (from 300,000 Daltons to over 1 million Daltons) can be partially attributed to an increase in the ethylene concentration at the active sites. However, the increase is greater than one might expect based on an increase in the ethylene concentration alone, and the authors could offer no explanation as to why. Furthermore, the increase in MW also corresponded to an apparent increase in the degree of crystallinity when ICA is higher in the composition of the gas. This was attributed mainly to the change in kinetics and mechanism of crystallization of polymer chains, with ICA acting as a local solvent. The samples with ICA presented (much) higher molecular weight, with values greater than one million when analyzed by rheology, than the HDPE produced in the absence of the ICA. In addition, the relaxation time of the polymer molecules with higher molecular weights was found to be orders of

magnitude higher than that of the reference polymer. Finally, it was also observed that raw reactor powder of high molecular weight PE produced in the presence of ICA was also more crystalline than that of the reference polymer.

The morphology of the final particles will depend strongly on the fragmentation step mentioned above [29, 30, 37] since the way in which the particles rupture will represent a trade-off between the rate of generation of stress caused by the polymerization on the one hand, and the ability of the particle to dissipate the mechanical energy on the other. Thus, the physical properties of the polymer during this part of the polymerization, and in particular the crystallinity [73] and relaxation time will have a strong influence on fragmentation. In addition, the crystallinity can influence monomer solubility[74], as well as the rates of diffusion [75] through the growing polymer particle.

1.3. Research statement

The aim of this thesis is to identify, question and critically evaluate the influence of ICA on the polymerization of ethylene in the gas phase in four main themes: i) polymerization temperature; ii) the presence of different concentrations of hydrogen; iii) incorporation of different comonomers iv) crystallization rate. Based on these themes, the strategy and structure of the thesis were formulated to answer several questions. In addition to this bibliographic review, this thesis is presented in four additional chapters and three appendices covering the major objectives, and answering the following questions:

Chapter 2: What happens when we change the operating temperature of the reactor in the presence of ICA?

Given that gas phase polymerizations can lead to important heat transfer resistance, it is important to understand what happens if particles heat up, and in particular, what, if anything, the presence of the ICA does to change this behavior. We will thus: i) provide experimental data on the behavior of ethylene homopolymerization rate at different temperatures and compare the molecular mass and crystallinity of the formed polymer; ii) evaluate experimental solubility data in the literature and correlate with the Sanchez Lacombe equation (SL-EOS) for

the studied systems; and iii) provide a simplified mathematical correlation that can compare the behavior of the particle temperature at the beginning and end of the reaction.

Chapter 3: What is the impact on the molecular weight in polyethylene, when we change the concentration of hydrogen in the presence of ICA?

All of the experimental data in the literature relating the impact of ICA and molecular weight were obtained almost with no hydrogen. However, this is virtually never done commercially, so it is important to consider the interaction between ICA and hydrogen. To achieve the objective, we will: i) provide experimental data on the behavior of ethylene homopolymerization rate in the combination of different concentrations of hydrogen and ICA; ii) provide an analytical database of the molecular mass and crystallinity of the polymers formed; iii) analyze the results of the matrix obtained, interpret them and criticize them from a statistical treatment.

Chapter 4: How does ICA influence the incorporation of a lighter (1-butene) and heavier (1-hexene) comonomer in the copolymerization of ethylene?

No data at all is available to look at the impact of ICA on comonomer incorporation, and given the significance of this last parameter, it is important to better understand this. To achieve the objective, we will: i) provide an experimental database on the behavior of the ethylene copolymerization rate in the combination of different concentrations of comonomers and ICA; ii) provide an analytical database of the molecular mass, crystallinity, and incorporation of the comonomers into the polymers formed; iii) analyze the results of the matrix obtained, interpret them and criticize them from a statistical treatment.

Chapter 5: What is the impact of ICA on the crystallization rate in the formation of polyethylene?

Clearly, ICA can plasticize PE under polymerization conditions, so it is important to know whether or not they can influence properties such as the rate of crystallization. To achieve the objective, we will: i) provide experimental data of isothermal curves and heating in blends of HDPE, produced in the laboratory with ICA by DSC analysis; ii) determine the equilibrium melt temperature of the blends and determine parameters of the crystallization kinetics.

Chapter 6 comprises an overview of the most important findings of the thesis, together with perspectives for future research.

Appendix I describes the experimental methodology in the synthesis of ethylene polymerization and the characterization analyzes; Appendix II shows the solubility equation, while appendix III deals with the statistical analysis.

Reference

- [1] E. Sagel, “Polyethylene Global Overview Today’ s,” *Foro Pemex*, 2012.
- [2] The Freedonia Group, “World Polyethylene,” pp. 1–495, 2014.
- [3] S&P Global Plantts, “Petrochemicals infographic: What’s in store for global polyethylene and polypropylene out to 2027? - The Barrel Blog,” 2017. [Online]. Available: <http://blogs.platts.com/2017/09/07/infographic-whats-store-global-polyethylene-polypropylene-2027/>. [Accessed: 31-May-2018].
- [4] F. Galiè, “Global Market Trends and Investments in Polyethylene and Polypropylene,” *Icis*, no. November, pp. 1–3, 2016.
- [5] J. K. and G. James Mark, Kia Ngai, William Graessley, Leo Mandelkern, Edward Samulski, *PHYSICAL PROPERTIES OF POLYMERS*, Third. 2003.
- [6] L. Mandelkern and Cambridge University Press., *Crystallization of Polymers Volume 2. Kinetics and Mechanisms*. Cambridge University Press, 2004.
- [7] P. C. Painter and M. M. Coleman, *Fundamentals of polymer science : an introductory text*. Technomic Pub. Co, 1997.
- [8] C. A. Harper, *Modern plastics handbook*. McGraw-Hill, 2000.
- [9] J. B. P. Soares and T. F. L. McKenna, *Polyolefin Reaction Engineering*. Weinheim, Germany: Wiley-VCH Verlag GmbH & Co. KGaA, 2012.
- [10] A. J. Peacock, *Handbook of polyethylene : structures, properties, and applications*. Marcel Dekker, 2000.
- [11] H. T. Liu, C. R. Davey, and P. P. Shirodkar, “Bimodal polyethylene products from UNIPOL™ single gas phase reactor using engineered catalysts,” *Macromol. Symp.*, vol. 195, pp. 309–316, 2003.
- [12] R. G. Alamo, “The role of defect microstructure in the crystallization behavior of metallocene and MgCl₂-supported Ziegler-Natta isotactic poly(propylenes),” *Polimeros*,

- vol. 13, no. 4, pp. 270–275, 2003.
- [13] M. Hamba and W. H. Ray, “Kinetic Study of Gas Phase Olefin Polymerization with a $\text{TiCl}_4 / \text{MgCl}_2$ Catalyst I. Effect of Polymerization Conditions,” no. September, pp. 2063–2074, 1996.
- [14] Y. V. Kissin, R. I. Mink, T. E. Nowlin, and A. J. Brandolini, “Kinetics and mechanism of ethylene homopolymerization and copolymerization reactions with heterogeneous Ti-based Ziegler-Natta catalysts,” *Top. Catal.*, vol. 7, pp. 69–88, 1999.
- [15] E. Work and F. Process, “Polyethylene, high density 1.,” vol. 1936, no. 13, 2004.
- [16] “Univation Technologies.” [Online]. Available: <http://www.univation.com/unipol.overview.php>. [Accessed: 03-Jun-2018].
- [17] V. Serini, “Polycarbonates,” *Ullmann’s Encycl. Ind. Chem.*, vol. 29, pp. 603–611, 2000.
- [18] G. A. Neumann and R. Gambetta, “Gas Fluidized Bed Polymerization.”
- [19] J. M. Jenkins, L. Russell, and T. M. Jones, “Fluidized Bed Reaction Systems,” US 4543399, 1985.
- [20] A. M. A.L. Duarte Bragança, A.L. Ribeiro de Castro Morschbaker, E. Rubbo, N. Cid Miro, T. Barlem, “Process for gas phase polymerization and copolymerization of olefin monomers,” EP001246853B1, 2004.
- [21] S. B. J.M. Jenkins III, R.L. Jones, T.M. Jones, “Method for fluidized bed polymerization,” US 4588790, 1986.
- [22] J. R. G. M.L. DeChellis, “Process for polymerizing monomers in fluidized beds,” US 5352749, 1980.
- [23] T. F. L. McKenna, “Condensed Mode Cooling of Ethylene Polymerization in Fluidized Bed Reactors,” *Macromol. React. Eng.*, vol. 1800026, 2018.
- [24] E. J. Nagel, V. A. Kirillov, and W. H. Ray, “Prediction of Molecular Weight Distributions for High-Density Polyolefins,” *Ind. Eng. Chem. Prod. Res. Dev.*, vol. 19, no. 3, pp. 372–379, 1980.
- [25] T. F. McKenna and J. B. P. Soares, “Single particle modeling for olefin polymerization on supported catalysts: A review and proposals for future developments,” 2001.
- [26] T. F. L. McKenna, A. Di Martino, G. Weickert, and J. B. P. Soares, “Particle growth during the polymerization of olefins on supported catalysts, 1 - Nascent polymer structures,” *Macromol. React. Eng.*, vol. 4, no. 1, pp. 40–64, 2010.
- [27] A. Alizadeh and T. F. L. McKenna, “Particle Growth during the Polymerization of Olefins on Supported Catalysts. Part 2: Current Experimental Understanding and

- Modeling Progresses on Particle Fragmentation, Growth, and Morphology Development,” *Macromol. React. Eng.*, vol. 12, no. 1, 2018.
- [28] M. G. Laurence, R. L. and Chiovetta, “Heat and Mass Transfer during Olefin Polymerization from the Gas Phase,” Munich, Germany, 1983.
- [29] B. Horáčková, Z. Grof, and J. Kosek, “Dynamics of fragmentation of catalyst carriers in catalytic polymerization of olefins,” *Chem. Eng. Sci.*, vol. 62, no. 18–20, pp. 5264–5270, 2007.
- [30] B. Lotz and S. Z. D. Cheng, “Polymer Crystallization Processes as Seen from the Growth Front’s Perspective,” *Polym. J.*, vol. 40, no. 9, pp. 891–899, 2008.
- [31] A. Mattozzi, B. Neway, M. S. Hedenqvist, and U. W. Gedde, “Morphological interpretation of n -hexane diffusion in polyethylene *,” vol. 46, pp. 929–938, 2005.
- [32] L. Theodore, *Chemical reactor analysis and applications for the practicing engineer*. John Wiley & Sons, Inc, 2012.
- [33] P. Kittilsen, H. Svendsen, and T. F. McKenna, “Modeling of transfer phenomena on heterogeneous Ziegler catalysts. IV. Convection effects in gas phase processes,” *Chem. Eng. Sci.*, vol. 56, no. 13, pp. 3997–4005, 2001.
- [34] S. Floyd, K. Y. Choi, T. W. Taylor, W. H. Ray, and F. E. T. Al, “Polymerization of Olefins through Heterogeneous Catalysis. 111. Polymer Particle Modelling with an Analysis of Intraparticle Heat and Mass Transfer Effects,” vol. 32, pp. 2935–2960, 1986.
- [35] S. Floyd, K. Y. Choi, T. W. Taylor, and W. H. Ray, “Polymerization of Olefins Through Heterogeneous Catalysis IV. Modeling of Heat and Mass Transfer Resistance in the Polymer Particle Boundary Layer,” vol. 31, pp. 2231–2265, 1986.
- [36] F. A.-O. Yahya Banat and A. K. Malek, “Olefin Gas Phase Polymerisation,” US 2014/0148563 A1, 2014.
- [37] R. P. White and J. E. G. Lipson, “Polymer Free Volume and Its Connection to the Glass Transition.”
- [38] M. Hedenqvist and U. W. Gedde, “Diffusion of small-molecule penetrants in semicrystalline polymers,” *Science (80-.)*, vol. 21, no. 95, pp. 299–333, 1996.
- [39] M. Chen, J. Wang, B. Jiang, and Y. Yang, “Diffusion measurements of isopentane, 1-hexene, cyclohexane in polyethylene particles by the intelligent gravimetric analyzer,” *J. Appl. Polym. Sci.*, vol. 127, no. 2, pp. 1098–1104, 2013.
- [40] J. M. Zielinski and J. L. Duda, “Predicting Polymer/Solvent Diffusion Coefficients Using Free-Volume Theory,” *AIChE J.*, vol. 38, no. 3, pp. 405–415, 1992.

- [41] Yampolskii Yu., I. Pinnau, and B. D. Freeman, *Materials science of membranes for gas and vapor separation*. John Wiley & Sons, 2006.
- [42] W. M. R. Parrish, "Solubility of isobutane in two high-density polyethylene polymer fluffs," *J. Appl. Polym. Sci.*, vol. 26, no. 7, pp. 2279–2291, 1981.
- [43] S. J. Moore and S. E. Wanke, "Solubility of ethylene, 1-butene and 1-hexene in polyethylenes," *Chem. Eng. Sci.*, vol. 56, no. 13, pp. 4121–4129, 2001.
- [44] C. Kiparissides, V. Dimos, T. Boulouka, A. Anastasiadis, and A. Chasiotis, "Experimental and theoretical investigation of solubility and diffusion of ethylene in semicrystalline PE at elevated pressures and temperatures," *J. Appl. Polym. Sci.*, vol. 87, no. 6, pp. 953–966, 2003.
- [45] J. Chmelař, K. Haškovcová, M. Podivinská, and J. Kosek, "Equilibrium Sorption of Propane and 1-Hexene in Polyethylene: Experiments and Perturbed-Chain Statistical Associating Fluid Theory Simulations," *Ind. Eng. Chem. Res.*, vol. 56, no. 23, pp. 6820–6826, 2017.
- [46] C. Wohlfarth, U. Finck, R. Schultz, and T. Heuer, "Investigation of phase equilibria in mixtures composed of ethene, 1-butene, 4-methyl-1-pentene and a polyethylene wax," *Die Angew. Makromol. Chemie*, vol. 198, no. 1, pp. 91–110, 1992.
- [47] L. M. Robeson and T. G. Smith, "Permeation of ethane–butane mixtures through polyethylene," *J. Appl. Polym. Sci.*, vol. 12, no. 9, pp. 2083–2095, 1968.
- [48] A. K. C. Chan and M. Radosz, "Fluid-liquid and fluid-solid phase behavior of poly(ethylene-co-hexene-1) solutions in sub- and supercritical propane, ethylene, and ethylene+hexene-1," *Macromolecules*, vol. 33, no. 18, pp. 6800–6807, 2000.
- [49] S. K. Nath, B. J. Banaszak, and J. J. De Pablo, "Simulation of ternary mixtures of ethylene, 1-hexene, and polyethylene," *Macromolecules*, vol. 34, no. 22, pp. 7841–7848, 2001.
- [50] A. Novak *et al.*, "Ethylene and 1-hexene sorption in LLDPE under typical gas-phase reactor conditions: Experiments," *J. Appl. Polym. Sci.*, vol. 100, no. 2, pp. 1124–1136, 2006.
- [51] C. S. Myers, "Solubility Characteristics of Polyethylene Resin," *J. Polym. Sci.*, vol. XIII, pp. 549–564, 1954.
- [52] W. Yao, X. Hu, and Y. Yang, "Modeling the solubility of ternary mixtures of ethylene, iso-pentane, n-hexane in semicrystalline polyethylene," *J. Appl. Polym. Sci.*, vol. 104, no. 6, pp. 3654–3662, Jun. 2007.

- [53] J. Sun, H. Wang, M. Chen, J. Ye, B. Jiang, J. Wang, Y. Yang, C. Ren, “Solubility measurement of hydrogen, ethylene, and 1-hexene in polyethylene films through an intelligent gravimetric analyzer,” *J. Appl. Polym. Sci.*, vol. 134, no. 8, pp. 1–7, 2017.
- [54] M. Namkajorn, a. Alizadeh, E. Somsook, and T. F. L. McKenna, “Condensed Mode Cooling for Ethylene Polymerisation : The Influence of Inert Condensing Agent on the Polymerisation Rate,” *Macromol. Chem. Phys.*, vol. 2014, no. 215, pp. 873–878, 2014.
- [55] A. Alizadeh, M. Namkajorn, E. Somsook, and T. F. L. McKenna, “Condensed Mode Cooling for Ethylene Polymerization: Part I. The Effect of Different Induced Condensing Agents on Polymerization Rate,” *Macromol. Chem. Phys.*, vol. 216, no. 8, pp. 903–913, Apr. 2015.
- [56] A. Alizadeh, M. Namkajorn, E. Somsook, and T. F. L. McKenna, “Condensed Mode Cooling for Ethylene Polymerization: Part II. From Cosolubility to Comonomer and Hydrogen Effects,” *Macromol. Chem. Phys.*, no. 216, pp. 985–995, 2015.
- [57] G. Sivalingam, V. Natarajan, K. R. Sarma, and U. Parasuveera, “Solubility of ethylene in the presence of hydrogen in process solvents under polymerization conditions,” *Ind. Eng. Chem. Res.*, vol. 47, no. 22, pp. 8940–8946, 2008.
- [58] P. Hamilton, D. R. Hill, and D. Luss, “Optical and infrared study of individual reacting metallocene catalyst particles,” *AIChE J.*, vol. 54, no. 4, pp. 1054–1063, Apr. 2008.
- [59] A. J. Cancelas, M. A. Plata, M. A. Bashir, M. Bartke, V. Monteil, and T. F. L. McKenna, “Solubility and Diffusivity of Propylene, Ethylene, and Propylene–Ethylene Mixtures in Polypropylene,” *Macromol. Chem. Phys.*, vol. 219, no. 8, pp. 1–13, 2018.
- [60] V. Kanellopoulos, D. Mouratides, P. Pladis, and C. Kiparissides, “Prediction of Solubility of *r*-Olefins in Polyolefins Using a Combined Equation of States Molecular Dynamics Approach,” pp. 5870–5878, 2006.
- [61] A. Krallis and V. Kanellopoulos, “Sanchez–Lacombe and Perturbed-Chain Statistical Associating Fluid Theory Equation of State Models in Catalytic Olefins (Co) polymerization Industrial Applications,” *Ind. Eng. Chem. ...*, vol. 52, pp. 9060–9068, 2013.
- [62] R. Alves, M. A. Bashir, and T. F. L. McKenna, “Modeling Condensed Mode Cooling for Ethylene Polymerization: Part II. Impact of Induced Condensing Agents on Ethylene Polymerization in an FBR Operating in Super-Dry Mode,” *Ind. Eng. Chem. Res.*, vol. 56, no. 46, pp. 13582–13593, 2017.
- [63] Y. Guerrieri, K. Valverde Pontes, G. Meyberg, N. Costa, and M. Embiruçu, “A Survey

- of Equations of State for Polymers,” *Intech*, pp. 357–402, 2012.
- [64] P. J. Flory, “Thermodynamics of High Polymer Solutions,” *J. Chem. Phys.*, vol. 10, no. 1, pp. 51–61, Jan. 1942.
- [65] M. L. Huggins, “Solutions of Long Chain Compounds,” *J. Chem. Phys.*, vol. 9, no. 5, pp. 440–440, May 1941.
- [66] I. C. Sanchez and R. H. Lacombe, “An Elementary Molecular Theory of Classical Fluids. Pure Fluids,” *J. Phys. Chem.*, vol. 80, p. 21, 1976.
- [67] F. Tumakaka, J. Gross, and G. Sadowski, “Modeling of polymer phase equilibria using Perturbed-Chain SAFT,” vol. 197, pp. 541–551, 2002.
- [68] W. G. Chapman, K. E. Gubbins, G. Jackson, and M. Radosz, “New Reference Equation of State for Associating Liquids,” *Ind. Eng. Chem. Res.*, vol. 29, no. 8, pp. 1709–1721, 1990.
- [69] N. Von Solms, M. L. Michelsen, and G. M. Kontogeorgis, “Equation of State for Highly Asymmetric and Associating Mixtures,” pp. 1098–1105, 2003.
- [70] A. Alizadeh, J. Chmelař, F. Sharif, M. Ebrahimi, J. Kosek, and T. F. L. McKenna, “Modeling Condensed Mode Operation for Ethylene Polymerization: Part I. Thermodynamics of Sorption,” *Ind. Eng. Chem. Res.*, vol. 56, no. 5, pp. 1168–1185, 2017.
- [71] J. A. Moebus and B. R. Greenhalgh, “Modeling Vapor Solubility in Semicrystalline Polyethylene,” *Macromol. React. Eng.*, vol. 12, no. 4, p. 1700072, 2018.
- [72] M. Namkajorn, A. Alizadeh, D. Romano, S. Rastogi, and T. F. L. McKenna, “Condensed Mode Cooling for Ethylene Polymerization: Part III. The Impact of Induced Condensing Agents on Particle Morphology and Polymer Properties,” *Macromol. Chem. Phys.*, vol. 217, no. 13, pp. 1521–1528, 2016.
- [73] A. S. Michaels and H. J. Bixler, “Solubility of gases in polyethylene,” *J. Polym. Sci.*, vol. 50, no. 154, pp. 393–412, Apr. 1961.
- [74] M. C. Kane, “Permeability, Solubility, and Interaction of Hydrogen in Polymers- An Assessment of Materials for Hydrogen Transport,” p. WSRC-STI-2008-00009, Rev. 0, 2008.
- [75] A. G. Fisch, J. H. Z. dos Santos, N. S. M. Cardozo, and A. R. Secchi, “Mass transfer in olefin polymerization: estimative of macro- and microscale diffusion coefficients through the swollen polymer,” *Chem. Eng. Sci.*, vol. 63, no. 14, pp. 3727–3739, Jul. 2008.

Chapter 2

The effect of temperature in the presence of Induced Condensing Agents

Abstract: An experimental investigation of the impact of changes in temperature on the observed rate of polymerization of ethylene in the gas phase using a commercial Ziegler Natta catalyst in the presence of induced condensing agents (ICA) revealed some unexpected behavior. In the absence of ICA, the effect of temperature was as expected: raising the temperature of the gas phase from 70°C to 90°C caused the observed rate of polymerization to increase monotonically. It has been demonstrated in the past that ICA can increase the rate of polymerization of the ethylene in the gas phase due to a cosolubility effect. However, in the current study it is shown that when ICA was present in the reactor, the same increase in temperature could actually lead to an observable decrease in the reaction rate under certain conditions of temperature and pressure. This was attributed to a lower impact of the ICA on the solubility of ethylene in the amorphous phase of the high-density polyethylene (HDPE) in the reactor at higher temperatures. An order of magnitude analysis also revealed that the presence of ICA can have an impact on the particle temperature as well.

2. INTRODUCTION

Polyethylene (PE) is the most widely used polymer in the world because it combines useful structural characteristics and properties at a low price. For this reason, it is expected that the worldwide output of PE will continue to increase for the foreseeable future. [1] To satisfy this increasing demand, either new capacity needs to be installed, or existing processes need to run at higher outputs. In either case, one of the greatest impediments to increasing production rates is the challenge of removing the heat from this highly exothermic reaction. This is even more difficult to do in gas phase polymerizations, than in slurry phase processes since the gaseous components typically have very low heat capacities and offer poor convective heat transfer. Despite this challenge, gas phase processes are widely used in commercial applications because they can be used to produce a much wider range of products than slurry processes, typically have lower operating costs, and have a lower environmental impact than the latter since they do not require large quantities of diluents.

The only reactor that can be used for gas phase polyethylene production is the Fluidized Bed Reactor (FBR) because the relative gas-particle velocities in the reactor are much higher than

in stirred bed reactors as well as the gas-solid mixing is appropriate in large scale processes. However as far back as the 1980s, the pressure to increase production rates made it necessary to find ways to improve heat removal from this type of reactor. One particularly effective means of removing heat from an FBR is to inject components referred to as Induced Condensing Agents (ICA). These components, typically C4 through C6 alkanes, are injected into the recycle loop of an FBR, and the feed is then cooled. If it is cooled to below the dew point of the mixture, then liquefied droplets of ICA are fed into the bottom of the reactor along with the gaseous species and the process is said to be operating in "condensed mode". The underlying concept is the second law of thermodynamics: the droplets vaporize in the reactor, and the latent heat of evaporation helps remove the heat of reaction. In addition, since these ICA typically have a higher heat capacity than ethylene and nitrogen (the other important process gases present in large quantities), this means that the vapor phase flowing through the reactor has a much higher heat capacity than that in a process without ICA. Finally, it should be noted that it has been shown that in the standard condensed mode of operation, the liquid droplets evaporate extremely rapidly, so most of the reactor will contain a mixture of vaporized alkanes along with the reactive components. [2, 3] The use of ICA in FBR for ethylene polymerization is clearly important from an industrial point of view, but it has not been extensively studied in the open literature.

Even though ICA are chemically inert, a recent series of articles from our research group [4-6] has shown that when these compounds are present in the reactor, they provoke an increase in the reaction rate due to the so-called cosolubility effect. This refers to the fact that the solubility of ethylene in the amorphous phase of the PE is higher in the presence of ICA than when ICA is not present and as a result the rate of reaction increases [4]. The heavier the ICA, the greater this effect is on the reaction rate. In addition, the ICA can impact the uptake of hydrogen and comonomers [5], as well as have an impact on the physical properties of the polymer and the morphology of the particles [6]. A summary of the findings from the paper by Alizadeh et al. [4] in terms of the impact of different ICA is shown in Figure 2.1, where the two hour productivity of ethylene polymerization on a commercial catalyst is shown for "dry mode" (no ICA, referred to as Base in Figure 2.1) compared with polymerizations of the same amount of ethylene pressure, but in the presence of n-hexane and n-pentane. It should be noted that all the experiments proposed in these references were performed at a reactor temperature of 80 °C. No information on the impact of the temperature of the continuous phase on the polymerization in the presence of ICA was provided. This is an important issue to consider as the operating

temperature is one of the primary levers for control of the process, so an understanding of how temperatures influence the polymerization of ethylene in condensed mode processes will be quite useful.

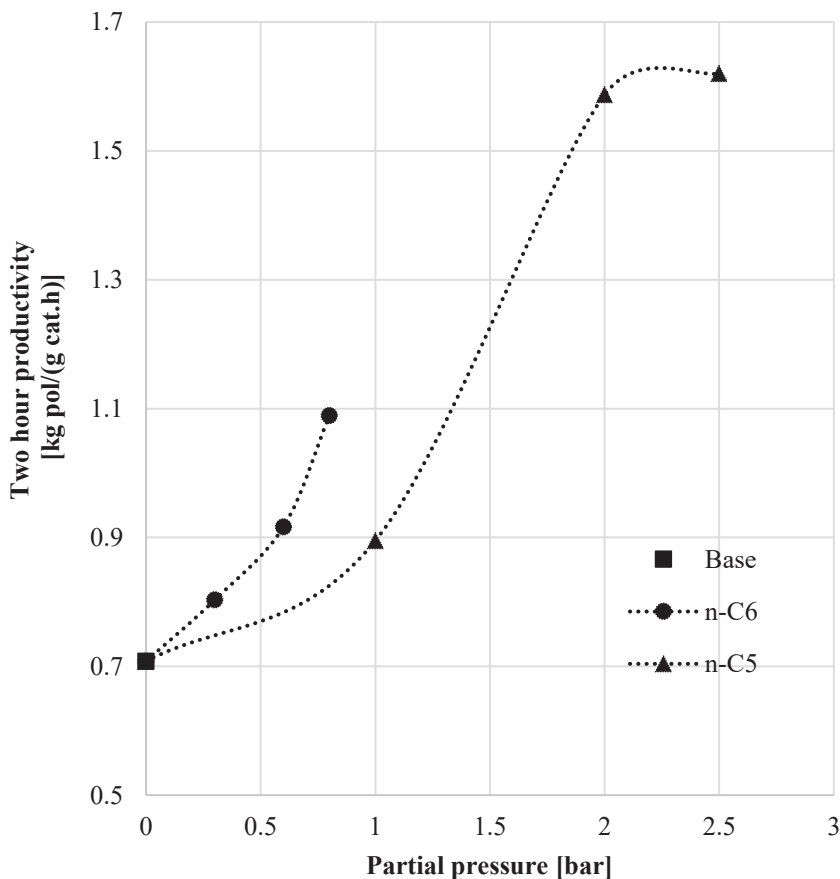


Figure 2.1. Two hours of productivity with n-hexane and n-pentane. Experimental data are taken from Alizadeh et al. [4].

In polymerizations conducted with heterogeneous Ziegler-Natta catalysts, it is possible that heat transfer limitations occur in the particles. They can generate strong effects on the rate of polymerization and its properties. Catalyst/polymer particle fragmentation and breakage, particle growth and morphological development, particles agglomeration and fine particles formation and particle overheating are other challenging problems arising when heterogeneous catalysts are used for olefin polymerization [7]. Kanellopoulos et al. [8] simulated in the single-particle growth model the effects of the initial size of the catalyst, among which the particle overheating of highly active Ziegler-Natta catalyst particles. It was shown that both the polymerization rate and particle overheating increase with increasing initial catalyst size and active metal concentration.

One expects that the temperature of the gas phase in the reactor will have several effects on the polymerization: increase in the rate of an exothermic reaction; influence the solubility of different components; soften the polymer and impact the particle morphology. In the current chapter, we will focus on the first two quantities and explore the effect of adding ICA to a polymerization reactor at different temperatures.

2.1. Experimental section

2.1.1. Materials

Ethylene with a minimum purity of 99.5% was obtained from Air Liquide (Paris, France) and was passed over purifying columns of zeolite and active carbon before use. Argon with a minimum purity of 99.5% (used to keep the reaction environment free of oxygen and other impurities) was obtained from Air Liquide and used as received. Triethylaluminium (TEA) co-catalyst was obtained from Witco (Germany). A commercial TiCl_4 supported on MgCl_2 Ziegler-Natta catalyst was used as the catalytic system with a Ti content of 2.8 wt% for all polymerizations. Sodium chloride (NaCl) with a minimum purity of 99.8% and used as a seedbed to disperse the catalyst particles. The salt was dried under vacuum for two hours at 200 °C and an additional 4 hours at 400 °C before use, to eliminate all traces of water. n-hexane and n-pentane (minimum purity 99%, from Sigma-Aldrich ICN - Germany) were purified by flowing it through 13X, and 3 - 4 Å mixed molecular sieves and stored in Schlenk flasks containing 13X molecular sieves.

2.1.2. Polymerization and characterization of polymer

The gas phase polymerization experiments are performed in the spherical stirred-bed semi-batch reactor where all descriptions are detailed in Appendix I. As well as the procedure of the analyzes to know the parameters of molecular weight and crystallinity of the polymer formed, analyzed by Size Exclusion Chromatography (SEC) and Differential Scanning Calorimeter (DSC) respectively.

In the current study, the experimental variables considered are the quantity and type of ICA (n-pentane, n-hexane), pressure (7 or 15 bars) and temperature (of 70, 80 and 90 °C), as can be seen in Table 2.1. The partial pressure of alkane injected into the reactor should be lower than the vapor pressure in the reactor temperature condition (Table 2.2) to ensure that no liquid is present in the reactor (the presence of liquid could lead to agglomeration of the particles). When the P_{ICA}/P^{vap} at the corresponding temperature is less than one, the condensation degree is total.

Table 2.1 Operation condition runs.

Run ^{a)}	$P_{reactor}$	$T_{reactor}$	$P_{Ethylene}$	$P_{n-Hexane}$	$P_{n-Pentane}$	Partial pressures	Activity Average
	[bar]	[°C]	[bar]	[bar]	[bar]	ratio - P_{ICA} / $P_{ethylene}$	[$g_{pol} \cdot g_{cat}^{-1} \cdot bar$ $C_2^{-1} \cdot h^{-1}$]
0 – 7 – 70	7	70	7	-	-	-	225
0 – 7 – 80	7	80	7	-	-	-	288
0 – 7 – 90	7	90	7	-	-	-	368
0 – 15 – 70	15	70	15	-	-	-	532
0.8 n-C6 – 7 – 70	7	70	6,2	0,8	-	0,13	610
0.8 n-C6 – 7 – 80	7	80	6,2	0,8	-	0,13	423
0.8 n-C6 – 7 – 90	7	90	6,2	0,8	-	0,13	208
0.8 n-C6 – 15 – 70	15	70	14,2	0,8	-	0,06	338
0.8 n-C6 – 15 – 80	15	80	14,2	0,8	-	0,06	278
0.8 n-C6 – 15 – 90	15	90	14,2	0,8	-	0,06	254
2.5 n-C5 – 7 – 70	7	70	4,5	-	2,5	0,56	668
2.5 n-C5 – 7 – 80	7	80	4,5	-	2,5	0,56	423
2.5 n-C5 – 7 – 90	7	90	4,5	-	2,5	0,56	283

^{a)} Sequence sample: ICA [bar] - Pressure [bar] – Temperature [°C]

Table 2.2 ICA proprieties.

ICA	P^{vap}			BP	MW
	[bar]			[°C]	
	70 °C	80 °C	90°C	at 1 atm	
<i>n</i> -Hexane	1.034	1.398	1.855	69	86.18
P_{ICA}/P^{vap}	0.77	0.57	0.43		
<i>n</i> -Pentane	2.802	3.637	4.645	36	72.15
P_{ICA}/P^{vap}	0.89	0.69	0.43		

2.1.3. Activity

The rate of polymerization was recorded by measuring the pressure decay profile in the ethylene reservoir and using the Soave-Redlich-Kwong (SRK) cubic equation of state to translate the pressure drop into a molar flow rate. The catalytic activity of the present study is the result of the arithmetic average of three experiments, and the data has been smoothed by fitting an exponentially decaying rate curve to the average activity curve.

2.2. Results and discussion

2.2.1. Rate of polymerization

In the first series of experiments, the quantity of ICA in the reactor was just sufficient to obtain a saturated vapor. This series of experiments was run to demonstrate that the addition of ICA leads to similar results as Namkajorn et al. [9] despite the change in catalyst between the current work and that in reference [9]. As can be seen in Figure 2.2, an increase in the ICA concentration in the reactor causes the rate of ethylene polymerization to increase by a factor of 2.5 (for a gas phase saturated in n-pentane) to 3 (for a gas phase saturated in n-hexane). This is in good agreement with the previously published results of Namkajorn et al. [9].

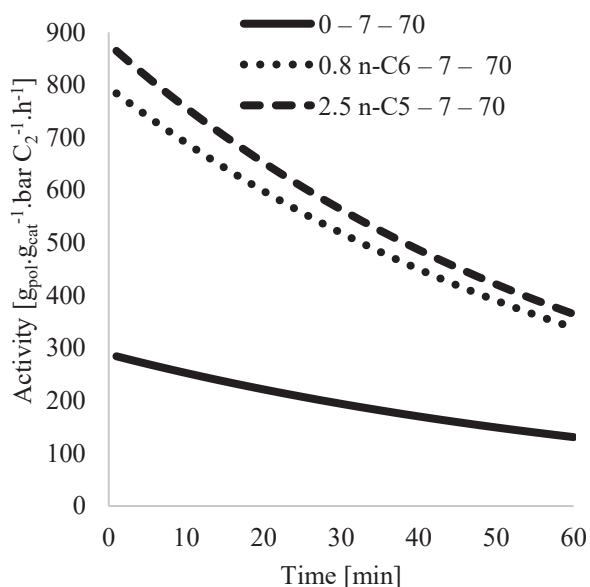


Figure 2.2. Activity of ethylene polymerization without/with ICA at 70°C and 7 bars of ethylene.

Let us now consider similar experiments at different temperatures. As can be seen in Figure 2.3, the results are not necessarily what one might immediately expect. In Figure 2.3a, it is seen that the observed rate of reaction increases with the temperature (for a fixed ethylene pressure) in “dry mode” (i.e. the absence of any ICA), as one would expect in an exothermic reaction. On the other hand, when we add ICA the situation changes. Figure 2.3b shows the impact of changing the temperature in the presence of 2.5 bars of pentane, and Figure 2.3c the same for 0.8 bars of n-hexane. In the presence of ICA, the exact opposite effect of temperature is observed with respect to dry mode: as the temperature increases, the observed rate of polymerization decreases. The same trend is observed for both n-pentane and n-hexane (recall also that each curve is the average of 3 runs).

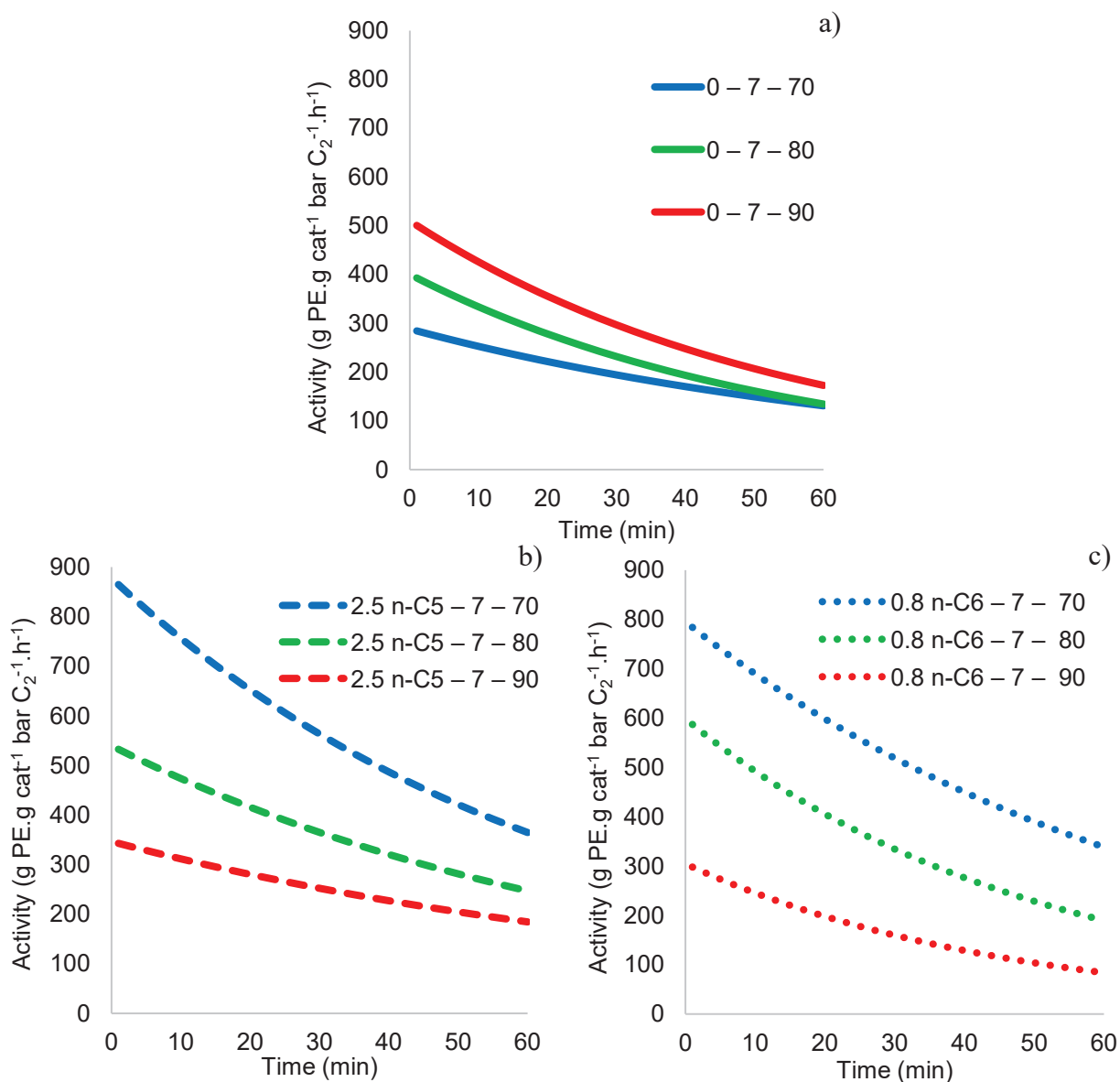


Figure 2.3. a) Rate of ethylene polymerization without ICA. b) Rate of ethylene polymerization with 2.5 bar n-pentane. c) Rate of ethylene polymerization with 0.8 bar n-hexane. Ethylene pressure in all experiments was 7 bars.

To better understand the relationship between T and the impact of ICA, the activity curves in the presence of ICA were normalized by the rate of polymerization of ethylene in dry mode at the same temperature. These results are shown in Figure 2.4.

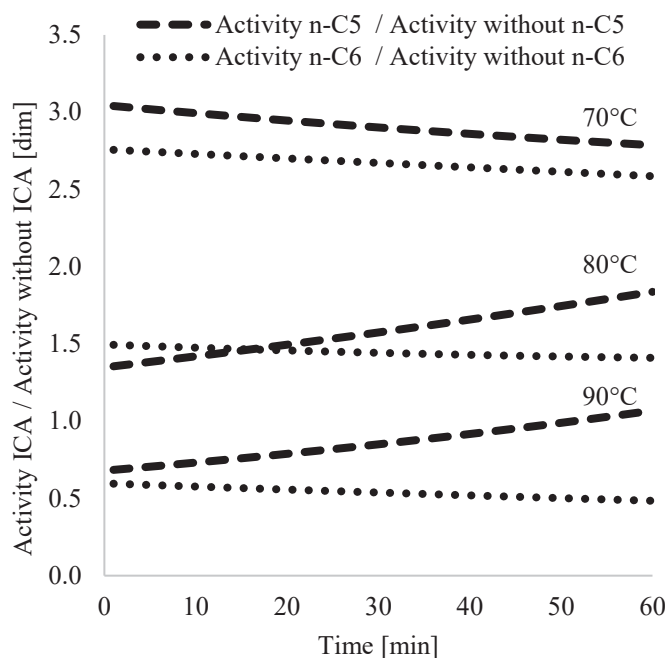


Figure 2.4. Enhancement factor of the rate polymerization ethylene

Figure 2.4 shows that at 70 °C, the presence of ICA enhances the rate of polymerization with respect to dry mode as discussed above. However, as the temperature of the gas phase increases, the effect is less and less pronounced, until at 90 °C we can see that the reactions in the presence of ICA are slower than those in the dry mode. Note again: we are referring to the temperature of the gas phase in the reactor at this point.

Polymerizations were also run at 15 bar, with and without ICA. It is shown in Figure 2.5a that, as expected, increasing the partial pressure of the monomer in the reactor leads to a higher rate of polymerization at 15 bars than at 7 bars in dry mode. However, the impact of ICA at different pressures of the reactor in the presence of 0.8 bar of n-hexane bar at 70 °C can also be seen in Figure 2.5a and b. In other words, when we increase the ethylene pressure to 15 bar, the influence of the ICA does not appear to be the same as at the lower pressure. Nevertheless, it can be seen from Figure 2.6 that the impact of changing the temperature at 15 bars of ethylene and 0.8 bars of n-hexane follows a similar if less pronounced trend as was observed at the lower pressure; the rate decreases slightly as the temperature increases.

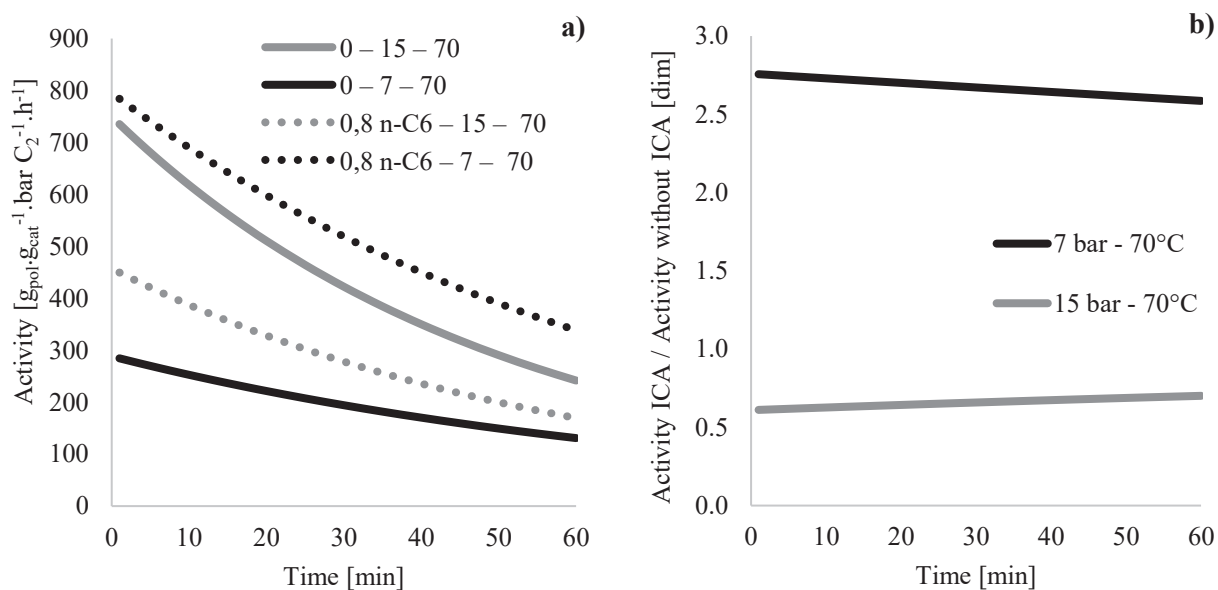


Figure 2.5. Rates of polymerization at 15 bars compared to the rates at 7 bars (activities normalized by pressure). a) Rate of ethylene polymerization with and without hexane. b) Enhancement of the rate polymerization ethylene in different monomer concentrations.

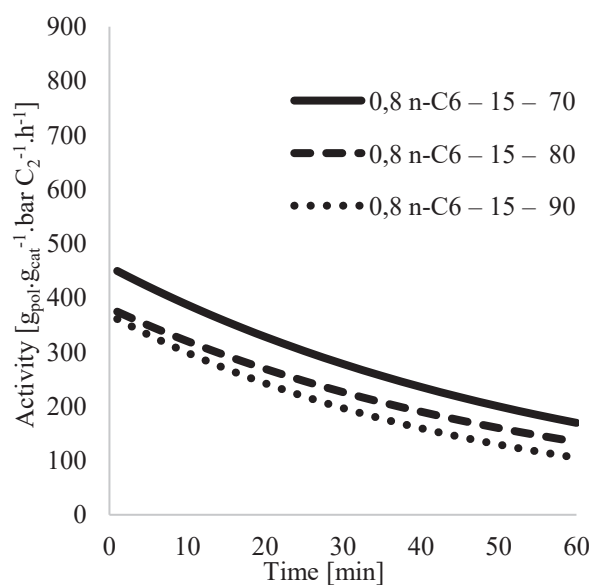


Figure 2.6. Rate of ethylene polymerization with 0.8 bar n-hexane in 15 bar.

The two major effects that can be seen here are those of temperature and of pressure. If one compares the results between the 7 bar and 15 bar experiments, at each pressure level the rates drop as temperature increases, but the effect is stronger for 7 bars of ethylene than at 15 bars. It is probable that while the cosolubility effect has an impact at both pressures, it will be less

significant at 15 bars than at 7 bars since the relative pressures of ethylene and of n-hexane are different at the different ethylene pressures. One would thus expect the relative impact of n-hexane on the ethylene pressure to be less significant at 15 bars.

However, to understand the other observations made above, we propose that one needs to consider challenges linked to heat transfer and the real temperatures of the particles since it is the particle temperature that determines both the reaction rate and the solubility of the compounds in the amorphous phase of the polymer. Ideally one would like to know what the particle temperature is, however, this would require knowledge of the flow field in the reactor, and in particular the relative gas particle velocities. Equally as important, one would also need a kinetic model and an accurate description of the complex thermodynamics of this multicomponent system. Much of this information is not available so we will have to content ourselves with an order of magnitude analysis of the possible explanations for the results we have obtained.

Since some thermodynamic data is available for the ethylene/*n*-hexane/PE system we will use the 7-bar experiments with n-hexane. The Sanchez–Lacombe equation of state (SL-EOS) [10] was used to model the solubility of ethylene in PE alone, and the solubility of a mixture of ethylene and n-hexane in PE. Alizadeh used the data of Yao et. al. [11, 12] and Castro et al. [13] to estimate the interaction parameters k_{13} and k_{23} (1 = ethylene, 2 = hexane or n-pentane, 3 = PE, assuming $k_{12} = 0$). The values as a function of temperature are shown in Figure 2.7. The solubility curves for the binary system of ethylene/PE (i.e. dry mode solubility) can be seen in Figure 2.8a for the temperatures of 70, 80 and 90 °C, and for the ternary system (PE/ethylene/n-pentane) Figure 2.8b and (PE/ethylene/ n-hexane) Figure 2.8c.

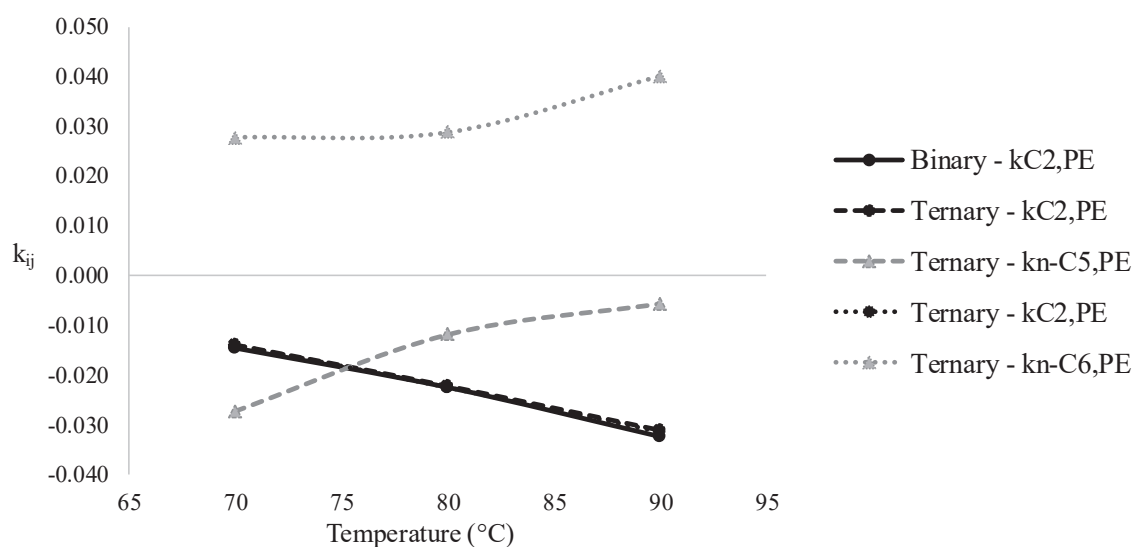


Figure 2.7. Interaction parameter (k_{ij}) as a function of temperature.

If we begin with the over-simplification that the particles have the same temperature as the gas phase, then the solubility results can help to partially explain the results shown above. Clearly, the concentration of ethylene is higher in the presence of n-hexane for a given temperature, and as the temperature increases, the ethylene solubility logically decreases. Also, the ethylene solubility is more sensitive to the temperature (in terms of the absolute value of g ethylene by gram of amorphous PE) in the presence of hexane than in the binary system. At 70 °C, the ethylene solubility in the ternary system is almost 33% higher than in the binary system at 70 °C. At 80 °C, the difference between the binary and ternary is slightly less than 15%, and at 90°C, it is only 3%. One would thus expect that anything that added to or perturbed this enhancement due to the cosolubility effect to have a greater impact at 70 °C than at 90 °C. In other words, as the temperature increases, the system becomes more and more like the dry mode system.

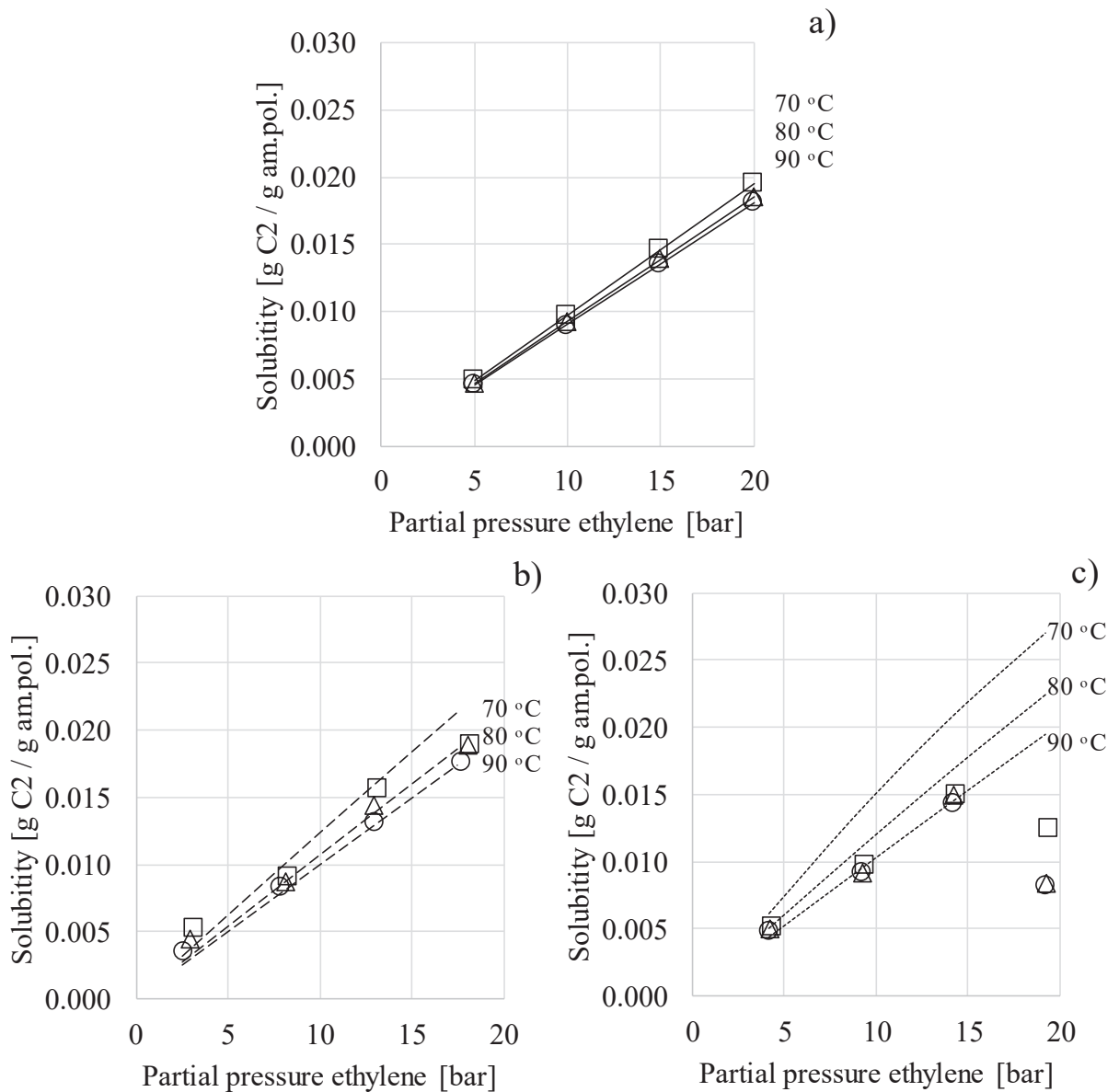


Figure 2.8. a) Binary Polyethylene / Ethylene Sanchez Lacombe Model. b) Ternary Polyethylene / 2.5 bar n-Pentane / Ethylene c) Ternary Polyethylene / 0.8 bar n-Hexane / Ethylene. Sanchez Lacombe Model. Data experimental \square 70 °C, Δ 80 °C and \circ 90 °C from Yao et al. [11,12].

However, we also need to think about the fact that the particles might not be at the same temperature as the continuous phase. In the work of Floyd et al. [15, 16], the authors use the well-known multigrain model (MGM) to analyze the temperature (and concentration) gradients inside the growing particles, as well as across the particle boundary layer. For reaction rates on the order of those observed in the current work, these authors show that it is far more likely that the exterior temperature gradients (i.e. between the bulk fluid and the surface of the particle)

will be more significant than the internal temperature gradient, and that this effect is more significant at the beginning of the reaction than once the particles have had the time to grow. One can use the graphs in reference [15] to estimate that the temperature rise in our polymerizations could be of the order of 5 - 10°C at the beginning of the polymerizations, and only a fraction of a degree after an hour. Of course, the temperature gradient will depend on different factors, including the relative gas-particle velocity, and the heat capacity of the gas phase. Figure 2.9 shows the impact of ICA on the heat capacity of the gas phase. Here it can be seen that the heat capacity of the gas phase is close to 27% higher in the presence of 11 mol% of *n*-hexane, the addition of 36 mol% of *n*-pentane leads to an increase of approximately 65% in the heat capacity of the gas phase. In other words, a small amount of ICA leads to a significant increase in the ability of the gas phase to absorb the heat produced by the reaction and to a higher heat transfer coefficient, which in turn would lead to a small increase in the value of *T* for systems containing ICA.

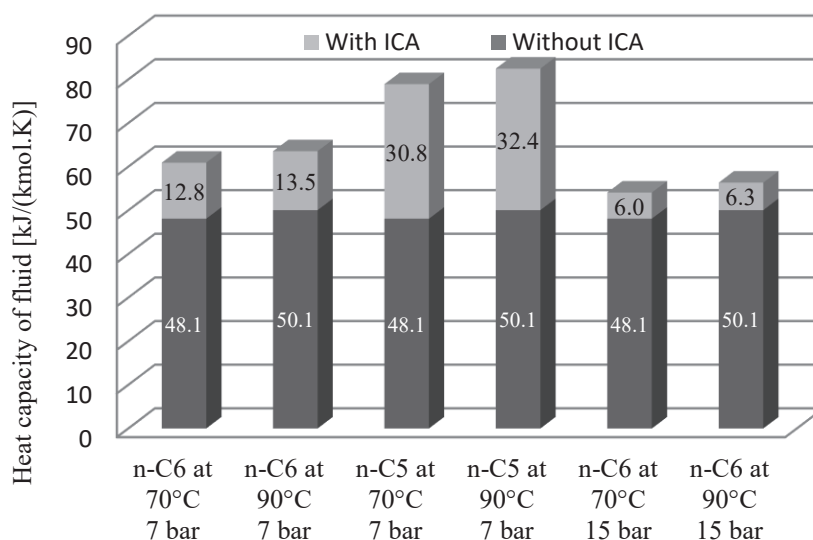


Figure 2.9. The increased heat capacity of the fluid in the presence of ICA for 7 and 15 bar of ethylene plus ICA.

Thus, the overall impact of increasing the temperature in the experiments presented here will be a tradeoff between competing effects: (1) activation energy - increasing the temperature will increase the propagation rate constant and should make the polymerization proceed faster (see dry mode results above); (2) heat capacity effect – or the degree of overheating of the particles. When the heat capacity of the gas phase is higher, it can absorb more heat and the particles will overheat less; (3) solubility - increasing the temperature of the particles will cause the ethylene

concentration to drop in the particles, and also that of n-hexane. The decrease in the n-hexane concentration will compensate for the decrease in the ethylene concentration due to the temperature rise since the cosolubility effect will be less significant as well.

If one considers Figure 2.4, the polymerization rate is enhanced by a factor of 2.6 to just over 3 for both ICA, but as the temperature increases the tradeoff between the two competing effects. At 90 °C the solubility of both ethylene and n-hexane are quite low, and as we saw above the solubility of ethylene in the dry mode with and without ICA will be very similar. However, in dry mode, the heat capacity of the gas phase is much lower than when the ICA is present, so the particle temperature will be lower in the presence of ICA than in dry mode, meaning that the enhancement effect will be less than one at the beginning of the reaction. The temperature gradient between the particle and the continuous phase will of course decrease until it is almost negligible by the end of the polymerization, so the tradeoff between the activation energy effect and the solubility effect will evolve. How this evolution of the enhancement effect develops will depend on the heat capacity of the gas phase, and the quantity and type of ICA in the gas phase. This explanation also appears to be valid for the results at 15 bars. The difference in the heat capacities is less significant, so the difference in temperature of the particles with, and without ICA is potentially less important. Although the overall tradeoffs are similar in nature, one can see from Figures 2.5 and 2.6 that they are less pronounced than at 7 bars.

2.2.2. Characterization

The polymers made in this part of the work were characterized in terms of the average molecular weights (weight-average molecular weight, M_w , and number-average molecular weight, M_n), the molecular-weight dispersity, PDI, as well as the total fraction of crystalline material (%wc) and the melting temperature (T_m). It was difficult to measure the M_w in of PE made in the presence of ICA because no hydrogen was used during the polymerization in order to remove a potentially confounding variable from the analysis. As noted by Namkajorn et. al. [6] the presence of ICA (*n*-hexane and *n*-pentane) leads to the production of HDPE with very high molecular weights (well in excess of one million, evaluated by Rheology) and increased crystallinity.

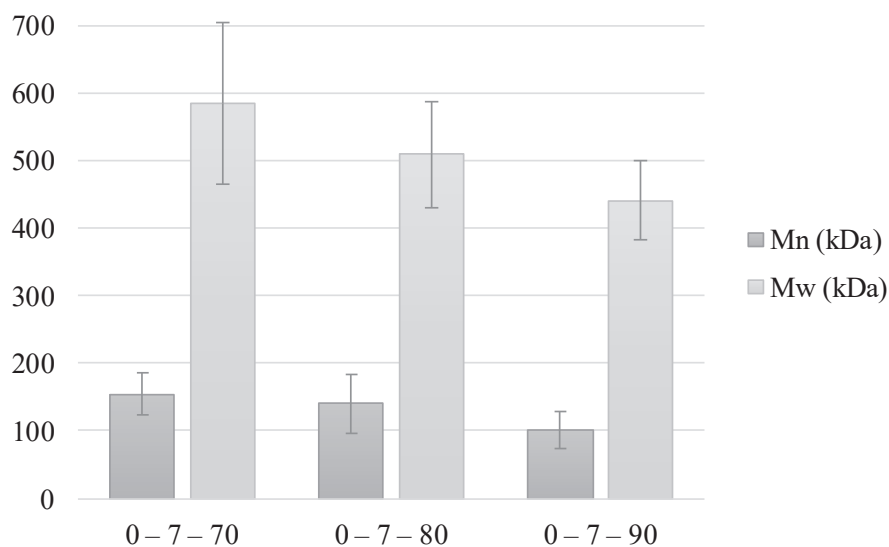


Figure 2.10. M_n and M_w average of samples without ICA.

The samples used for the molecular weight measurements underwent a long dilution process. The dilution was done by cycles of 30 minutes of heating (at 150 °C) and cooling (at room temperature) for 8 hours, using trichlorobenzene (TCB) as a solvent, and was then analyzed in SEC. This method allows a relaxation of the polymer chain which facilitated the dilution and avoided operational problems in the SEC equipment. Although we are able to dilute part of the polymer in the TCB, this does not guarantee a real reading, since larger molecules were possibly retained in the exclusion column of the equipment. However, the data allow us to evaluate a tendency for the different reaction temperatures analyzed in the presence and absence of ICA. The reproducibility was evaluated for the three samples without presence of ICA, shown in Figure 2.10. This is likely to be true for the other samples.

The data on crystallinity was performed by two different thermogram methods and compared values of the second heat. The crystallinity in the first heat is 15 - 20% higher because it considers artifacts occurring in the reactor environment, as discussed by Namkajorn et. al. The difference between the methods stems from annealing time of 10 and 30 minutes at temperature 180 and -20 °C, respectively. This evaluation was used because some samples needed more time to relax the molecules. The annealing effect relates to characteristics of the thickening process, which stabilizes the polymer crystals. Here the effect of partial melting and molecular weight distribution causes difficulties in defining the melting temperature. The higher the annealing time, the longer the spacing of crystals [17].

Table 2.3 Characterization parameters of the polymers.

Run	M _w kDa	PDI	%wt insoluble	%w _c 10 min	%w _c 30 min	T _c °C	T _m °C
0 – 7 – 70	585	4.14	27	50	57	118	135
0 – 7 – 80	509	4.07	36	59	54	119	136
0 – 7 – 90	441	4.62	26	62	49	119	136
0 – 15 – 70	693	4.04	22	69	42	118	137
0.8 nC6 – 7 – 70	631	3.19	22	73	56	118	136
0.8 nC6 – 7 – 80	523	8.02	19	69	53	119	136
0.8 nC6 – 7 – 90	453	6.75	19	90	67	118	135
0.8 nC6 – 15 – 70	601	3.65	13	56	56	118	136
0.8 nC6 – 15 – 80	509	6.54	12	64	50	119	136
0.8 nC6 – 15 – 90	476	7.30	14	71	64	119	136
2.5 nC5 – 7 – 70	842	4.52	39	45	42	118	137
2.5 nC5 – 7 – 80	735	5.08	39	35	46	118	136
2.5 nC5 – 7 – 90	578	7.80	45	40	43	123	136

Table 2.3 shows the results of the characterization, as well as the fraction of insoluble in the reading of the SEC. We can observe:

- i) A large fraction of insoluble materials leads us to believe that there might be a significant error in the absolute values of the molecular weight;
- ii) M_w decreases with increasing temperature (expected) for a given composition.
- iii) The presence of ICA increases the molecular weight at 7 bars. For samples with n-C5, the differences were more significant. The increase in the ethylene partial pressure, ie higher C2/n-C6 ratio, did have the same trends at 70 °C (Figure 2.11a), but there is not enough data at other temperatures to draw a strong conclusion.
- iv) The PDI of polymers made without ICA is similar, regardless of the temperature. On the other hand, the PDI values increase consistently from 70 °C to 90 °C, when ICA is present.
- v) No impact was observed on the degree of crystallinity between different temperature and pressure conditions, (Figure 2.11b) for an annealing time 10 min which is not seen for a time of 30 min. Peak Crystal temperature was the same for all samples, on average 118.9 ± 1.1 °C.
- vi) No variation in the melting temperature was observed, with an average of 136.0 ± 0.6 °C.

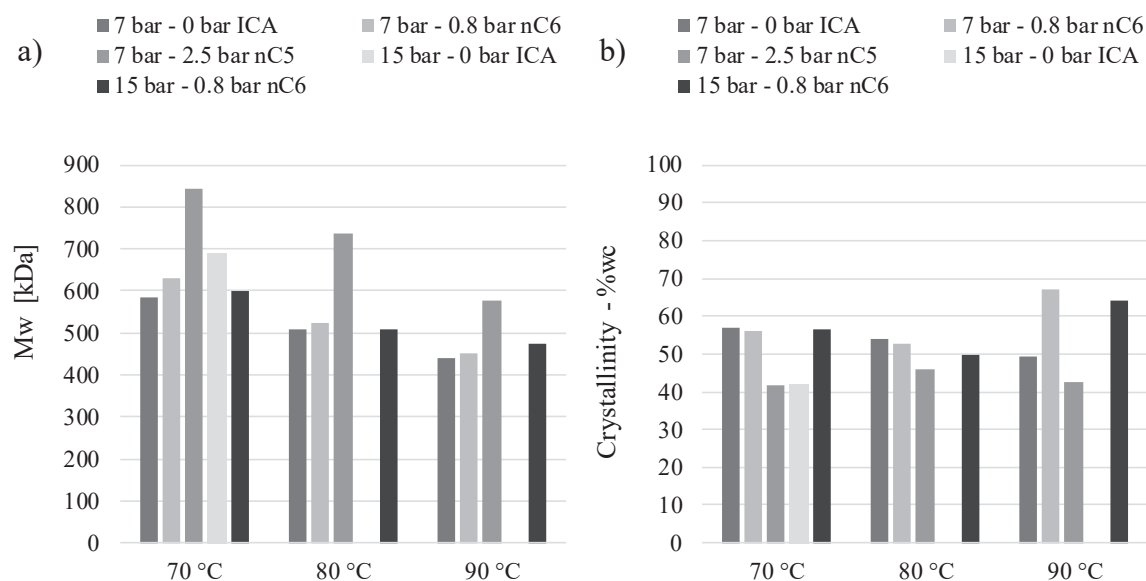


Figure 2.11. a) M_w for all samples b) Degree of crystallinity for all samples.

2.3. Conclusions

In the current study, the behavior of the catalytic activity of the homopolymerization of ethylene in the presence of ICA at different temperatures was evaluated at 70 °C, 80 °C and 90 °C. The results obtained at 2 industrially relevant pressures show that the evolution of the reaction rate as a function of temperature is not what one might expect in the presence of ICAs, with the rate decreasing as the temperature increases.

This observation is attributed to tradeoffs between the competing effects caused by increasing the reaction temperature. On the one hand, increasing the temperature in the reactor should increase the polymerization rate due to the activation energy of the exothermic reaction. This is indeed what one sees in dry mode. However, increasing the temperature decreases the solubility of the gas phase species in the amorphous phase of the reaction. In addition, the presence of ICA in the gas phase also increases the heat capacity of the latter. This means that the difference between the particle temperature (especially at the beginning of the polymerization) and the gas phase will be smaller when ICA is present than it is in dry mode. The sum of the combination of these competing effects leads us to situations where the effective reaction rate is lower for higher temperatures in the presence of ICA.

With regards to the characterization of this experimental series, as seen in the literature, the presence of ICA increases the concentration of the polymer chain, as seen by the Mw and the degree of crystallinity, it is not observed a great impact of the ICA when analyzed by a higher annealing time.

Clearly, these issues will be very important if we wish to develop working models of fluidized bed reactors operating in condensed mode or in the presence of vaporized alkanes in the reactor feed stream. The results of this study also point to the need for more detailed thermodynamic studies that allow us to develop models of solubility in multicomponent systems over a range of temperatures and pressures.

References

- [1] Polyethylene (PE) Typical Properties Generic HDPE, MMW | UL Prospector. Available at: <https://plastics.ulprospector.com/generics/27/c/t/polyethylene-pe-properties-processing/sp/10>. (Accessed: 23rd February 2017)
- [2] Alizadeh, A. & McKenna, T. F. L. Condensed Mode Cooling in Ethylene Polymerisation: Droplet Evaporation. *Macromol. Symp.* 2013, 333, 242–247.
- [3] Chinh J-C.; Filippelli M.C.H; Newton D.; Power M.B. *Polymerization Process.* 1996, US 5,541,270.
- [4] Alizadeh, A., Namkajorn, M., Somsook, E. & McKenna, T. F. L. Condensed Mode Cooling for Ethylene Polymerization: Part I. The Effect of Different Induced Condensing Agents on Polymerization Rate. *Macromol. Chem. Phys.* 2015, 216, 903–913.
- [5] Alizadeh, A., Namkajorn, M., Somsook, E. & McKenna, T. F. L. Condensed Mode Cooling for Ethylene Polymerization: Part II. The Effect of Different Condensable Comonomers and Hydrogen on Polymerization Rate. *Macromol. Chem. Phys.* 2015, 216, 985–995.
- [6] Namkajorn, M., Alizadeh, A., Romano, D., Rastogi, S. & McKenna, T. F. L. Condensed Mode Cooling for Ethylene Polymerization: Part III. The Impact of Induced Condensing Agents on Particle Morphology and Polymer Properties. *Macromol. Chem. Phys.* 2016, 217, 1521–1528.

- [7] McKenna TF, Di Martino A, Weickert G, Soares JBP (2010) Particle growth during the polymerization of olefins on supported catalysts, 1-nascent polymer structures. *Macromol React Eng* 2010, 4, 40–64.
- [8] Kanellopoulos V, Dompazis G, Gustafsson B, Kiparissides C (2004) Comprehensive analysis of single-particle growth in heterogeneous olefin polymerization: The random - pore polymeric flow model. *Ind Eng Chem Res* 2004, 43, 5166-5180.
- [9] Namkajorn, M., Alizadeh, A., Somsook, E. & McKenna, T. F. L. Condensed-Mode Cooling for Ethylene Polymerization: The Influence of Inert Condensing Agent on the Polymerization Rate. *Macromol. Chem. Phys.* 2014, 215, 873–878.
- [10] Sanchez, I. C. & Lacombe, R. H. An elementary molecular theory of classical fluids. Pure fluids. *J. Phys. Chem.* 1976, 80, 2352–2362.
- [11] Yao, W., Hu, X. & Yang, Y. Modeling solubility of gases in semicrystalline polyethylene. *J. Appl. Polym. Sci.* 2007, 103, 1737–1744.
- [12] Yao, W., Hu, X. & Yang, Y. Modeling the solubility of ternary mixtures of ethylene, iso-pentane, n-hexane in semicrystalline polyethylene. *J. Appl. Polym. Sci.* 2007, 104, 3654–3662.
- [13] Castro, E. F.; Gonzo, E. E.; Gottifredi, J. C. Thermodynamics of the absorption of hydrocarbon vapors in polyethylene films. *Journal of Membrane Science* 1987, 31 (2-3), 235-248.
- [14] Alizadeh, A., Ph.D. Thesis, Department of Chemical Engineering, Queen’s University, Kingston, ON, Canada, July, 2014 (also available at https://qspace.library.queensu.ca/bitstream/handle/1974/12281/Alizadeh_Arash_201407_PhD.pdf, last accessed 10 May, 2017)
- [15] Floyd, S., Choi, K. Y., Taylor, T. W. & Ray, W. H. Polymerization of olefins through heterogeneous catalysis. III. Polymer particle modeling with an analysis of intraparticle heat and mass transfer effects. *J. Appl. Polym. Sci.* 1986, 32, 2935–2960.
- [16] Floyd, S., Choi, K. Y., Taylor, T. W. & Ray, W. H. Polymerization of olefins through heterogeneous catalysis IV. Modeling of heat and mass transfer resistance in the polymer particle boundary layer. *J. Appl. Polym. Sci.* 1986, 31, 2231–2265.
- [17] E. W. Fischer, “Effect of annealing and temperature on the morphological structure of polymers,” *Pure Appl. Chem.*, vol. 31, no. 1–2, pp. 113–131, 1972.

Chapter 3

The impact of Induced Condensing Agents in the presence of hydrogen

Abstract: Polymerization of ethylene in the presence of hydrogen was performed in the gas phase using a commercial Ziegler Natta catalyst and the addition of Induced Condensing Agents (ICA). Experimental planning and statistical analysis techniques were used to evaluate the effects of the concentration of hydrogen and n-pentane (the ICA) on the yield and properties of polyethylene (molecular weight and crystallinity). Although there is no effect on the mutual interaction between hydrogen and pentane in the response variables, the hydrogen concentration is an important variable. Affecting molecular weight and short chain branching, there is no major impact of ICA under conditions where the ICA concentration is less than the hydrogen concentration. For an ICA/C₂ ratio much larger than the H₂/C₂ ratio, the effect of ICA may interfere with the decrease of the hydrogen effect on the ethylene polymerization reactions.

3. INTRODUCTION

As mentioned previously, a gas phase reactor operating in either super dry or condensed mode will contain monomer(s), hydrogen, inert gases such as nitrogen to control partial pressures, as well as chemically inert species referred to as induced condensing agents (ICA), used in principle to enhance the rate of heat removal from the reactor.

Hydrogen is used as a chain transfer agent to control molecular weight in most polymerization reactions performed with Ziegler Natta catalysts. Essentially molecular hydrogen inserts itself between the active site and the growing polymer chain, causing the chain to transfer off the active site. One atom of hydrogen saturates the chain end, and the other stays on the active (titanium) site, forming dormant site [1]. This, in turn, can lead to a decrease in the polymerization rate of ethylene. The higher the concentration of hydrogen at the active site, the more likely it is that a chain transfer will occur, so the shorter the polymer chains will become, but also the more dormant sites we have, the dormant site can be reactivated, but as this event takes a certain time, increasing hydrogen concentration leads to a decrease in the polymerization rate of ethylene.

On the other hand, we know that increasing the concentration of inert species such as Induced Condensing Agents (ICA), can lead to increasing the rate of ethylene polymerization due to the cosolubility effect [2], [3]. This increase is observed because ICA allows greater sorption and mobility of smaller molecules in the polymer matrix. What is not clear at the current time is whether or not ICA has a significant cosolubility effect on hydrogen. It is found in the literature that increasing ethylene concentration in a hydrogen-ethylene-liquid hydrocarbon system can provoke an increase in the solubility of hydrogen in hexane, cyclohexane, and benzene [4]. There are some data for binary hydrogen-PE systems, and experiments show that the solubility of the hydrogen in the polymer matrix is very low; typically on the order of 10^{-4} g H₂ / g amorphous polymer [5]–[7]. Unfortunately, there is no solubility data for hydrogen / ethylene / polyethylene system in the literature.

Knowing that ICA contributes to increased concentrations of ethylene (and propylene [8]) in the polymer matrix, the question is whether or not ICA enhances the solubility of hydrogen? Since it is difficult to directly measure the solubility of hydrogen in PE in a standard laboratory set-up, we decided to design a series of experiments combined with a statistical analysis to estimate the effects of changes caused by different ICA and H₂ levels.

Due to the complex nature of the polymerization system, it is not a simple task to determine the effect of several process variables independently. In this scenario, experimental planning tools can be used to evaluate the effect of process variables on both the polymerization behavior and the final polymer properties. To perform an orthogonal factorial design, we first need to specify the q -levels at which each k -factor will be evaluated, that is, the experimental range of values that will be employed in the trials. An orthogonal factorial design presents a matrix of qk experimental runs. To study the effect of the factor on the response it is necessary to make it vary and observe the result of this variation. This obviously implies running experiments on at least two levels, to have a complete orthogonal factorial design. [9].

According to Box and Wilson [10] statistical analysis of an orthogonal factorial design is based on the following sequence:

- i) Statement of the problem with the formulation of hypotheses;
- ii) Choice of factors (independent variables);

- iii) Choice of the experimental setup and analytical techniques to provide information on the response;
- iv) Choice of variables to be measured;
- v) Determination of the rules and procedures by which the different treatments (combination of factor levels) are assigned to the experimental procedure;
- vi) Statistical analysis of results.

As previously stated, experimental planning tools can be successfully used to describe the influence of control variables, the relationship on the polymerizations behavior and, to establish a clear relationship between them and response variables. This analysis allows are to accept or reject the hypotheses formed by the experimental matrix. Statistical techniques are used to analyze, interpret and present information from planned experiments.

This study was developed to understand the impact of hydrogen in the presence of ICA, such as n-pentane on productivity, molecular weight distribution (MWD), and the crystallinity of the polyethylene formed, varying the concentration of hydrogen and ICA.

3.1. Experimental section

3.1.1. Materials

Ethylene with a minimum purity of 99.5% was obtained from Air Liquide (Paris, France) and was passed over purifying columns of zeolite and active carbon before use. Hydrogen minimum purity of 99.5% was obtained from Air Liquide (Paris, France). Argon with a minimum purity of 99.5% (used to keep the reaction environment free of oxygen and other impurities) was obtained from Air Liquide and used as received. Triethylaluminium (TEA) co-catalyst was obtained from Witco (Germany). A commercial TiCl_4 supported on MgCl_2 Zeigler-Natta catalyst was used as the catalytic system for all polymerizations. Sodium chloride (NaCl) with a minimum purity of 99.8% and used as a seedbed to disperse the catalyst particles. The salt was dried under vacuum for two hours at 200 °C and more 4 hours at 400 °C before use to eliminate all traces of water. The anhydrous n-pentane (minimum purity 99%, from Sigma-

Aldrich ICN - Germany) was purified by flowing it through 13X and 3 - 4 Å mixed molecular sieves and stored in Schlenk flasks containing 13X molecular sieves.

3.1.2. Homopolymerization and characterization of the polymer

The ethylene homopolymerization protocol is described in Appendix I, along with the characterization methodologies. The polymers were characterized in terms of their average molecular weights and molecular weight distribution (MWD) by size exclusion chromatography (SEC), and the crystallization and the melting temperatures using differential scanning calorimetry (DSC).

3.1.3. Experimental design

An orthogonal factorial design consisting of a three-level factorial experimental design and two independent variables (hydrogen and n-pentane partial pressure) was employed to evaluate quantitatively the effect of factors (independent variables) on the response variables (polymer yield, average molecular weights, and crystallinity). There are nine experiments plus three repetitions of the intermediate point to evaluate the pure error. The study also includes three extra points, which allow us to extrapolate the statistical model by evaluating the impact in the absence of hydrogen.

Experimental runs based on a 3^2 factorial design were carried out to characterize the behavior of ethylene polymerizations and give insight into the effect of independent variables on the polymer properties, as depicted in Tables 3.1 and 3.2.

Table 3.1 3^2 Factorial design.

Variable		Level		
		-1 Low	0 Middle	1 High
$x_1 =$	p H₂ [bar]	1	2	3
$x_2 =$	p n-C₅ [bar]	0	1	2

The experimental limits for the independent variables were defined based on patents [11 – 14], focusing the condensed mode polyethylene production. Based on the conditions of factorial design levels, the partial pressure lying in the range from 0.14 to 0.43 H₂ / C₂ ratio and in the range from 0 to 0.29 for n-C₅ / C₂ ratio. In the current study the experimental variables ICA (n-pentane) and hydrogen, were varied based on Table 2. The experiments were performed in random order and the ethylene pressure (7 bar) and reactor temperature (80 °C), were kept constant for all experimental conditions.

Table 3.2 Operation conditions for different runs.

N°	Notation	Experimental matrix		Run name ^{a)}	p H ₂ [bar]	p n-C ₅ [bar]	Partial pressure ratio	
		x ₁	x ₂				p H ₂ / p C ₂	p n-C ₅ / p C ₂
1		-1	-1	80 - 7C2 - 1H2 - 0nC5	1	0	0.14	-
2		1	-1	80 - 7C2 - 3H2 - 0nC5	3	0	0.43	-
3		-1	1	80 - 7C2 - 1H2 - 2nC5	1	2	0.14	0.29
4	3 ²	1	1	80 - 7C2 - 3H2 - 2nC5	3	2	0.43	0.29
5	Factorial	-1	0	80 - 7C2 - 1H2 - 1nC5	1	1	0.14	0.14
6	design	0	-1	80 - 7C2 - 2H2 - 0nC5	2	0	0.29	-
7		1	0	80 - 7C2 - 3H2 - 1nC5	3	1	0.43	0.14
8		0	1	80 - 7C2 - 2H2 - 2nC5	2	2	0.29	0.29
9		0	0	80 - 7C2 - 2H2 - 1nC5	2	1	0.29	0.14
10	Replica of	0	0	R-I	2	1	0.29	0.14
11	the	0	0	R-II	2	1	0.29	0.14
12	intermediate point (R)	0	0	R-III	2	1	0.29	0.14
13		-	-	80 - 7C2 - 0H2 - 0nC5	0	0	-	-
14	Extra points	-	-	80 - 7C2 - 0H2 - 1nC5	0	1	-	0.14
15		-	-	80 - 7C2 - 0H2 - 2nC5	0	2	-	0.29

^{a)} Sequence sample: Temperature [°C] - Ethylene pressure [bar] - Hydrogen pressure [bar] - ICA pressure [bar]

The treatment of the factorial design was performed using multiple regression to estimate the parameters related to the isolated variables and their interactions and the quadratic terms. The linear model for factorial design 3² (factor A and B with three levels) is detailed in Appendix III.

The effects are studied using *Pareto diagram*, where parameters with p values less than 0.05 do not have significant statistical value. The validity of these parameters is defined considering the pure error with repetition of the intermediate point, represented by the parameter R^2 . The evaluation of the model can also be done by observing the regression model prediction considering a confidence interval of 95%. Analysis of variance (ANOVA) was used as a technique for analysis of variance. To express any trends observed, effects will be presented as a *response surface*. Statistica version 10 was used for analysis. The second-order linear regression model for general factorial design is presented in more detail in Appendix III.

The second-order linear regression model can be expressed generically as:

$$Y = \beta_0 + \sum_{i=1}^k \beta_i x_i + \sum_{i=1}^k \sum_{\substack{j=1 \\ i \leq j}}^k \beta_{ij} x_i x_j + \varepsilon \quad (3.1)$$

where Y represents the dependent variable (response), β_i ($i = 0, 1, \dots, k$) are the linear regression coefficients, x_i are the independent variables and ε is the unobserved random error associated with the experimental conditions.

The regression coefficients β_i are estimated according to the least square method, considering the least square function (\mathfrak{S}) to be minimized as expressed by Equation 3.2:

$$\mathfrak{S} = \sum_{i=1}^n \varepsilon^2 = \sum_{i=1}^n \left[Y - \left(\beta_0 + \sum_{i=1}^k \beta_i x_i + \sum_{i=1}^k \sum_{\substack{j=1 \\ i \leq j}}^k \beta_{ij} x_i x_j \right) \right]^2 \quad (3.2)$$

3.2. Results and discussion

The production profile for each experimental condition can be seen by the rate of ethylene polymerization (or activity) as a function of time, shown in Figure 3.1. These profiles demonstrate that the increase of the hydrogen concentration at the same operating conditions leads to a lower rate of polymerization at constant ICA pressure, as expected. There is no visible difference in the rates between 1 and 2 bar of hydrogen in these experimental.

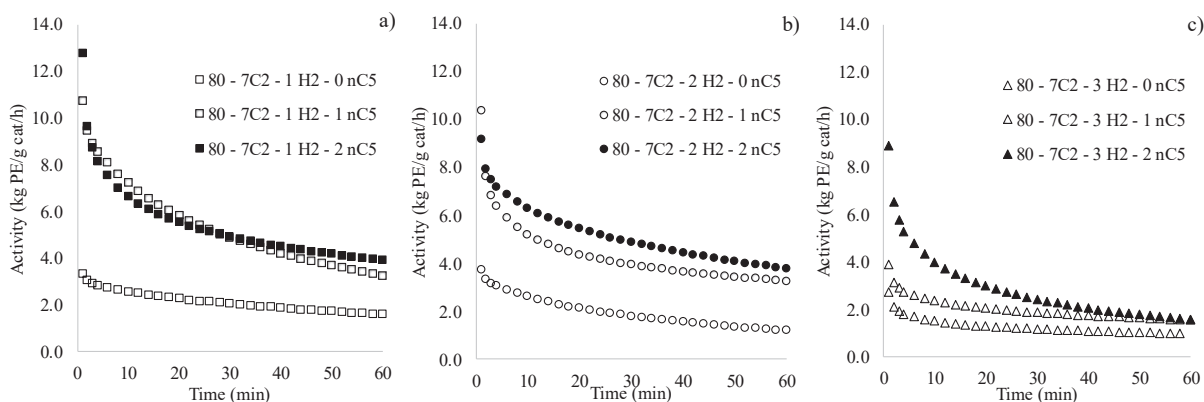


Figure 3.1 Activity of ethylene polymerization of factorial design 3^2 . Constant pressure of hydrogen a) $p_{H_2} = 1$ bar; b) $p_{H_2} = 2$ bar; c) $p_{H_2} = 3$ bar with the variation of the partial pressure of n-C5.

We can also see in these profiles that the increase of the partial pressure of n-C5, as ICA, leads to an increase of the ethylene activity which is in agreement with previous studies of our group [2].

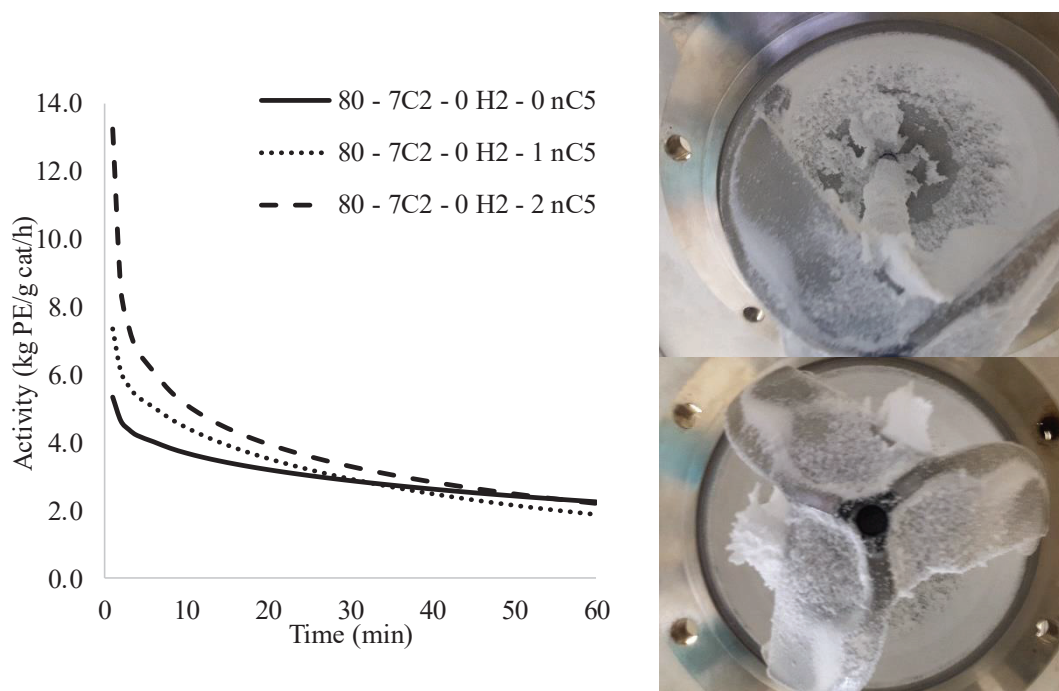


Figure 3.2 Activity of ethylene polymerization without hydrogen with 0, 1 and 2 bar nC5, as ICA.

Let us now consider similar experiments at different n-pentane partial pressure without the presence of hydrogen. As can be seen graphics in Figure 3.2, here we can clearly observe a higher activity at the beginning of the reaction with very rapid decay convergence to activity around $2.5 \text{ kg PE} \cdot \text{g cat}^{-1} \cdot \text{h}^{-1}$, independently of the pentane pressure. The polymer formed in the

reactions presents agglomerations and fouling on the reactor walls and on the agitator, which may justify a rapid decrease in activity from the beginning. The formation of melting and agglomeration can be seen in Figure 3.2. These agglomerations are more pronounced in the reactions without hydrogen, when the minimum hydrogen is added, the polymer is formed with more quality and the temperature controlled. This formation of lumps and agglomerates has a significant impact during particle growth, mass transfer rates and sorption of the monomer will have a strong influence on the rate of polymerization [15], [16]. However, if we consider the production of a quarter of the total reaction time, we can compare with the reactions in the presence of hydrogen (Figure 3.3).

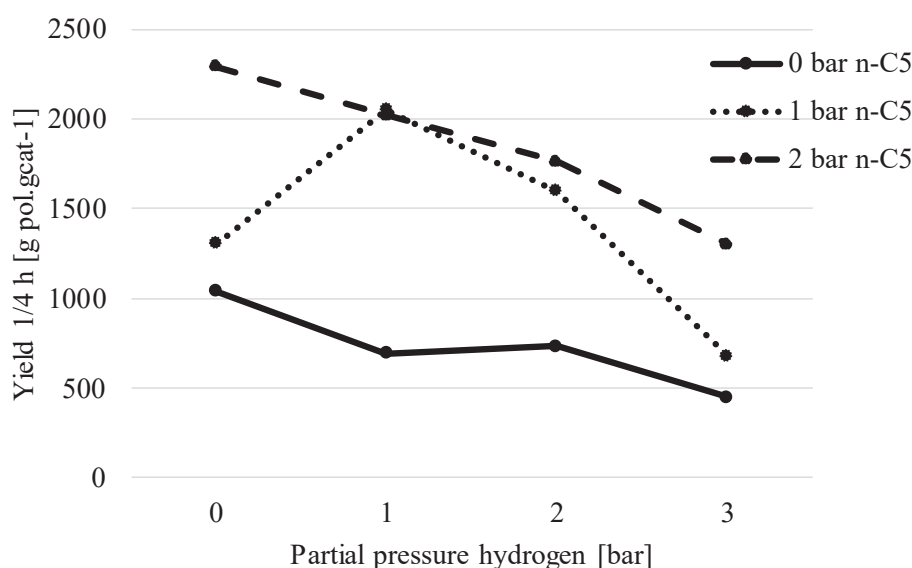


Figure 3.3 Yield at 1/4 reaction time.

About 35% of the polyethylene production in this series of experiments occurs in 1/4 of the total reaction time. Although productivity decreases with increasing H₂ / C₂ ratio, the influence of the nC₅ / C₂ ratio is quite significant. This suggests little influence of hydrogen on the co-solubility effect caused by the presence of ICA (and no impact of the ICA on the hydrogen).

The Sanchez-Lacombe state equation (SL-EOS) was used to model the hydrogen solubility in the H₂ / LLDPE binary system (Figure 3.4a) and the ethylene solubility in the Ethylene / HDPE binary system and Ethylene / Iso-pentane / HDPE ternary system (Figure 3.4b). The numerical mathematical aspects for solving this equation, as well as the related SL parameters in these

systems are detailed in Appendix II. The interaction parameters for the evaluated systems are expressed in Table 3.3, which were estimated from experimental data found in the literature.

Table 3.3 Interaction parameters.

System	Penetrant/PE	k_{ij} at 80°C	Reference experimental data
Binary	H ₂ / LLDPE	$k_{H_2,PE}$ -1.7284	[7]
	C ₂ / HDPE	$k_{C_2,PE}$ -0.0226	[17]
Ternary		k_{C_2,nC_5} 0	
	C ₂ /nC ₅ / HDPE	$k_{C_2,PE}$ -0.0223	[17]
		$k_{nC_5,PE}$ -0.0118	

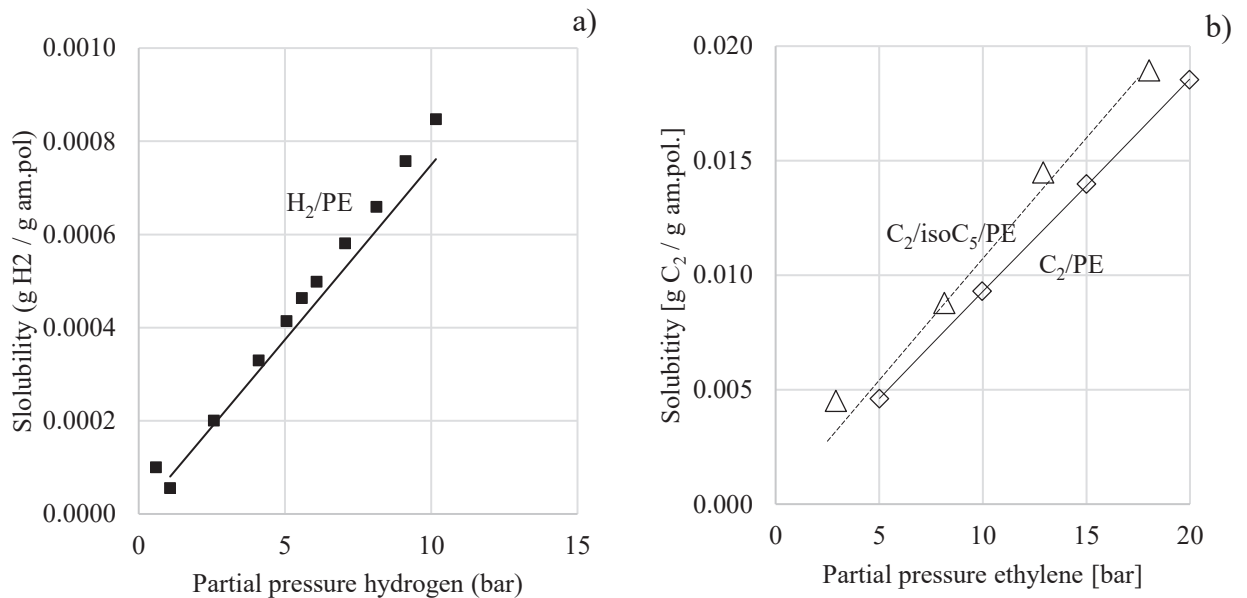


Figure 3.4 Solubility at 80°C a) Binary system to H₂/LLDPE and b) Ternary system C₂/isoC₅/HDPE.

As noted above, an evaluation of the H₂/PE binary system shows that the solubility of hydrogen in the amorphous phase is very low; on the order of 10^{-4} g_{H₂}.g_{am.pol.}⁻¹ (Figure 3.4a). In the literature there is no experimental data for H₂/C₂/PE systems, so the impact of the presence of hydrogen on the solubility of ethylene in the gas phase polyethylene is very difficult to evaluate (and probably negligible). However, there are studies that evaluate solution systems using hexane, cyclohexane or benzene, which show that there is a significant decrease in ethylene solubility upon the addition of H₂. This implies that the presence of hydrogen under polymerization conditions could decrease the ethylene concentration in the amorphous phase and thus decrease the rate of polymerization [4]. Nevertheless, we know that in the ternary

system $C_2/\text{iso}C_5/\text{PE}$, the ethylene solubility in the amorphous phase increases with respect to the C_2/PE binary system. Future solubility studies for more complex systems such as $H_2/C_2/\text{PE}$ and/or $H_2/C_2/\text{ICA}/\text{PE}$ would contribute to the evaluation of the physical effects and interactions of these components in the ethylene polymerization reaction.

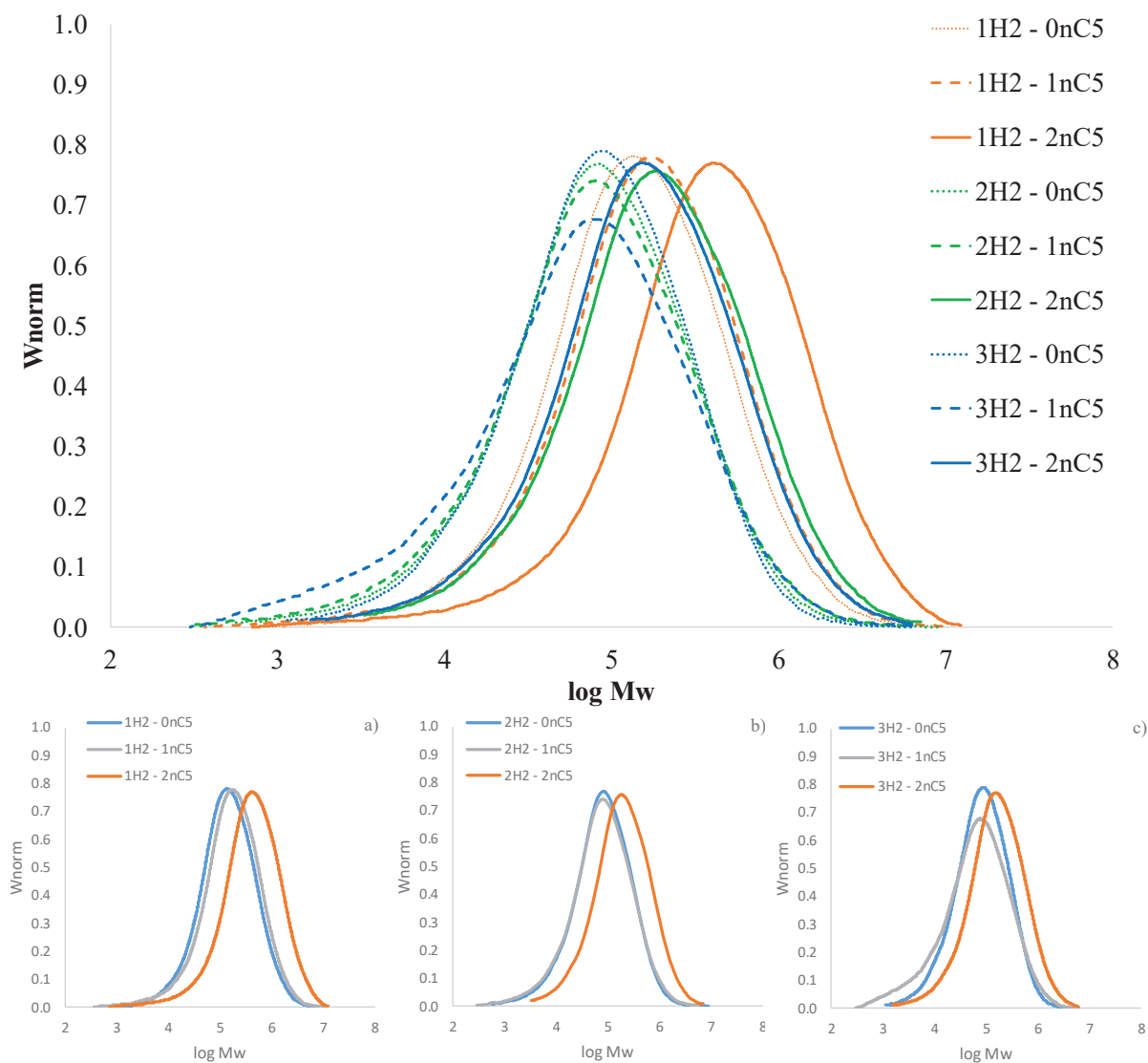


Figure 3.5 Molecular weight distribution based on the orthogonal factorial design of experiments. a) MWD to 1 bar hydrogen; b) MWD to 2 bar hydrogen and c) MWD to 3 bar hydrogen with the variation of the partial pressure of n-C5.

Figure 3.5 shows the molecular weight distributions (MWD) for the runs of the factorial design. We can divide the MWD into three groups, first a left-shift distribution with runs of greater hydrogen presence; the second group presents an intermediate distribution that demonstrates a race with the minimum of hydrogen and other races a balance between hydrogen and n-pentane; and finally a single run, 80 - 7C2 - 1H2 - 2nC5, shows an MWD displaced to the right, ie, higher

molecular weight. We can see in Figures 3.5a – 3.5c the weight-average molecular weight is increased as the ICA pressure is increased, exhibiting a more pronounced difference when the ICA pressure is equal to 3 bar. For a better understanding of the effects of the factors (hydrogen partial pressure and n-pentane) on the molecular weight, the parameters Mw and Mn will be evaluated by the statistical method. We will also do this with the crystallinity, where the average crystallization temperature is 117.5 ± 2.4 °C and the average melting temperature is 133.6 ± 0.9 °C.

The statistical analysis of the response variables of the interaction between the partial hydrogen and n-pentane pressures of the factorial design is the productivity, Mn, and Mw referring to the molecular weight and the degree of crystallinity. All data used in this study can be found in Table 3.4.

Yield

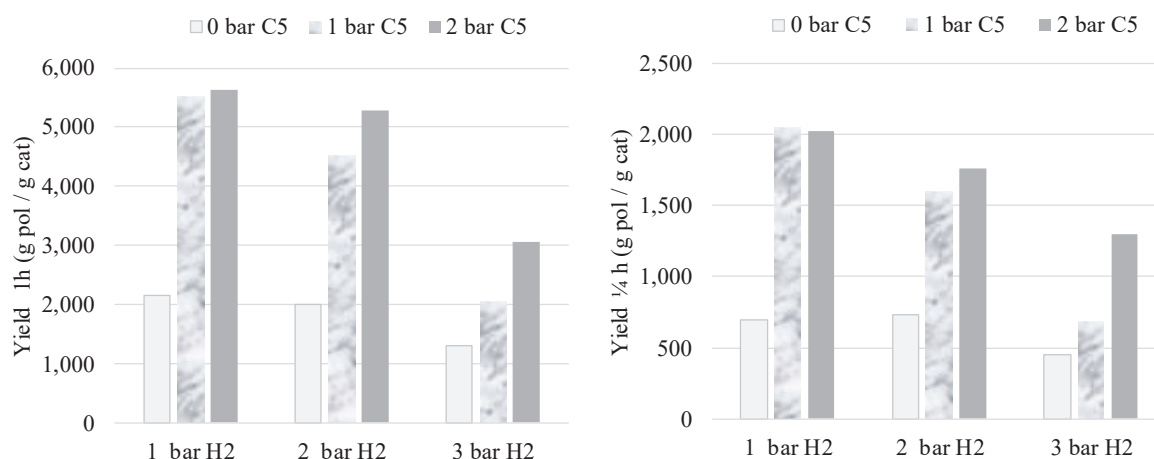


Figure 3.6 Yield to all points of orthogonal factorial design a) Yield to 1 h and b) Yield 1/4 h.

The studies of the ethylene polymerization rate performed in the presence of ICA present a common point in any operating condition, in which an increase production is observed at the beginning of the reaction [18], [19]. For this reason, the statistical analysis will take place for the total reaction time (1 hour) and 1/4 of that total time (15 min). Figure 3.6a shows productivity in one hour and Figure 3.6b shows the productivity of 1/4 h.

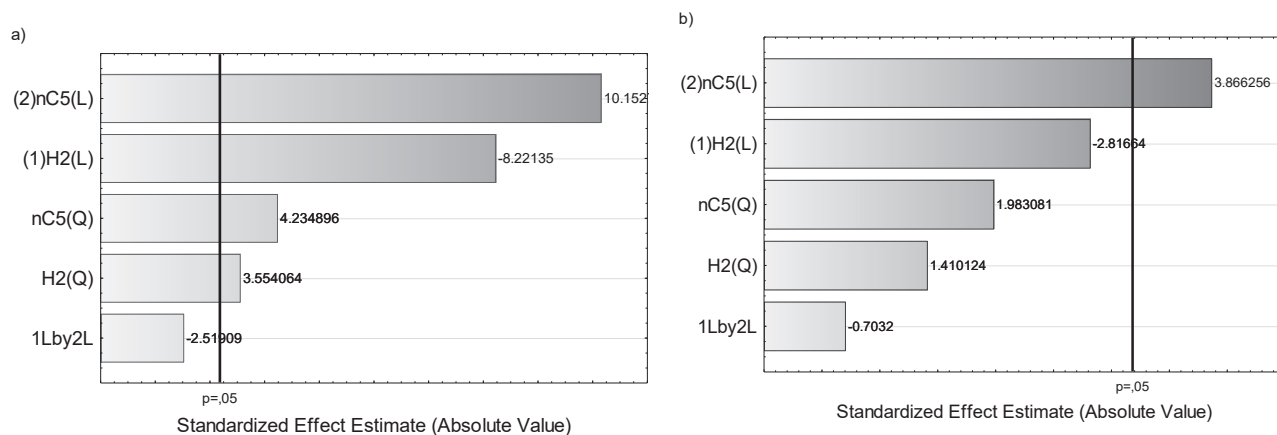


Figure 3.7 Pareto diagram to yield. a) 1 h with $R^2 = 0.9426$ and b) $\frac{1}{4}$ h with $R^2 = 0.8448$.

The regression model for 1h yield is expressed by equation 3.3 and $\frac{1}{4}$ h yield in the equation 3.4, we can see that in $\frac{1}{4}$ h of polymerization productivity is only dependent on n-C5, whereas for one hour the productivity has a negative effect of hydrogen.

$$\varphi_{1h \text{ Yield}} = 3,538 - 1,147 \cdot H_2 + 372 \cdot H_2^2 + 1,417 \cdot nC5 + 443 \cdot nC5^2 \quad (3.3)$$

$$\varphi_{\frac{1}{4}h \text{ Yield}} = 1,298 + 1,071 \cdot nC5 \quad (3.4)$$

The main effect of each factor had different results, in Figure 3.7a yield 1h shows both a positive effect of pentane and a negative effect of hydrogen. While in Figure 3.7b there is no significant effect of hydrogen during $\frac{1}{4}$ h yield, there is a permanent positive effect of n-pentane. As for the interaction of the factors, there is no significant effect, this means that in the production of ethylene polymerization under these conditions the hydrogen maintains its role as a transfer chain agent regardless of the ICA performance.

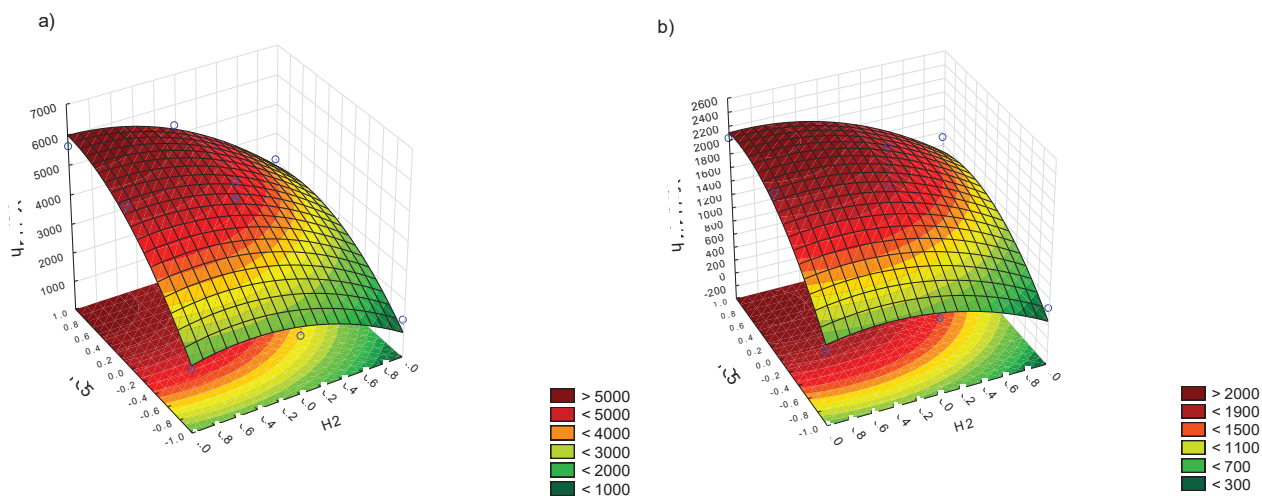


Figure 3.8 Response surface to the polymer yield. a) 1 h with $R^2 = 0.9426$ and b) $\frac{1}{4}$ h with $R^2 = 0.8448$.

Figure 3.8 shows the productivity response surface at the different reaction times as a function of the hydrogen and n-pentane factors, generated from the adjusted model. Red indicates that the factor in question has a stronger impact, and green shows an owner one. The yield of $\frac{1}{4}$ h (Figure 3.8.b) is more influenced by the effect of the n-pentane factor that is the 1h yield (Figure 3.8.a). It is also observed that the presence of hydrogen translates into lower yield (green area). This result also shows that the best yield result (both cases) is when we have the maximum of pentane (2 bar) with the minimum of hydrogen (1 bar).

Molecular weight (Mn and Mw)

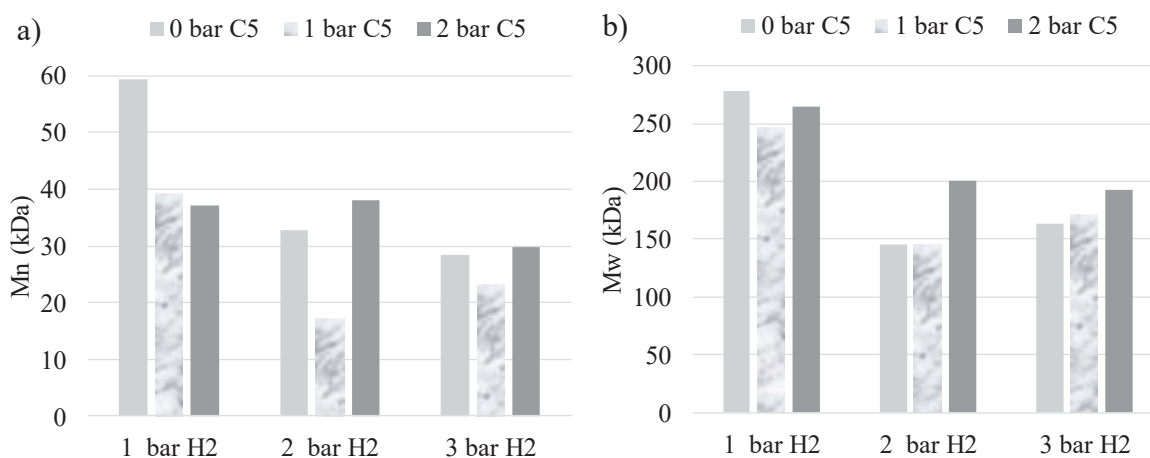


Figure 3.9 Molecular weight to all points of orthogonal factorial design a) Mn and b) Mw.

In a polymerization reaction, the chains increase in a differentiated way influenced by the reaction medium. The parameters M_n and M_w represent this characteristic that has great importance in the mechanical properties of the polymer. These values presented in Figure 3.9, in the different combinations, alone do not provide clear information about the effect of the factors.

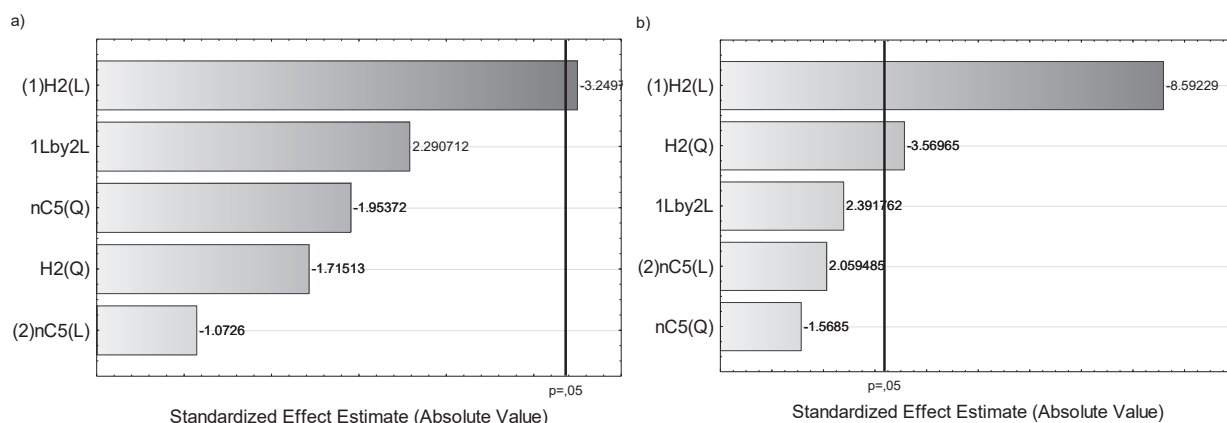


Figure 3.10 Pareto diagram to molecular weight. a) M_n with $R^2 = 0.7763$ and b) M_w with $R^2 = 0.9521$.

$$\varphi_{M_n} = 35 - 16 \cdot H_2 \quad (3.5)$$

$$\varphi_{M_w} = 203 - 99 \cdot H_2 - 31 \cdot H_2^2 \quad (3.6)$$

The second-order linear regression model for M_n is expressed by equation 3.5 and M_w in equation 3.6, both are affected only by hydrogen. Figure 3.10a shows that hydrogen has significant value on M_n , as well as on M_w , shown in Figure 3.10b. In fact, it appears from this data set that hydrogen has a stronger influence on M_w than on M_n .

The response surface for molecular weight (Figure 3.11) shows an intense influence (red region) only on the minimum value of the hydrogen factor, for both M_n and M_w . However, we can also clearly observe that the increase in the presence of hydrogen, dearly drives these quantities to decrease. Although not significant, the presence of n-pentane increases these parameters.

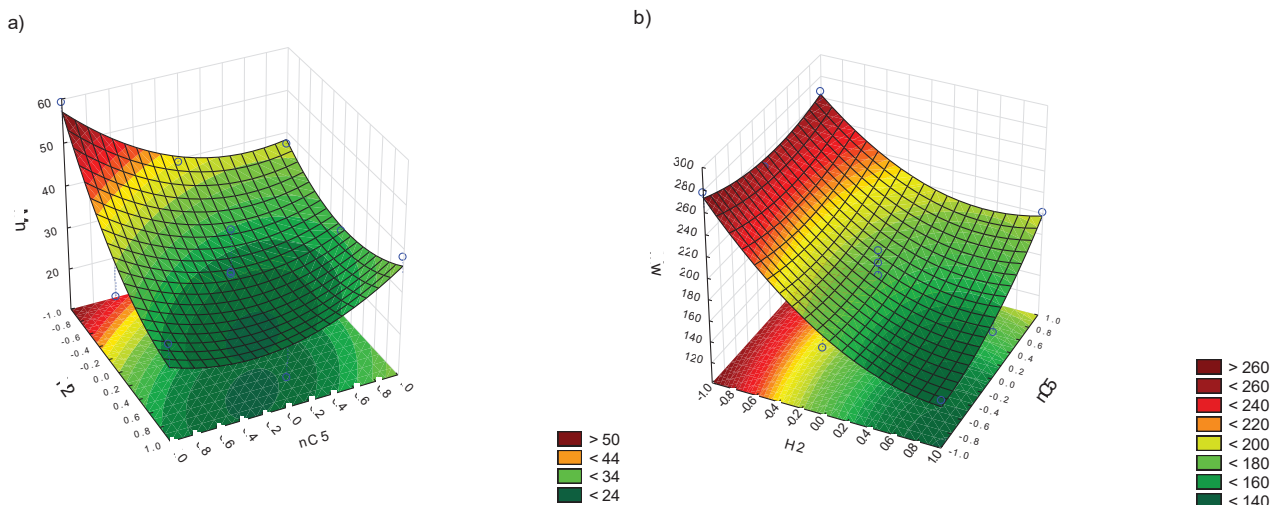


Figure 3.5. Response surface to molecular weight. a) Mn with $R^2 = 0.7763$ and b) Mw with $R^2 = 0.9521$.

For the samples of extra points 14 and 15, i.e. absence of hydrogen and partial pressure of 1 and 2 bar of n-pentane, the measured Mw was 672 and 565 kDa, respectively. While in the absence of n-pentane (sample 13), Mw is 491 kDa. These values are probably higher in reality because of the difficulty with properly diluting the samples that were discussed earlier. Nevertheless, we see that the presence of ICA increases by about 25% molecular weight. We can conclude that the increase in Mw caused by adding ICA in the absence of hydrogen is essentially negated when we add the latter.

Degree of crystallinity

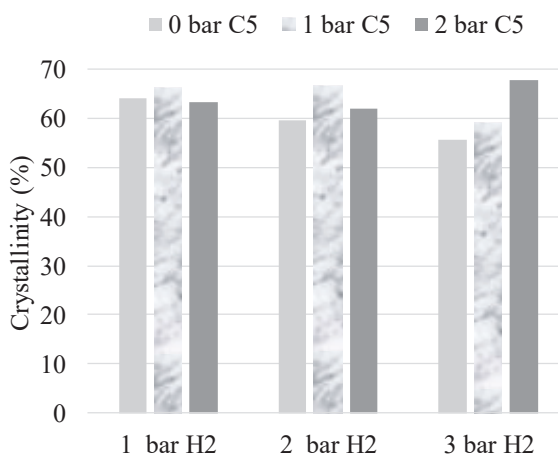


Figure 3.12 Degree of crystallinity to all points of orthogonal factorial design.

The semi-crystalline state of the polymer represents its importance as it has a significant influence on the diffusion of reactive species from the amorphous phase of polymers to the active sites of the catalyst. We know that the presence of ICA allows greater mobility of the molecules at this stage, which contributes positively to the increase of the ethylene diffusion, but the impact on the molecular organization is still little explored. The crystallinity based on DSC measurements of the polymers synthesized under the different conditions of the factorial design (Figure 3.12) varied in a narrow range of values in response to the experimental conditions adopted in the planning of experiments. The evaluation of the linear and quadratic model for crystallinity was performed. Despite improving the fit of the data from 48% to 87%, respectively, no impact of the factors on the crystallinity was observed, as we can see in Figure 3.13.

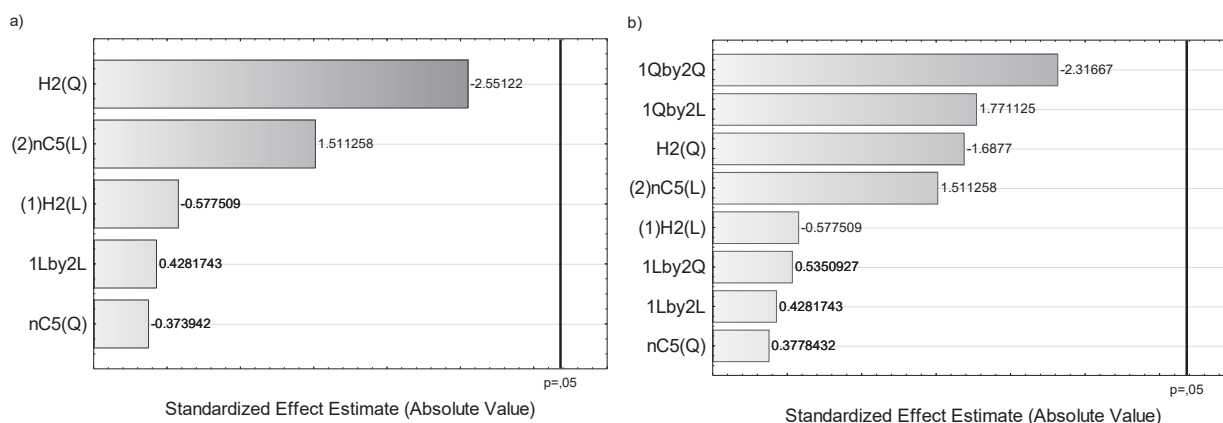


Figure 3.13 Pareto diagram to crystallinity. a) Linear model - $R^2 = 0.4826$ and b) Quadratic model - $R^2 = 0.8683$.

The pure error calculated in these linear model responses applied for yield and the molecular weight is acceptable. Indicated by the coefficient of determination R^2 of 94% for yield 1h, 84% for yield $\frac{1}{4}$ h, 78% for M_n and 95% for M_w . here values can explain when the variation around the reproducibility of the intermediate point.

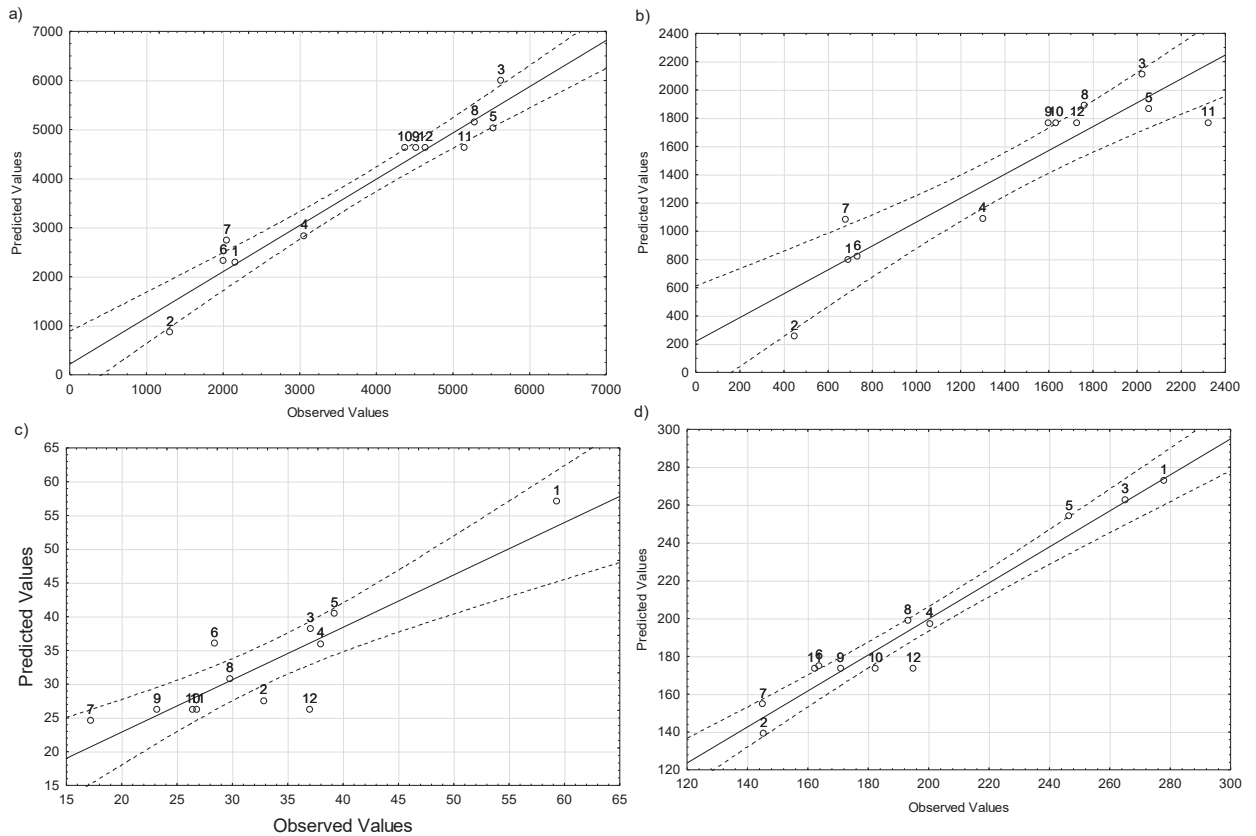


Figure 3.14 Regression model prediction. a) Yield to 1 h with $R^2 = 0.9426$, b) Yield $\frac{1}{4}$ h with $R^2 = 0.8448$, c) Mn with $R^2 = 0.7763$, d) Mw with $R^2 = 0.9521$.

The evaluation of the model can also be done by observing the predicted values versus the observed values shown in Figure 3.14. The values predicted by the model are represented by the straight line, while the observed values are represented by the points. We can observe that the predicted values approximate the observed values. The small fluctuations of the experimental points observed in the prediction of the regression model are due to the influence of the variations of the intermediate point. These experimental data present their relevance in the calculation of the experimental error of the factorial plan, which shows a good model for most of the evaluated responses.

Table 3.4 Response variables for all samples.

Run	Yield		SEC		DSC		
	¼ hour	One-hour	Mn	Mw	%w/c	T _c °C	T _m °C
	g _{pol} /g _{cat}	g _{pol} /g _{cat}	kg/gmol	kg/gmol			
80 - 7C2 - 0H2 - 0nC5	1,037	3,132					
80 - 7C2 - 0H2 - 1nC5	1,306	3,401					
80 - 7C2 - 0H2 - 2nC5	2,293	4,101					
80 - 7C2 - 1H2 - 0nC5	693	2,158	59	278	64	115	134
80 - 7C2 - 1H2 - 1nC5	2,054	5,524	39	247	62	115	133
80 - 7C2 - 1H2 - 2nC5	2,023	5,630	37	265	63	120	134
80 - 7C2 - 2H2 - 0nC5	734	2,008	28	164	60	115	134
80 - 7C2 - 2H2 - 1nC5	1,599	4,515	23	171	59	120	133
80 - 7C2 - 2H2 - 2nC5	1,763	5,286	30	193	68	120	133
80 - 7C2 - 3H2 - 0nC5	448	1,312	33	145	60	115	132
80 - 7C2 - 3H2 - 1nC5	681	2,055	17	145	56	116	132
80 - 7C2 - 3H2 - 2nC5	1,301	3,062	38	200	62	115	133
R-I: 80 - 7C2 - 2H2 - 1nC5	1,037	3,132	26	182	54	120	135
R-II: 80 - 7C2 - 2H2 - 1nC5	1,306	3,401	27	162	51	120	135
R-III: 80 - 7C2 - 2H2 - 1nC5	2,293	4,101	37	195	58	120	135
<i>Standard deviation of the intermediate point</i>	<i>468</i>	<i>549</i>	<i>5</i>	<i>12</i>	<i>3</i>	<i>0.2</i>	<i>0.7</i>

3.3. Conclusion

The homopolymerization of ethylene in the presence of hydrogen was performed in the gas phase in the presence of Induced Condensing Agents (ICA) to evaluate the interaction at different concentrations. Experimental planning and statistical analysis techniques were used to evaluate the effects and interactions of the concentration of hydrogen and n-pentane, such as ICA on polyethylene reactions. It was evaluated how these factors influence the yield and properties of polyethylene (molecular weight and crystallinity). A linear model was found to better fit the data, with a regression coefficient greater than 0.78 for all evaluated responses. The conditions of factorial design levels, the partial pressure lying in the range from 0.14 to 0.43 H₂/C₂ ratio and in the range from 0 to 0.29 for the n-C₅/C₂ ratio.

The productivity for the total reaction time (one hour) analyzed showed that there is an individual effect of hydrogen and n-pentane, but in the first 15 minutes of the reaction, only the individual effect of n-pentane is observed. Therefore, no effect of the mutual interaction between these two components was observed on productivity under the reaction conditions studied.

As for the properties, the combinations evaluated in the molecular weight only the individual effect of the hydrogen interfered the Mn and Mw. It did not the present individual effect of n-pentane nor of the mutual interaction between them. The optimum region (maximum or minimum) of the investigated response surface showed that only the minimum region of hydrogen observed the effect of any ICA concentration on the increase of Mw, which is not seen for Mn. Regarding the crystallinity of the polymer, no significant impact was observed in the data obtained from this experimental study. The crystalline total of the polymer under the conditions evaluated is on average 60%.

The experiments revealed that high concentrations of ICA cause high activity at the beginning of the reaction, having control by the presence of hydrogen with the decrease of the polymerization rate throughout the reaction. Although there is no effect on the mutual interaction between hydrogen and pentane in the response variables, the hydrogen concentration is an important variable. Affecting molecular weight and short chain branching, there is no major impact of ICA under conditions where the ICA concentration is less than the hydrogen concentration. For an ICA/C₂ ratio much larger than the H₂/C₂ ratio, the effect of ICA may interfere with the decrease of the hydrogen effect on the ethylene polymerization reactions.

Basically, what we see in all these results is that the higher the presence of hydrogen the lower the productivity and the molecular mass of the polymer and an inverse tendency when we increase the pentane concentration, therefore, there is no interaction between these components. However, for more accuracy on this system, more experiments are needed, especially in less time and with other types of ICA.

Reference

- [1] J. B. P. Soares, T. F. L. McKenna, *Polyolefin Reaction Engineering*. Weinheim, Germany: Wiley-VCH Verlag GmbH & Co. KGaA, 2012.
- [2] A. Alizadeh, T. F. L. McKenna, "Condensed Mode Cooling for Ethylene Polymerization: The Influence of the Heat of Sorption," *Macromol. React. Eng.*, vol. 8, no. 5, pp. 419–433, 2014.
- [3] C. V. L. M. V. Ker, S. Kumar Goyal, M. Kelly, Y. Jiang, "Enhanced Catalyst Productivity," US 2007/0060724 A1, 2007.
- [4] G. Sivalingam, V. Natarajan, K. R. Sarma, U. Parasuveera, "Solubility of ethylene in the presence of hydrogen in process solvents under polymerization conditions," *Ind. Eng. Chem. Res.*, vol. 47, no. 22, pp. 8940–8946, 2008.
- [5] M. C. Kane, "Permeability, Solubility, and Interaction of Hydrogen in Polymers- An Assessment of Materials for Hydrogen Transport," p. WSRC-STI-2008-00009, Rev. 0, 2008.
- [6] F. Reinertz, T. Schober, W. A. Oates, and H. Wenzl, "Solubility of Hydrogen in NiAl," *Z. für Phys. Chem.*, vol. 183, no. 2, p. 99, 1994.
- [7] J. Sun, H. Wang, M. Chen, J. Ye, B. Jiang, J. Wang, Y. Yang, C. Ren, "Solubility measurement of hydrogen, ethylene, and 1-hexene in polyethylene films through an intelligent gravimetric analyzer," *J. Appl. Polym. Sci.*, vol. 134, no. 8, pp. 1–7, 2017.
- [8] A. R. Martins, A. J. Cancelas, T. F. L. McKenna, "A Study of the Gas Phase Polymerization of Propylene: The Impact of Catalyst Treatment, Injection Conditions and the Presence of Alkanes on Polymerization and Polymer Properties," *Macromol. React. Eng.*, vol. 11, no. 1, pp. 1–14, 2017.
- [9] G. E. P. Box, W. G. Hunter, J. S. Hunter, *Statistics for experimenters: an introduction to design, data analysis, and model building*. Wiley, 1978.
- [10] G. E. P. Box, K. B. Wilson, "On the Experimental Attainment of Optimum Conditions," *Journal of the Royal Statistical Society. Series B (Methodological)*, vol. 13. WileyRoyal Statistical Society, pp. 1–45, 1951.
- [11] J. M. Jenkins, L. Russell, T. M. Jones, "Fluidized Bed Reaction Systems," US 4543399, 1985.
- [12] S. B. J.M. Jenkins III, R.L. Jones, T.M. Jones, "Method for fluidized bed polymerization," US 4588790, 1986.

- [13] A. M. A. L. Duarte Bragança, A.L. Ribeiro de Castro Morschbaker, E. Rubbo, N. Cid Miro, T. Barlem, “Process for gas phase polymerization and copolymerization of olefin monomers,” EP001246853B1, 2004.
- [14] T. KOCIAN, Harvey; REBHAN, David; PARRISH, John; PILGRAM, “Control of gas phase polymerization reactions,” EP1000097B1, 2002.
- [15] T. F. L. McKenna, “Growth and evolution of particle morphology: An experimental & modeling study,” *Macromol. Symp.*, vol. 260, pp. 65–73, 2007.
- [16] C. Martin, T. F. McKenna, “Particle morphology and transport phenomena in olefin polymerization,” *Chem. Eng. J.*, vol. 87, no. 1, pp. 89–99, 2002.
- [17] W. Yao, X. Hu, Y. Yang, “Modeling the solubility of ternary mixtures of ethylene, isopentane, n-hexane in semicrystalline polyethylene,” *J. Appl. Polym. Sci.*, vol. 104, no. 6, pp. 3654–3662, Jun. 2007.
- [18] A. Alizadeh, M. Namkajorn, E. Somsook, T. F. L. McKenna, “Condensed Mode Cooling for Ethylene Polymerization: Part II. From Cosolubility to Comonomer and Hydrogen Effects,” *Macromol. Chem. Phys.*, no. 216, pp. 985–995, 2015.
- [19] F. N. Andrade, T. F. L. McKenna, “Condensed Mode Cooling for Ethylene Polymerization: Part IV. The Effect of Temperature in the Presence of Induced Condensing Agents,” *Macromol. Chem. Phys.*, vol. 218, no. 20, pp. 1–8, 2017.
- [20] M. Namkajorn, A. Alizadeh, D. Romano, S. Rastogi, T. F. L. McKenna, “Condensed Mode Cooling for Ethylene Polymerization: Part III. The Impact of Induced Condensing Agents on Particle Morphology and Polymer Properties,” *Macromol. Chem. Phys.*, vol. 217, no. 13, pp. 1521–1528, 2016.

Chapter 4

The impact of Induced Condensing Agents in the presence of a comonomer

Abstract: Gas phase copolymerizations of ethylene were performed using a commercial Ziegler-Natta catalyst in the presence of n-pentane as an Induced Condensing Agent (ICA). Experimental design and statistical analysis techniques were used to evaluate the effect of independent factors on the response variables. The impact of these factors the yield and final polyethylene properties such as the average molecular weights, crystallinity, and incorporation of comonomer (CH₃/1000C) was studied. It has been shown that the comonomer effect is more intense in the presence of ICA. It showed what cosolubility and comonomer effects are additive. It also appears that adding ICA to the copolymerizations changes the comonomer incorporation with respect to similar copolymerizations performed without ICA. It is postulated that when the ICA is lighter than the comonomer, it has an antisolvent effect on the better, leading to an increased ethylene/comonomer ratio at the active sites and thus a higher crystallinity. When n-hexane is used as ICA, it appears that its cosolubility effect on ethylene also leads to a higher ethylene/comonomer ratio at the active sites, and thus a lower number of CH₃ per 1000 carbons than in dry mode.

4. INTRODUCTION

Linear low-density polyethylene (LLDPE) is produced using α -olefin comonomers, to provoke the formation of short chain branching. Commonly used α -olefins include 1-butene, 1-hexene, 1-octene and 4-methyl-1-pentene [1]. The main effect of the copolymer on the final is the reduction of crystallinity and the melting temperature of the final polymer [2]. Another observed effect is the rate-enhancement, seen when a moderate amount of α -olefin comonomers are present; known as “comonomer effect”, which can be seen in different catalysts, processes, including different types of polymers [3]–[9].

For some authors, it is generally agreed that the comonomer effect can be argued for by : i) decrease in crystallinity around the catalyst a polymer layer is formed by incorporation of α -olefin into the polymer matrix, allowing the monomers to diffuse more easily; [10]–[12]; ii) structural change, i.e., an increase in the porosities of the growing particles [10], [13], [14] and iii) formation of new active sites with more suitable binder due to the stronger coordination of

α -olefin [15], [16], related to the “trigger mechanism” as proposed by Steven [17]. Mc Daniel [18] rigorously evaluated the comonomer effect on chromium polymerization catalysts in which he concluded that the effect is more associated with the change in the chemistry of the active sites in the coordination of the electron-rich α -olefin. However, studies with different α -olefin comonomers/ethylene ratios [19], [20] show that high concentrations of comonomer resulted in a decreasing rate of ethylene consumption. Lower reactivity may occur with increasing length of the olefin chain.

Although the solubility of comonomers in different polymers has been widely studied for binary systems (1 polymer + 1 penetrant) for both molten and solid polymers, there is little information available for multiple penetrants in the gas phase [21] – [27]. The solubility of α -olefin comonomers in polymers increases as the size of the molecules increases and is inversely proportional to temperature, similar to what is observed for alkane solubility. For multicomponent systems, Sun et al. [28] evaluated ethylene/1-hexene/LLDPE system and concluded that the co-solubility measured in a gas mixture is almost 10% smaller than the sum of the pure-component solubilities under the same conditions but in a binary system.

The impact of combining induced condensing agents (ICA) and comonomers was studied experimentally by Alizadeh et al. [29], who evaluated the effect of n-hexane partial pressure on the formation of poly(ethylene-co-1-hexene). Figure 4.1 shows the average catalytic activity for a two-hour polymerization as a function of the partial pressure of n-hexane and/or 1-hexene. The ICA increases the rate of polymerization when its concentration is increased; while the comonomer effect is seen only in the presence of 0.3 and 0.8 bar of 1-hexene, but not at 0.6 bar of 1-hexene (this is likely an outlier as there is no particular reason for that data point to not follow the trend). However, the rate in the presence of 0.6 bar of 1-hexene and 0.6 bar of n-hexane is observed an increase factor of about 1.5. This implies that the presence of ICA in the copolymerization plays a fundamental role in physical phenomena, therefore it may interfere with the chemical phenomena observed in the copolymer reactions.

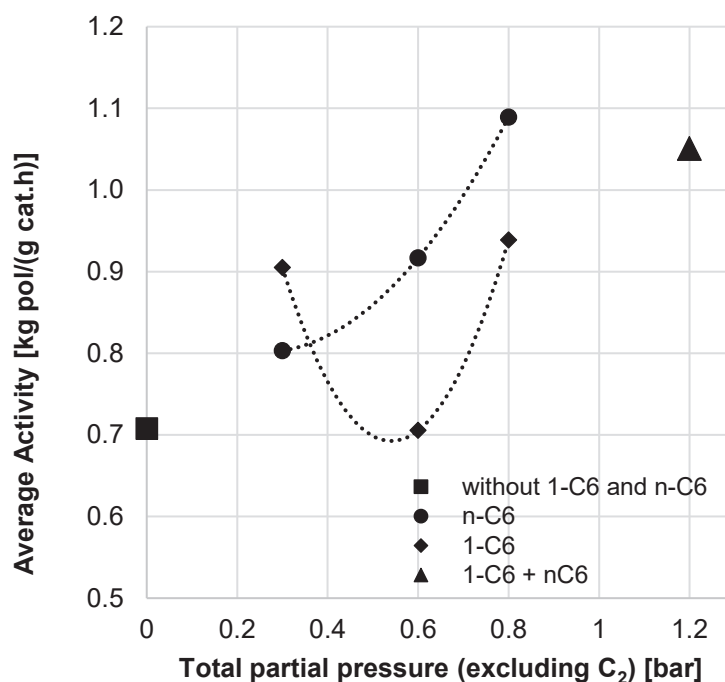


Figure 4.1 Two hours of productivity with n-hexane and 1-hexene. Experimental data are taken from Alizadeh et al. [29].

In order to better elucidate any eventual interactions of ICA and comonomers, experimental design and statistical analysis were proposed to study their impact on the rate of polymerization and some physical properties.

4.1. Experimental section

4.1.1. Materials

Ethylene with a minimum purity of 99.5% was obtained from Air Liquide (Paris, France) and was passed over purifying columns of zeolite and active carbon before use. Hydrogen and argon with a minimum purity of 99.5% (Argon used to keep the reaction environment free of oxygen and other impurities) was obtained from Air Liquide and used as received. Comonomers 1-Butene minimum purity of 99% was obtained from Air Liquide and 1-Hexene minimum purity of 97% was obtained from Sigma-Aldrich ICN (Germany). As ICA, anhydrous n-pentane (minimum purity 99%, from Sigma-Aldrich ICN - Germany) and propane with a minimum purity of 99.5 % from Air Liquide. Triethylaluminium (TEA) co-catalyst was obtained from Witco (Germany). A commercial TiCl₄ supported on MgCl₂ Zeigler-Natta catalyst was used as

the catalytic system for all polymerizations. Sodium chloride (NaCl) with a minimum purity of 99.8% and used as a seedbed to disperse the catalyst particles.

4.1.2. Copolymerization and copolymer characterization

The ethylene copolymerization synthesis protocol is described in Appendix I, along with the characterization methodologies. The copolymers were characterized in terms of their average molecular weights and molecular weight distribution (MWD) by size exclusion chromatography (SEC), the crystallization and the melting temperatures using differential scanning calorimetry (DSC), and crystallization elution fractionation (CEF) analyses were performed to evaluate the presence of comonomers in the synthesized copolymer.

4.1.3. Experimental design

An orthogonal factorial design consisting of three-level factorial design and two independent variables (partial pressure of 1-butene and n-pentane) and six extra conditions, was used to study of a variation of ICA/comonomer species (pentane/1-hexene and propane/1-butene), as shown in Tables 4.1 and 4.2.

The factorial design allows a qualitative evaluation of the effect of factors (independent variables) on the response variables (copolymerization yield, average molecular weights, crystallinity, melting temperature and comonomer incorporation with $\text{CH}_3/1000\text{C}$). The number of experiments with all combinations will be from nine experimental trials based on a 3^2 factorial design to characterize the behavior of ethylene polymerizations and provide important information about the effect of independent variables on the properties of the polymer. The extra conditions will be used to evaluate the influence of ICAs in a reaction where the comonomer has a lower molecular weight than the ICA.

Table 4.1 3² Factorial design.

Variable		Level		
		-1	0	1
		Low	Middle	High
x ₁ =	p 1-C ₄ [bar]	0	1	2
x ₂ =	p n-C ₅ [bar]	0	1	2

The experimental limits for the independent variables were defined based on patents [30 – 34]. Based on the conditions of factorial design levels, the partial pressure ratios should lie in the range from 0 to 0.29 for 1-C₄ / C₂ and n-C₅ / C₂. The experiments were performed in random order and the ethylene pressure (7 bar), hydrogen pressure (1 bar) and reactor temperature (80 °C), were kept constant for all experimental conditions. The presence of 1 bar of hydrogen is kept constant since there was no significant impact on the corelacao H₂-ICA for this catalyst, as seen in chapter 3 of this study. The presence of hydrogen is also important to avoid too many changes, but also too keep Mw easily measurable range, in addition to what is approaching the industrial conditions.

Table 4.2 Operation conditions for different runs.

N°	Matriz experimental		Run name ^{a)}	p 1-C ₄	p n-C ₅	Partial pressure ratio	
	x ₁	x ₂		[bar]	[bar]	P _{C₂} / P _{C₂}	P _{ICA} / P _{C₂}
1	-1	-1	80 - 7C2 - 1H2 - 0 1-C4 - 0 nC5	0	0	-	-
2	1	-1	80 - 7C2 - 1H2 - 2 1-C4 - 0 nC5	2	0	0.29	-
3	-1	1	80 - 7C2 - 1H2 - 0 1-C4 - 2 nC5	0	2	-	0.29
4	1	1	80 - 7C2 - 1H2 - 2 1-C4 - 2 nC5	2	2	0.29	0.29
5	-1	0	80 - 7C2 - 1H2 - 0 1-C4 - 1 nC5	0	1	-	0.14
6	0	-1	80 - 7C2 - 1H2 - 1 1-C4 - 0 nC5	1	0	0.14	-
7	1	0	80 - 7C2 - 1H2 - 2 1-C4 - 1 nC5	2	1	0.29	0.14
8	0	1	80 - 7C2 - 1H2 - 1 1-C4 - 2 nC5	1	2	0.14	0.29
9	0	0	80 - 7C2 - 1H2 - 1 1-C4 - 1 nC5	1	1	0.14	0.14
10	-	-	80 - 7C2 - 1H2 - 0.8 1C6 - 0 nC5	0.8	0	0.11	-
11	-	-	80 - 7C2 - 1H2 - 0.8 1C6 - 1 nC5	0.8	1	0.11	0.14
12	-	-	80 - 7C2 - 1H2 - 0.8 1C6 - 2 nC5	0.8	2	0.11	0.29
13	-	-	80 - 7C2 - 1H2 - 1 1-C4 - 5 nC3	1	5	0.14	0.71
14	-	-	80 - 7C2 - 1H2 - 1 1-C4 - 10 nC3	1	10	0.14	1.43
15	-	-	80 - 7C2 - 1H2 - 1 1-C4 - 15 nC3	1	15	0.14	2.14

^{a)} Sequence sample: Temperature [°C] - Ethylene pressure - Hydrogen pressure - Comonomer pressure - ICA pressure [bar]

The treatment of the factorial design was performed using multiple regression to estimate the parameters related to the isolated variables, their interactions, and the quadratic terms. The second-order linear regression model for general factorial design is presented in more detail in Appendix III.

4.2. Results and discussion

4.2.1. Ethylene / 1-butene copolymerizations in the presence of n-pentane

Rate of polymerization and yield

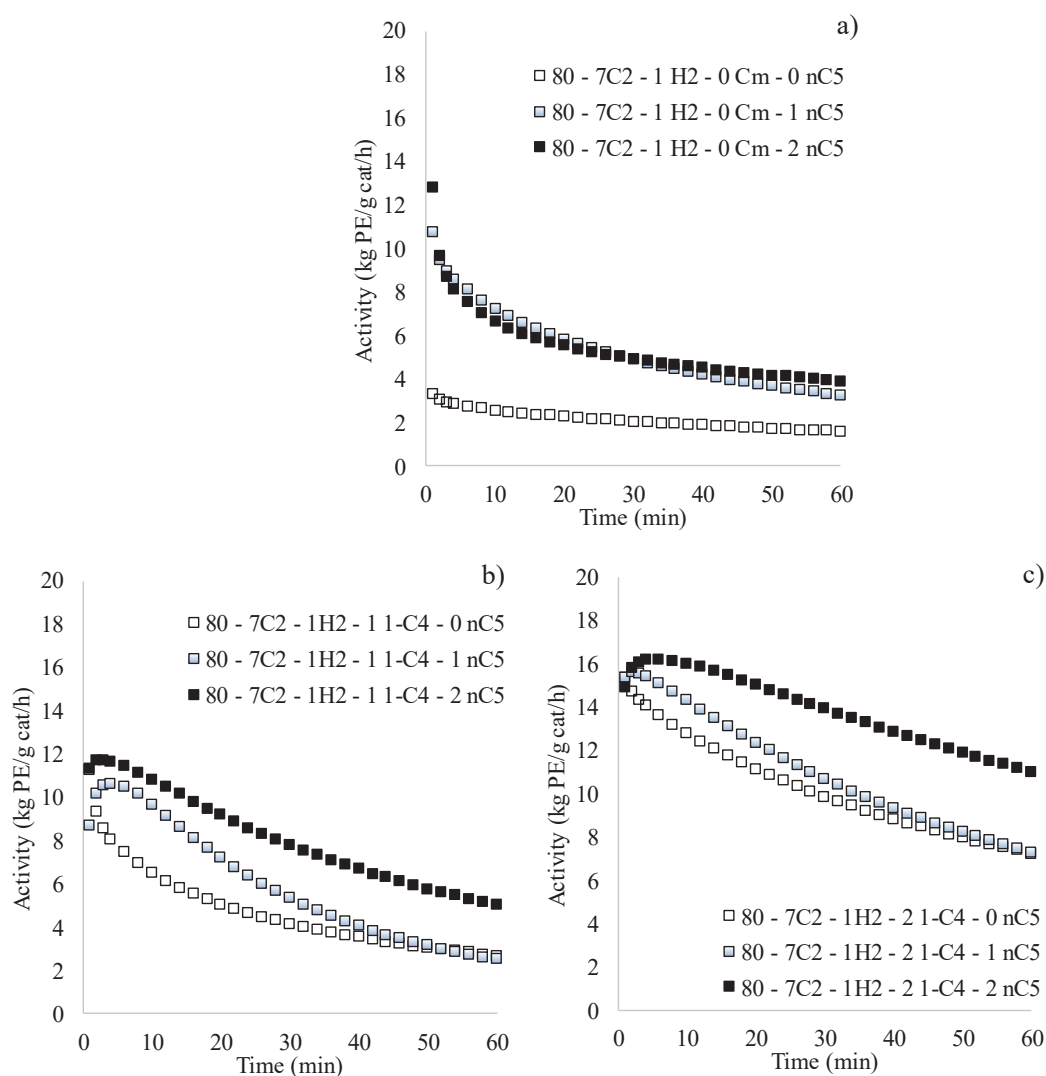


Figure 4.2 Rate of ethylene polymerization: a) Without comonomer, b) 1 bar of 1-butene and c) 2 bar of 1-butene.

The copolymerization rates a function of time are shown in Figure 4.2, where we can see the combined influence of changing the comonomer and ICA partial pressure. Figure 4.2a shows the effect of the presence of n-pentane, as the ICA in the absence of a comonomer, at higher pressures one observes an increase of 2.6 times in the rate with respect to the rate found in the absence of ICA. Unexpectedly, there is little difference in the polymerization rates at 1 and 2 bar of n-pentane (n-C5) - this is most likely due to some experimental error. Notice that the comonomer and ICA curves show different activation this then just ICA or just comonomer. While this is out of the scope of the current work, one could postulate that this might be due to different fragmentation behavior in the owner of the softest polymers. Figure 4.2b and 4.2c show the impact of the variation of n-C5 in the presence of 1 bar and 2 bars of 1-butene (1-C4), respectively. Once again, increases the n-C5 levels leads to an increase in the polymerization rate for a given concentration of 1-C4. The comonomer effect is visible from the rates with a comonomer and no n-C5. Furthermore, this series of graphs also shows a combined effect of n-C5 plus 1-C4, where they both increase the polymerization rate in a similar manner.

To evaluate the comonomer and ICA effects we will use the polymer yield as a response factor in the statistical analysis. The Pareto diagram for a one-hour yield of copolymerization (Figure 4.3a) shows that there is a statistically significant impact of the individual effects of n-C5 and 1-C4, the comonomer effect being about twice as significant as the ICA effect, but also that there is no statistically significant effect of the mutual interaction of the species. In other words, the effects on the yields appear to be additive.

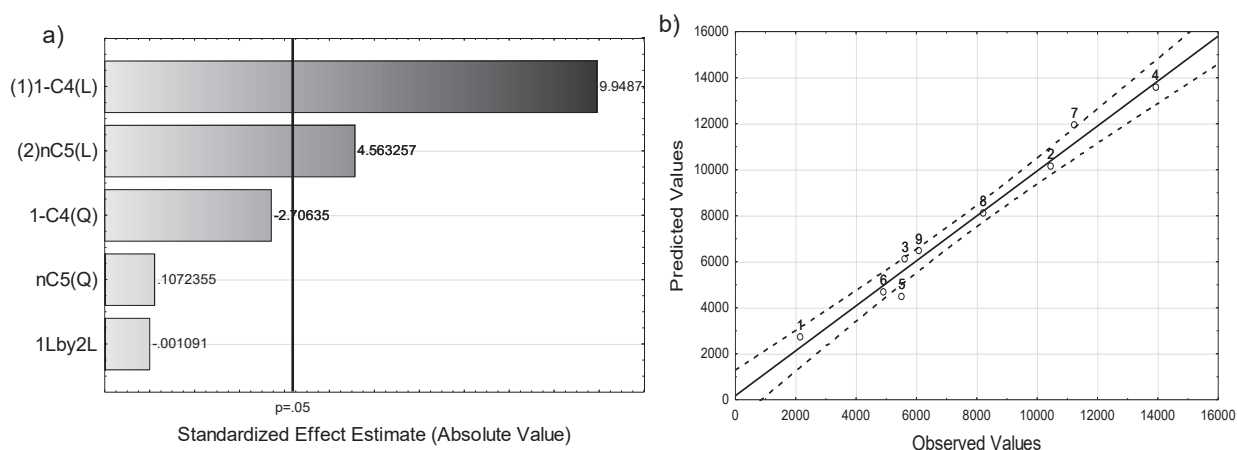


Figure 4.3 a) Pareto diagram and b) regression model prediction to one-hour - $R^2 = 0.9770$.

Based on the Pareto diagram and the regression models, the polymerization rates are strongly dependent on 1-C4 and n-C5, both contributing positively to the polymer yield (ϕ). Figure 4.3b illustrates the regression model prediction, which agrees very well with the experimental data, expressing a correlation coefficient (R^2) equal to 97.70%. Equation 4.1 used to describe the behavior of the polymer yield considers a 95.0% confidence interval along with the terms statistically significant.

$$\phi_{1h\ yield} = 7,575 + 3,723 \cdot 1-C4 + 1,708 \cdot nC5 \quad (4.1)$$

In recent studies, we saw that the ICA effect is much more pronounced at the beginning of the reaction and in these copolymerizations, the 1-C4 / C2 ratio in the gas phase of the reactor decreases with the reaction time, so it is reasonable to perform a yield analysis at the beginning of the reaction [36]. Then a study of the effects on yield to ten minutes of reaction can be seen in Figure 4.4.

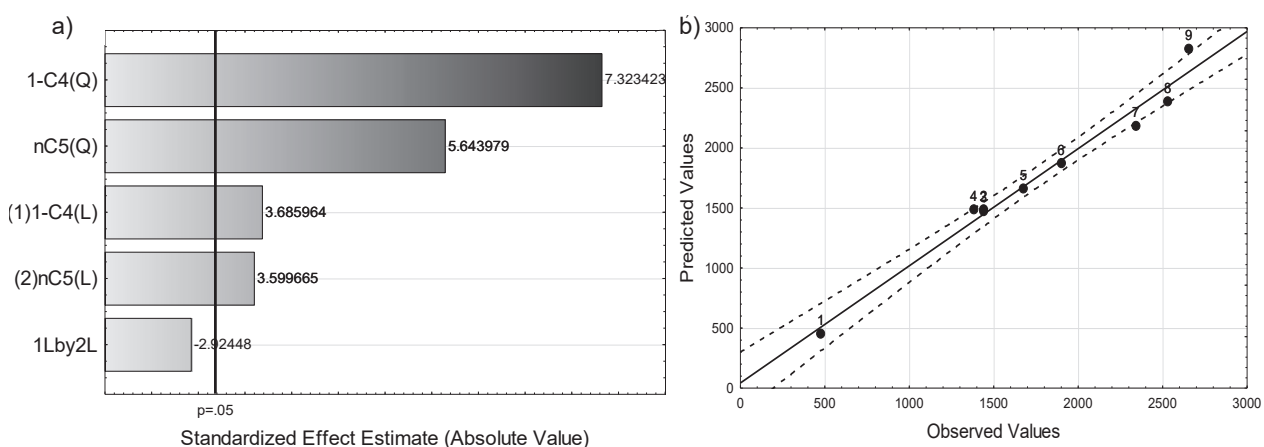


Figure 4.4 a) Pareto diagram and b) regression model prediction to ten minutes yield - $R^2 = 0.9757$.

As can be observed in Figure 4.4a, the main effects of 1-C4 (positive) and nC5 (positive), the quadratic effects of 1-C4 (positive) and nC5 (positive) were significant. The polymer yield in 10 minutes of reaction there is a smaller proportion between comonomer effect and ICA effect than Figure 4.3a.

$$\phi_{10\ min\ yield} = 1,760 + 525 \cdot 1-C4 + 903 \cdot 1-C4^2 + 512 \cdot nC5 + 696 \cdot nC5^2 \quad (4.2)$$

The proposed model for describing the polymer yield with 95% confidence interval is given by Equation 4.2, considering all significant independent variables, binary interactions of variables, and the quadratic contributions of the independent variables. Figure 4.4b portrays the quality of regression model prediction, which agrees very well with the experimental data, exhibiting a good correlation coefficient (R^2) of 97.57%.

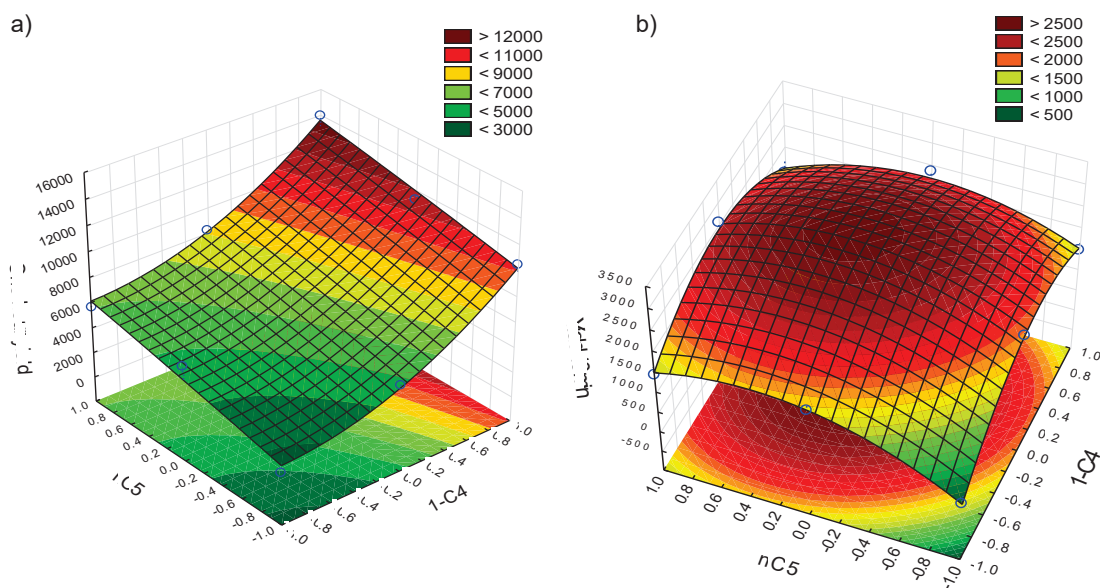


Figure 4.5 Response surface to yield. a) One-hour yield and b) Yield to 10 minutes.

When the yield response surface is observed between one hour and 10 minutes of copolymerization in Figure 4.5 it is clear that the ICA has a strong impact in 10 minutes of reaction (Figure 4.5b), where the red region represents the value of statistical relevance. Figure 4.5a, the one-hour yield is more pronounced for a greater amount of comonomer (2 bar of 1-C4) and an impact of the presence of ICA is observed, with an increase in yield from about 10,000 to 14,000 g_{pol}/g_{cat} . This impact is even greater in the yield in 10 minutes, as seen in Figure 4.4b, where an optimum region, productivity greater than 2,500 g_{pol}/g_{cat} in 10 minutes, can be seen at the same ratio of 1-C4/n-C5 between the range of partial pressure of 0.4 – 1.4 bar.

The results of the characterization of the copolymer samples will be presented in Table 4.3 and parameters of the analyses were evaluated with statistical methods to evaluate the impact of the ICA.

Table 4.3 Characterization of the copolymer.

Run	SEC			%wt insoluble	%wc	DSC				CEF	
	Mn kDa	Mw kDa				T _{c on} °C	T _c °C	T _{c end} °C	T _m °C	CH ₃ / 1000C	T _{elution} °C
80 - 7C2 - 1H2 - 0 1-C4 - 0 nC5	75	247		18	64	119	115	107	134		
80 - 7C2 - 1H2 - 0 1-C4 - 1 nC5	70	234		21	63	118	114	106	132		
80 - 7C2 - 1H2 - 0 1-C4 - 2 nC5	82	248		15	66	118	115	107	133		
80 - 7C2 - 1H2 - 1 1-C4 - 0 nC5	29	146		16	36	115	112	108	124	5.7	106.8
80 - 7C2 - 1H2 - 1 1-C4 - 1 nC5	32	159		11	53	116	113	108	125	3.7	107.8
80 - 7C2 - 1H2 - 1 1-C4 - 2 nC5	35	158		27	52	116	114	109	126	3.4	108.6
80 - 7C2 - 1H2 - 2 1-C4 - 0 nC5	66	240		23	37	112	109	103	122	5.4	107.6
80 - 7C2 - 1H2 - 2 1-C4 - 1 nC5	64	240		24	37	112	109	104	123	5.5	106.7
80 - 7C2 - 1H2 - 2 1-C4 - 2 nC5	27	146		25	46	115	113	109	125	4.0	107.6

Molecular weight

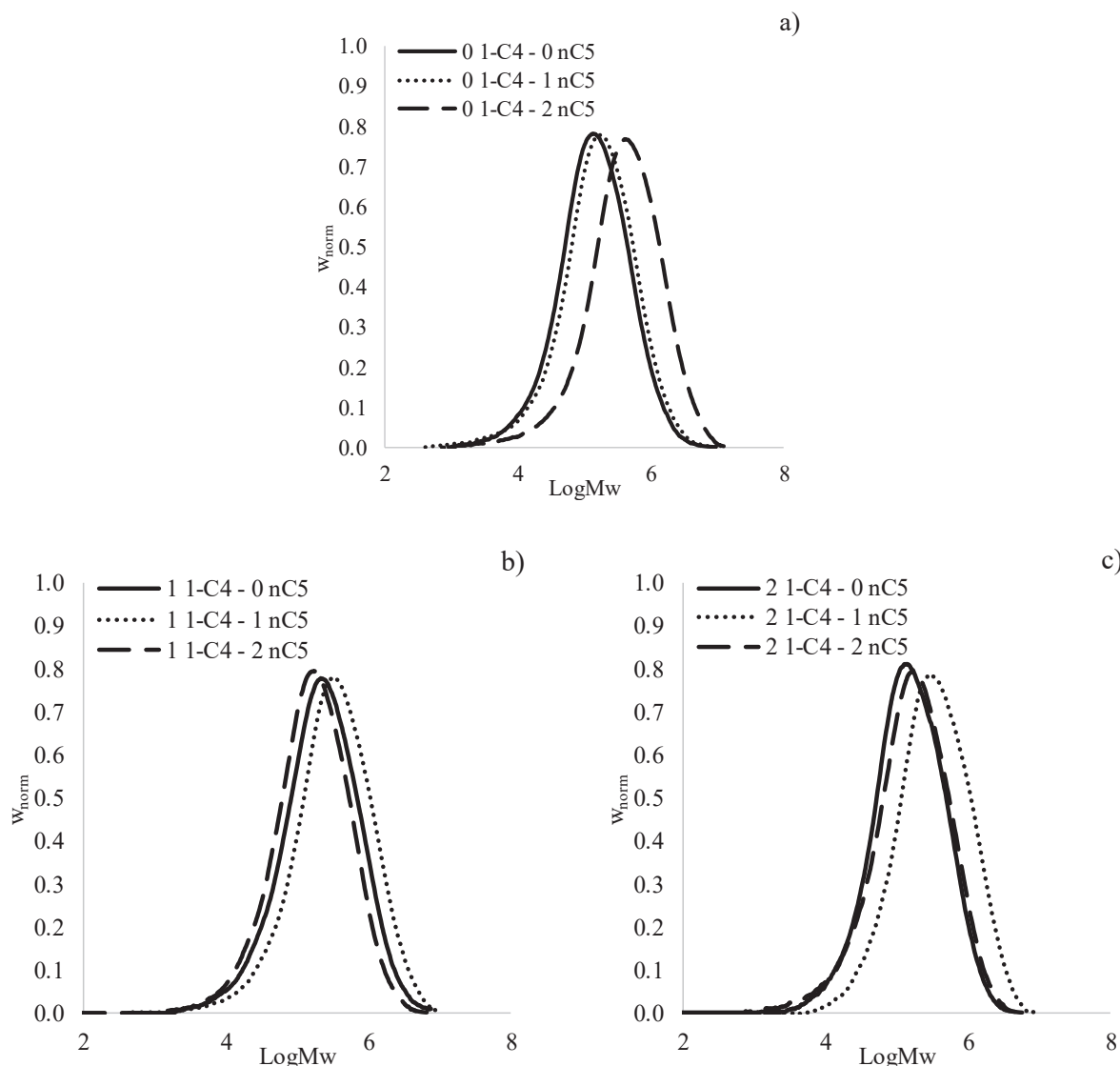


Figure 4.6 Molecular weight distribution. a) 0 bar 1-C4, b) 1 bar 1-C4 and c) 2 bar 1-C4.

In order to compare the MWD essays were carried out based on the factorial design conditions as shown in Figure 4.6. It is observed that the presence of ICA in the copolymerization does not have the same tendency as in homopolymerization (Figure 4.6a). The increase of the ICA concentration on homopolymerization shows an increase in molecular weight. On the other hand, for the copolymers (Figure 4.6b and 4.6c), the MWD obtained with 2 bar of nC5 approaches the MWD of the comonomer without nC5. While the MWD profile increases in comonomers obtained in the presence of 1 bar nC5.

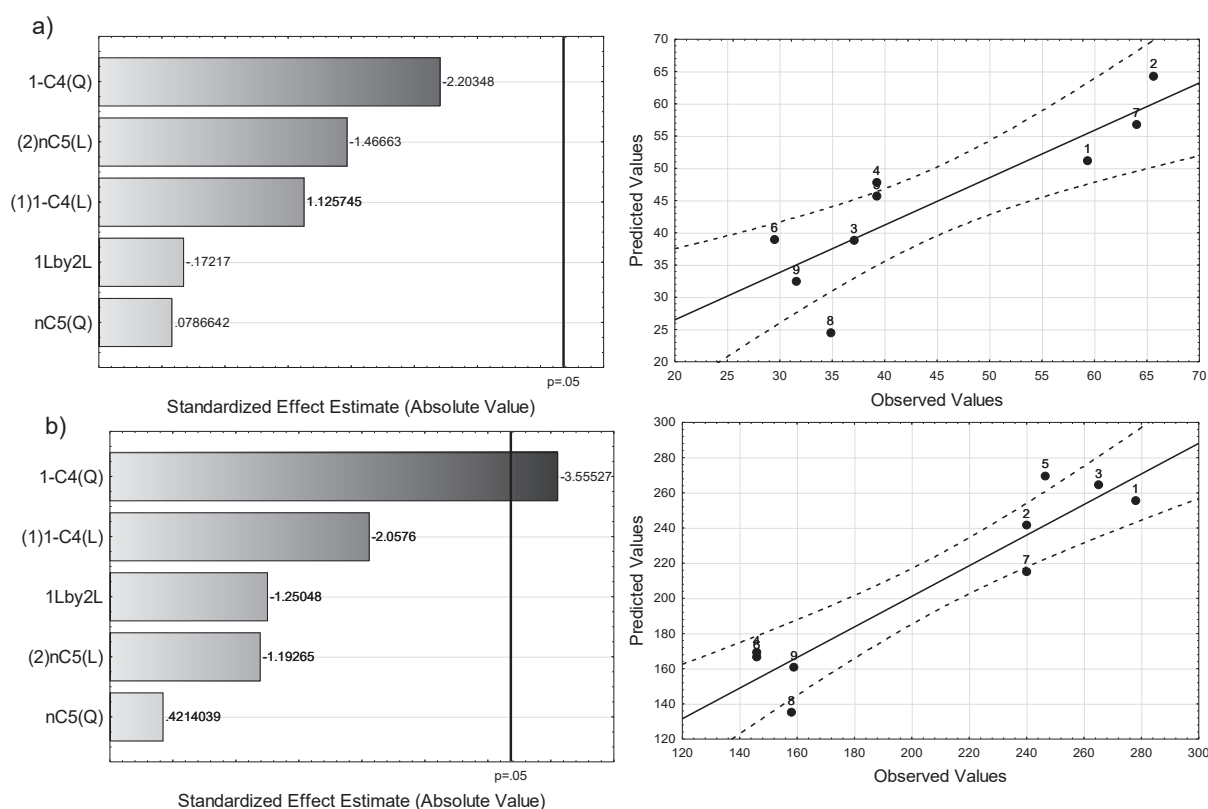


Figure 4.7 Pareto diagram and regression model prediction to molecular weight: a) Mn - $R^2 = 0.7347$ and b) Mw - $R^2 = 0.8698$.

The Pareto diagram shown in Figure 4.7 shows a single linear effect of the comonomer on Mw for the copolymers formed, with no significant impact of ICA or mutual interaction between species. The evaluation of the model can also be done by observing the regression model (Equation 4.3) with a correlation coefficient of 86.98%. Mn has nevertheless a correlation coefficient low, with no effect of ICA and comonomer.

$$\rho_{Mw} = 209 - 82 \cdot 1-C4^2 \quad (4.3)$$

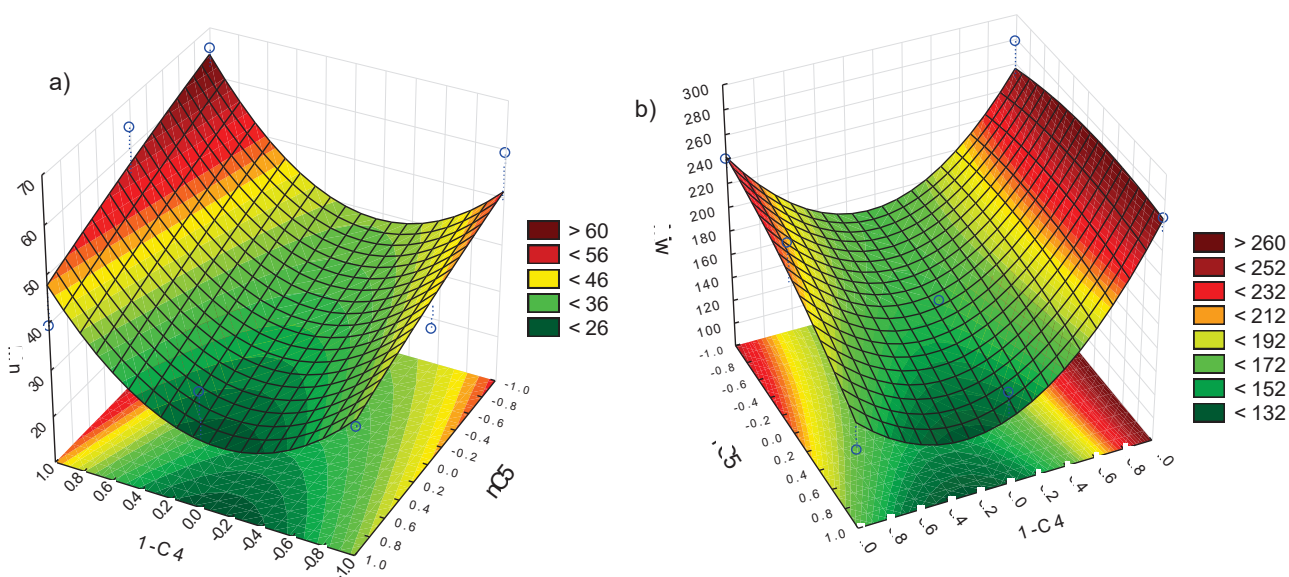


Figure 4.8 Response surface to molecular weight: a) Mn and b) Mw.

According to the molecular weight response surface, a maximum point of Mn > 60 kDa (Figure 4.8a) can be seen for combinations with higher concentrations of comonomer and ICA and maximum point Mw > 235 kDa (Figure 4.8b) for lower concentrations of comonomer, with no impact of ICA. For maximum concentrations of ICA, minimum points are seen: Mn values lower than 36 kDa for a wide range of 0.2 – 1.6 bar of 1-butene, while Mw values lower than 152 kDa for a range of 1 – 1.6 bar of 1-butene. This means a low impact of ICA on the molecular weight of the comonomers formed based on these experiments.

Crystallinity and melting temperature

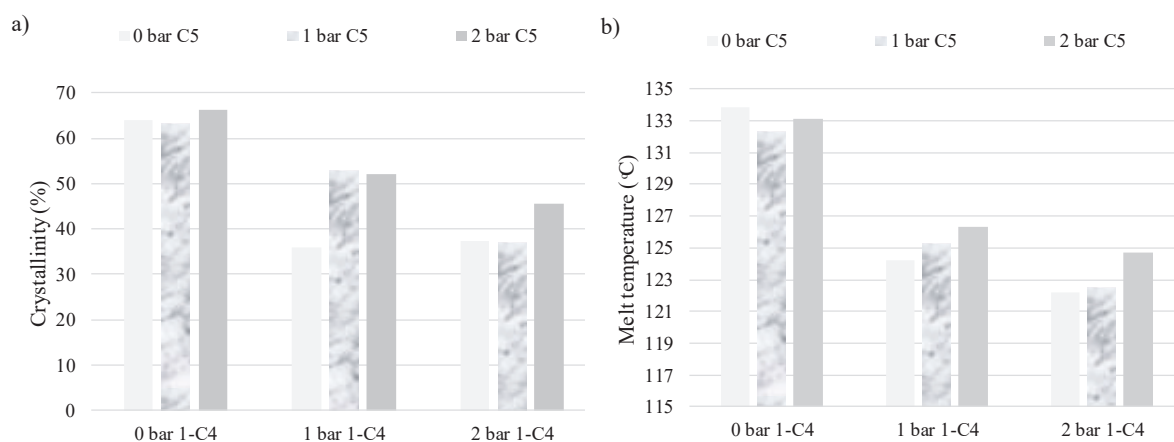


Figure 4.9 DSC analysis: a) Crystallinity and b) Melting temperature.

Thermal analysis was used to determine the crystallization and melting temperatures of the polymer material. The samples obtained based on the factorial design that did not contain 1-butene had a crystallinity around 60% and a melting temperature around 133 °C, while in the presence of the comonomer the crystallinity and the melting temperature had lower values, as expected. The impact of ICA on crystallinity can be seen in Figure 4.9a, samples with different amounts of ICA show an increase of about 25%, except when the amount of comonomer is greater than that of ICA in the reaction. In the same way, the melting temperature can be seen in Figure 4.9b, where the impact of ICA increases slightly to T_m .

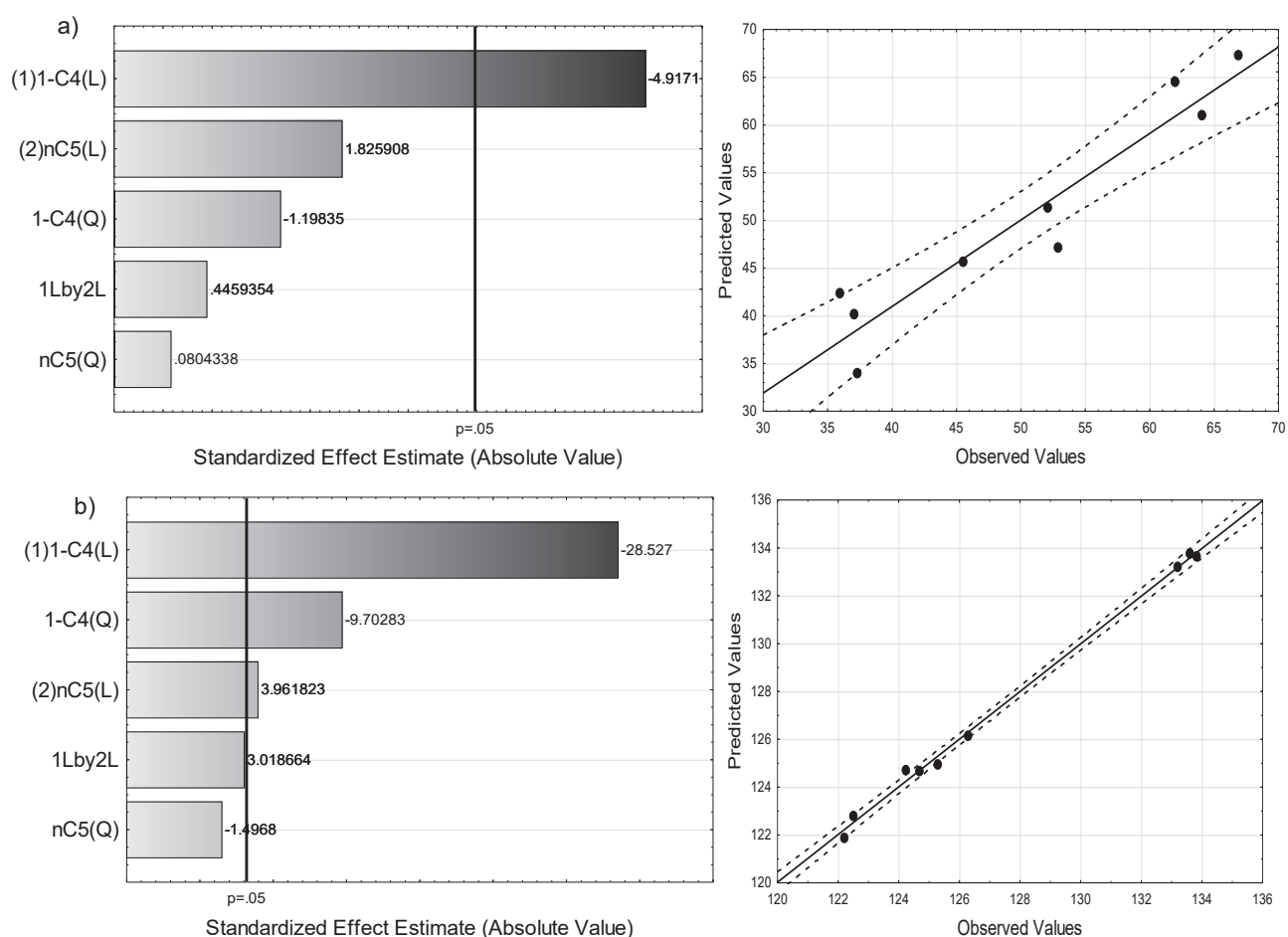


Figure 4.10 Pareto diagram and regression model prediction to: a) Crystallinity - $R^2 = 0.9067$ and b) Melt temperature - $R^2 = 0.9968$.

$$\rho_{\%wc} = 50 - 24 \cdot 1-C4 \quad (4.4)$$

$$\rho_{T_m} = 127 - 10 \cdot 1-C4 - 3.1 \cdot 1-C4^2 + 1.4 \cdot nC5 \quad (4.5)$$

Statistical analysis helps us to understand the significant impact of the factors. For the crystallinity (Figure 4.10a) the only significant effect was the comonomer, although the fraction of the variation in the statistical model was relatively low. While the polynomial fit for the melting temperature (Figure 4.10b) is a statistic factory, showing a large negative linear and quadratic effect of the comonomer, and a slight positive effect of the presence of ICA.

The response surface clearly shows a decrease in crystallinity (Figure 4.11a) and melt temperature (Figure 4.11b) when we increased the concentration of 1-butene in the reaction. This is obviously to be expected. While the impact of ICA can be seen clearly in the crystallinity, by lowering the ICA concentration, there is a lower crystalline content in the copolymer. For the melt temperature and impact of the ICA is more pronounced in the reaction of 2 bar of each species (1-butene and n-pentane), an increase of 3 °C.

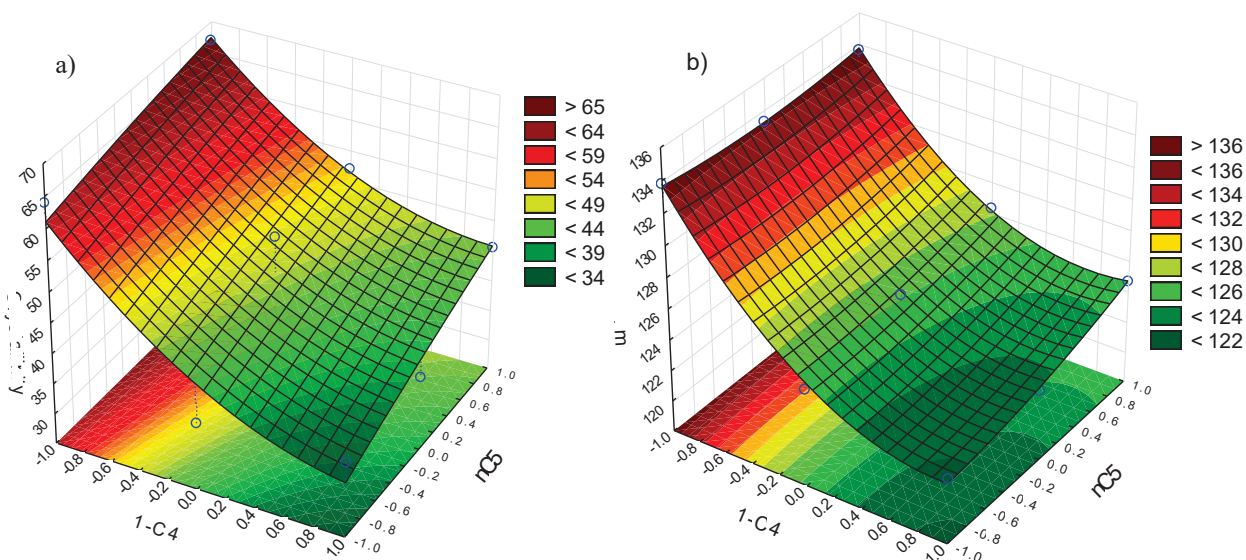


Figure 4.11 Response surface a) Crystallinity and b) Melting temperature.

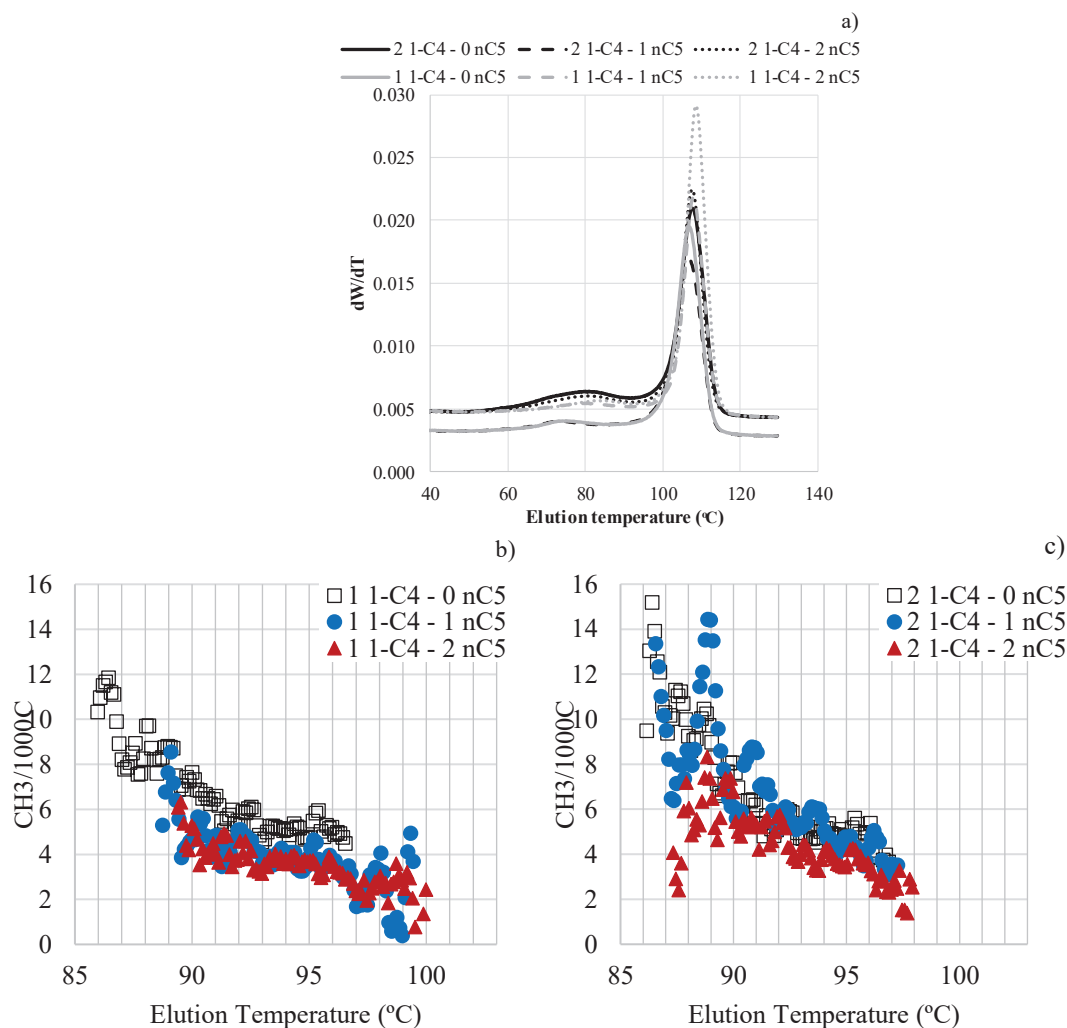
Comonomer incorporation ($CH_3/1000C$)

Figure 4.12 CEF analysis for factorial design sample. a) Copolymer composition distribution, b) $CH_3/1000C$ to 1 bar 1-C4 and c) $CH_3/1000C$ to 2 bar 1-C4.

As discussed in the previous chapters, ICA plays an important role as it increases the ethylene concentration at the active sites, which leads us to question the impact of the comonomer content incorporated in the copolymerizations. Through the crystallization elution fractionation technique it was possible to evaluate the incorporated comonomer content expressed as the number of methyl branches per 1000 carbon atoms ($CH_3/1000C$). Figure 4.12a shows the distribution of the copolymer composition, where the temperature is similar for all samples, while Figure 4.12b and 4.12c show the number of methyls as a function of temperature for 1 and 2 bars of 1-C4 respectively. The overall number of $CH_3/1000C$ is given in Table 4.3. The data in Table 4.3 show that overall there is a reduction in $CH_3/1000C$ values as the amount of

ICA increases in the reactor. This trend can be seen in Figure 4.12b, and quite clearly for 2 bar of C5, where the ICA-free polymerizations have a higher number of methyl groups. The difference between 0, 1 and 2 bars of n-C5 is still observable, but less pronounced at 2 bars of -C4. While cosolubility data for 1-C4/n-C5/LLDPE cannot be found in the literature, it is reasonable to suppose that n-C5 will increase the concentration of 1-C4 in the polymer, but probably only slightly; most likely the enhancement of 1-C4 due to n-C5 will be less significant than the enhancement of C2 solubility by n-C5. This implies that the impact of n-C5 in decreasing the presence of methyl branches can be explained by a lower ratio of 1-C4/C2 at the active sites in the presence of n-C5. The fact that the decrease in methyl branching is less pronounced in the case where we have 2 bars of 1-C4 also supports this reasoning as the C4 concentration will be higher and the impact of ICA as the 1-C4/C2 ratio will be less important.

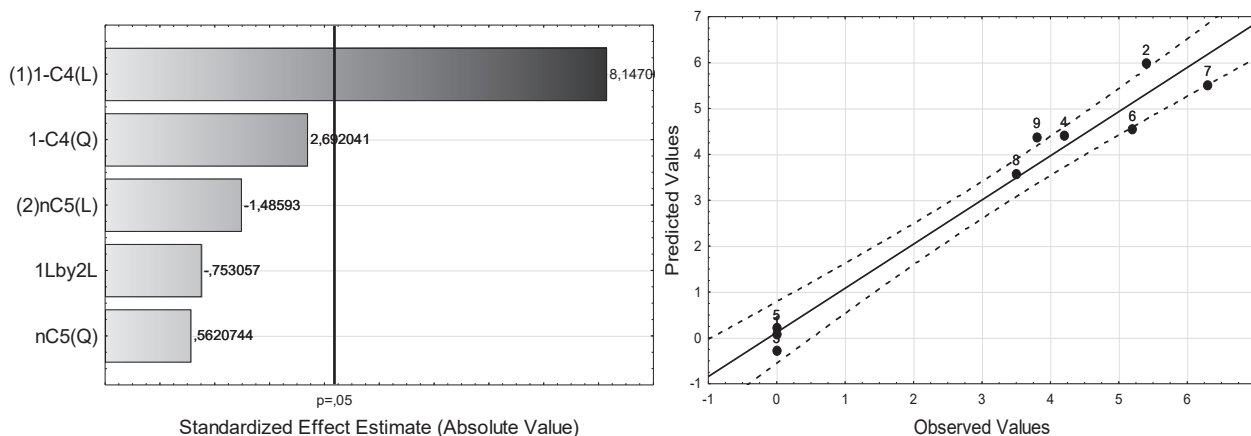


Figure 4.13 Pareto diagram and regression model prediction to $CH_3/1000C$ - $R^2 = 0.9624$.

$$\rho_{CH_3/1000C} = 3.2 + 2.7 \cdot 1-C4 \quad (4.6)$$

The statistical model for observed values of $CH_3/1000C$ showed a good prediction (Figure 4.13), showing only a positive effect of the comonomer and although the effect of the ICA is not significant in this experimental arrangement; the value of the effect is negative; that is, the ICA may decrease comonomer incorporation. This impact can be seen on the response surface (Figure 4.14) in samples with 2 bar of 1-butene, where the $CH_3/1000C$ value decreases by about 30% with increasing ICA concentration and for 2 bar of 1-butene, this figure will decrease by 57%.

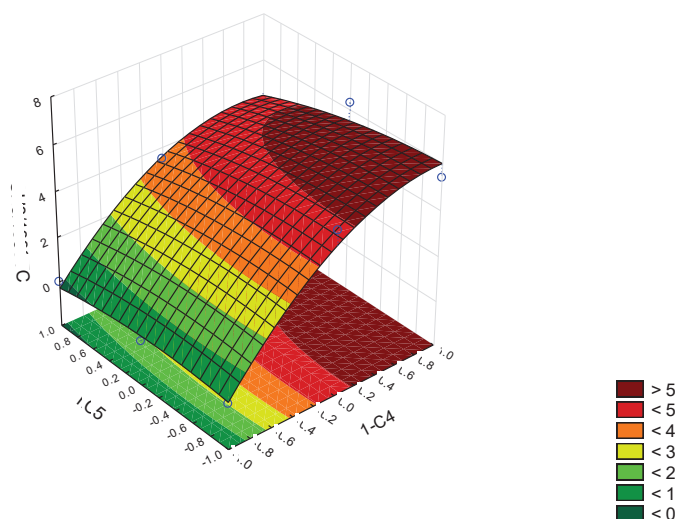


Figure 4.14 Response surface to $\text{CH}_3/1000\text{C}$.

4.2.2. Combinations of light ICA with a heavier comonomer

Different systems were also analyzed by varying the concentration of light ICA combined with heavier comonomer: poly(ethylene-*co*-1-butene) + propane and poly(ethylene-*co*-1-hexene) + n-pentane.

Figure 4.15 shows the copolymerization rate of these systems in the absence of both species, including the curve only with the comonomers (Partial pressure: 1 bar of 1-C₄ and 0.8 bar 1-C₆) and curves in the presence of different ICA compositions (5, 10 and 15 bar C₃ and to 1 and 2 bar nC₅). In all cases, there is an increase in the copolymerization rate in relation to the rates seen without ICA. Once again, we can also see a significant comonomer effect both for 1 bar of 1-C₄ and 0.8 bar of 1-C₆.

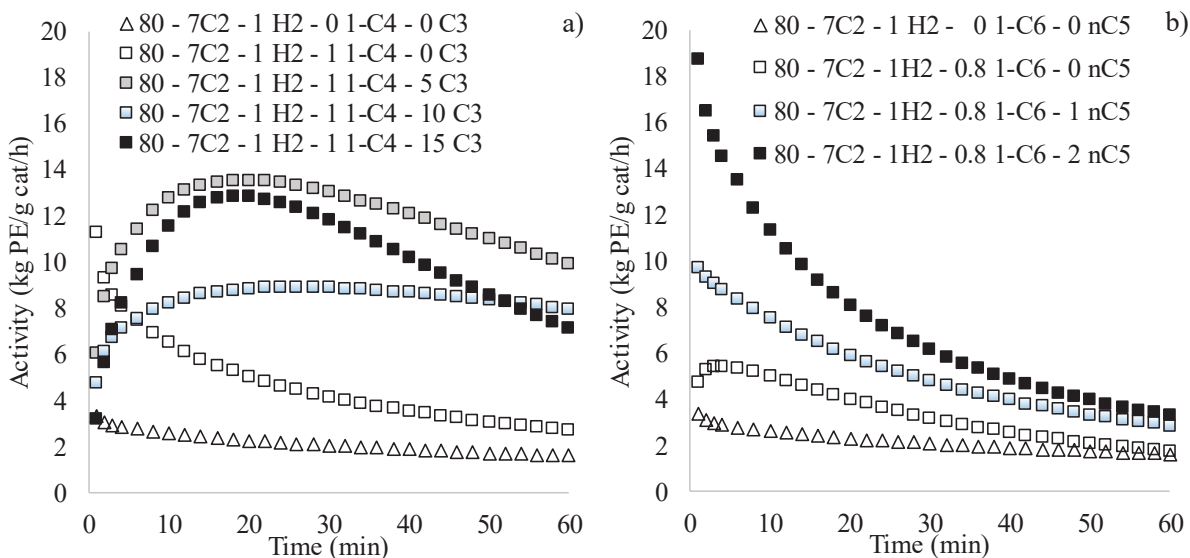


Figure 4.15 Rate of ethylene polymerization: a) poly(ethylene-co-1-butene) + propane and b) poly(ethylene-co-1-hexene) + pentane.

When we evaluate the behavior of propane variation (Figure 4.15a) the rate does not necessarily increase with increasing ICA concentration, the presence of 5 and 15 bar of propane presents similar profile, whereas in the presence of 10 bar of propane has a production smaller and more stable. In presence of pentane (Figure 4.15b) the copolymerization rate increases with an increase in the ICA concentration lighter and much more pronounced at the beginning of the reaction.

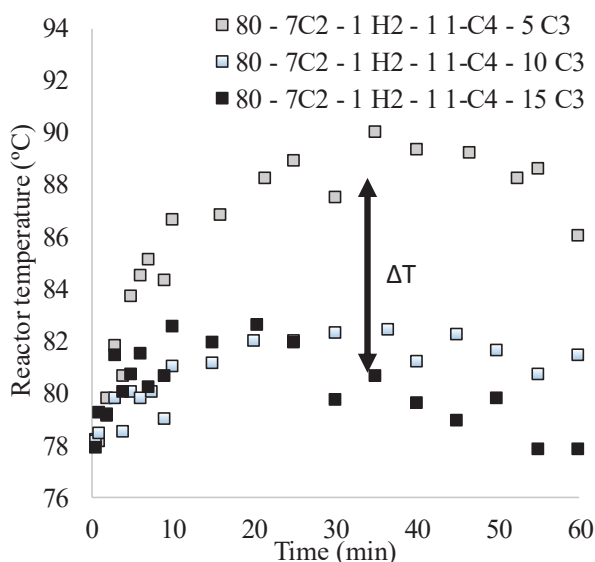


Figure 4.16 Reaction temperature of copolymerization of poly(ethylene-co-1-butene) + propane.

The ICA effect should be considered with constant temperature in the reactor, as for example, the polymerization rate with 5 bars of propane is the highest in comparison to the series of

reactions. Figure 4.16, where it shows the temperature profile as a function of the time of the copolymerization with propane, we see an increase in the temperature of the copolymerization with 5 bars of propane, on average 85.3 °C, while for copolymerization with 10 and 15 bars of propane the average temperature is 80.5 °C. Temperature profiles show that the experiments are not all comparable. This implies that the copolymerization rate also has the effect of the temperature variation of the reactor, so the high copolymerization rate of 5 bar of propane has an ICA and thermal effects. The thermal capacity produced in the presence of 5 bar of propane is not enough to control the temperature, so in the characterization analysis, the copolymer in the presence of 5 bar of propane will be discarded.

Table 4.4 shows the same data of copolymerization reactions, where for all reactions with propane, 14% of the total copolymer formed were produced within 10 minutes of reaction, whereas in reactions with 1 and 2 bar n-pentane produced in 27 minutes 27 and 31% of the total copolymer formed, respectively.

Table 4.4 Data summary of copolymerization reactions and characterization of copolymers.

Run	Cp _{gas} kJ/kgmol.°C	Yield		SEC		DSC			CEF			
		10 min g _{pol} /g _{cat}	One-hour g _{pol} /g _{cat}	Mn kg/gmol	Mw kg/gmol	%wt insoluble	%wC	T _{c on} °C	T _{c end} °C	T _m °C	CH ₃ / 1000C	T _{elution} °C
80 - 7C2 - 1H2 - 0 Cm - 0 ICA	47	477	2,158	75	247	18	64	119	115	107	134	
80 - 7C2 - 1H2 - 1 1-C4 - 0 nC3	53	1,383	4,912	29	146	16	36	115	112	108	124	5.7
80 - 7C2 - 1H2 - 1 1-C4 - 10 nC3	77	1,151	8,211	68	198	21	55	117	114	110	126	3.6
80 - 7C2 - 1H2 - 1 1-C4 - 15 nC3	85	1,326	9,969	58	213	20	54	116	114	108	128	3.9
80 - 7C2 - 1H2 - 0.8 1-C6 - 0 nC5	57	862	3,416	29	177	11	71	118	116	108	128	2.7
80 - 7C2 - 1H2 - 0.8 1-C6 - 1 nC5	66	1,437	5,378	32	182	24	50	117	115	110	127	3.6
80 - 7C2 - 1H2 - 0.8 1-C6 - 2 nC5	75	2,432	7,736	41	196	20	67	119	116	109	129	3.9

The Mw of the copolymers decreases as the comonomer pressures increase when the reactions are carried out without ICA, but with 10 and 15 bar of propane, Mw increases around 40%, whereas there is a 10% increase for 2 bar of n-pentane (neglecting possible experimental errors). The ICA effect on increasing crystallinity was seen only in the presence of propane, whereas with pentane the crystalline total is high even for dry comonomer. There was no significant change in the incorporation of the comonomer in the presence of pentane, but in the presence of propane the CH₃/1000C value decreased by 20%, this is most likely explained in the same manner as we saw for 1-C4 and nC5 above.

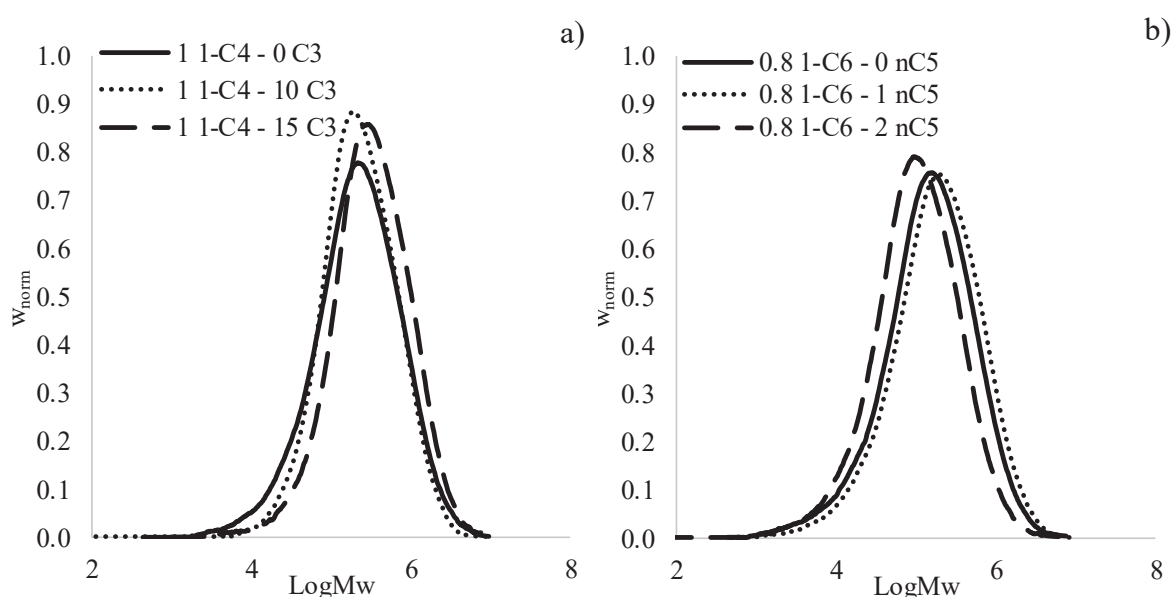


Figure 4.17 Molecular weight distribution: a) poly(ethylene-co-1-butene) + propane and b) poly(ethylene-co-1-hexene) + pentane.

Figure 4.17 shows the molecular weight distribution (MWD) for the evaluated cases since there is no significant change between copolymers in the presence of ICA with respect to copolymers in the absence. However, conditions tested with higher amounts of ICA tend to be less. The interaction of ICA with comonomer seems to minimize the impact of ICA on MWD seen in homopolymerization.

Figure 4.18a shows the CH₃ / 1000C distribution where the presence of propane significantly decreased the amount of methyl in the poly(ethylene-co-1-butene), while Figure 4.18b shows the presence of pentane slightly increases the amount of methyl in the poly(ethylene-co-1-hexene). The microstructure of the comonomer depends directly on the type and distribution of

the comonomer used, the branching content and the molecular weight, so the impact of the ICA observed in these analyses has relevance in the formation of the polymer.

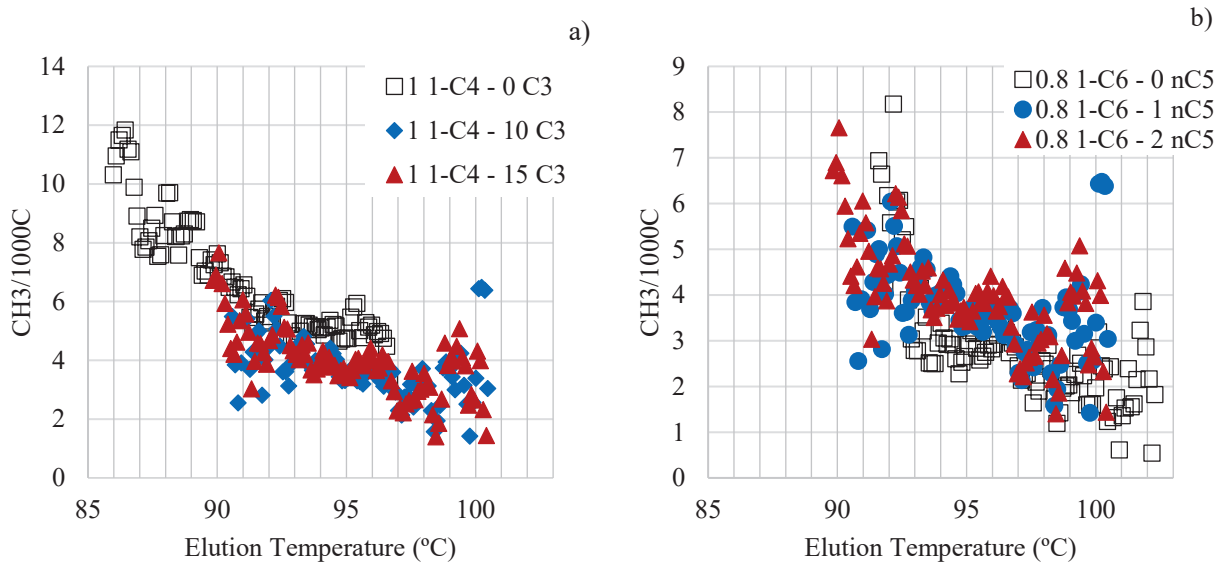


Figure 4.18 CH3/1000C distribution: a) poly(ethylene-co-1-butene) + propane and b) poly(ethylene-co-1-hexene) + pentane.

4.2.3. Solubility of comonomer in polymer

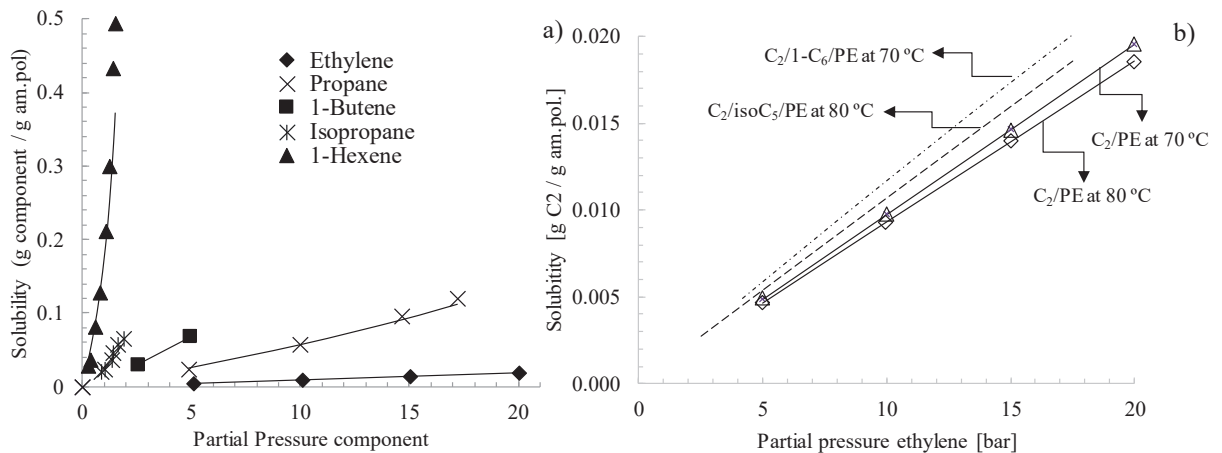


Figure 4.19 Solubility: a) Binary systems at 80 °C and b) Comparison of ethylene solubility between binary and ternary systems (C2/1-C6/PE at 70°C and C2/C5/PE at 80°C).

The solubility of alkanes (and probably alkenes) in the polymer matrix increases with increasing carbon number, as shown in Figure 4.19a. The figure describes a relationship between solubility coefficient as a function of the pressure increase of the components (studied in this chapter) for

binary system component i and polyethylene j . We observed an increase in the solubility coefficient for heavier compounds, under a constant temperature of 80 °C.

In this study, the ethylene solubilities in the ternary systems C2 / 1-C6 / PE at 70 °C and C2 / isoC5 / PE at 80 °C were compared at the pressures of ICA used in the experiments presented above. The comparison of the solubility data for this system aimed to show how soluble ethylene is in the presence of 1-hexene or iso-pentane. Figure 4.18b demonstrates that the solubility of ethylene in the presence of 0.8 bar of 1-hexene and in the presence of 2 bar of iso-pentane is greater than the binary system (C2 / PE) at the corresponding temperatures. However, it is still unknown about the solubility behavior of a smaller penetrant in the presence of more than one penetrant that favors its solubilization in the polymer chain.

All species solubility data in LLDPE for different systems presented adequate adjustment to that predicted by the Sanchez model (Appendix II) and the interaction parameters of the species are presented in Table 4.5.

Table 4.5 Interaction parameters.

System	Penetrant/PE	k_{ij}	Reference experimental data
Binary	Ethylene / LLDPE	$k_{C2,PE}$	-0.0226 [35]
	Propane / LLDPE	$k_{C3,PE}$	0.00051 [27]
	1-Butene / LLDPE	$k_{1-C4,PE}$	0,0150 [27]
	Iso-Pentane / LLDPE	$k_{iso-C5,PE}$	0,0247 [35]
	1-Hexene / LLDPE	$k_{1-C6,PE}$	-0,0121 [27]
Ternary	C2 /isoC5 / LLDPE at 80 °C	$k_{C2,nC5}$	0
		$k_{C2,PE}$	-0.0223 [35]
		$k_{nC5,PE}$	-0.0118
	C2 /1-C6 / LLDPE at 70 °C	$k_{C2,1-C6}$	0
		$k_{C2,PE}$	-0.0125 [28]
		$k_{1-C6,PE}$	0.0314

4.3. Conclusion

In this chapter we present a study focused on identifying certain physical phenomena that occur during the ethylene copolymerization of 1-butene and 1-hexene in the presence of propane and n-pentane as ICA. It has been shown that the comonomer effect on the rate of polymerization is more intense in the presence of ICA.

It was also observed that the comonomer / ICA combination is more important in the initial stages because after 10 minutes of reaction there is an impact on productivity for virtually all the concentrations analyzed. Despite having a less pronounced ICA effect in the one-hour reaction, the impact of ICA can still be seen for most of the physical properties studied. The statistical study confirmed that there is an increase of M_n in the presence of ICA, but that when ICA is present, the M_n is independent of the amount of comonomer, whereas the increase of M_w is seen when there are few presences of comonomer and this is more expressive in the homopolymerization process. The presence of ICA increases the degree of crystallinity of the copolymer while the impact on the melting temperature is seen only on the effect of the comonomer. The study of the impact on the incorporation of the comonomer, represented by $CH_3/1000C$, showed that high concentrations of ICA impact the decrease of the number of methyl groups. We have interpreted this on the basis that the ICA probably increases the solubility of ethylene and has little effect on the comonomers used in this chapter. This means that the ratio comonomer/ethylene is probably lower at the active sites in the presence of an ICA than in a dry system.

Different systems were analyzed by varying the concentration of light ICA combined with the heavier comonomer. Where it is observed that a light ICA causes influence even when combined with a higher comonomer in the copolymerization rates that presented higher productivities in the presence of propane and pentane. Propane increased M_w by about 40% of poly (ethylene-co-1-butene), while pentane increased by 10% M_w of poly (ethylene-co-1-hexene). Only propane increased the crystallinity of the copolymer and we saw a significant increase in the amount of methyl, about 20%. The effects of the nC5 / 1-C6 combination were less pronounced than the C3 / 1-C4 combination, although the copolymerization rates were higher in the presence of pentane. Perhaps the presence of the heavier comonomer has a greater

contribution to the phenomena of solubility and diffusion of the reactants, being more selective than the ICA in the polymer matrix.

Reference

- [1] V. Serini, "Polycarbonates," *Ullmann's Encycl. Ind. Chem.*, vol. 29, pp. 603–611, 2000.
- [2] S. Clas, D. C. Mcfaddin, and K. E. Russell, "Melting Points of Homogeneous Random Copolymers of Ethylene and 1-Alkenes," vol. 25, pp. 3105–3115, 1987.
- [3] J. Koivumiiki, J. V. Seppalft, "Observations on the Rate Enhancement Effect with $MgCl_2/TiCl_4$ and $CpZrCl_2$ Catalyst Systems upon 1-Hexene Addition," *Macromolecules*, vol. 26, no. 9, pp. 2226–5535, 1993.
- [4] D. Harrison et al., "Olefin polymerization using supported metallocene catalysts: Development of high activity catalysts for use in slurry and gas phase ethylene polymerizations," *J. Mol. Catal. A Chem.*, vol. 128, no. 1–3, pp. 65–77, 1998.
- [5] R. Van Grieken, C. Martín, J. Moreno, O. Prieto, and J. M. Bravo, "Ethylene/1-butene copolymerization over heterogeneous metallocene catalyst," *Macromol. Symp.*, vol. 259, pp. 174–180, 2007.
- [6] J. A. M. Awudza and P. J. T. Tait, "The 'comonomer effect' in ethylene/ α -olefin copolymerization using homogeneous and silica-supported Cp_2ZrCl_2/MAO catalyst systems: Some insights from the kinetics of polymerization, active center studies, and polymerization temperature," *J. Polym. Sci. Part A Polym. Chem.*, vol. 46, no. 1, pp. 267–277, Jan. 2008.
- [7] J. Moreno, B. Paredes, A. Carrero, and D. Vélez, "Production of bimodal polyethylene on chromium oxide/metallocene binary catalyst: Evaluation of comonomer effects," *Chem. Eng. J.*, vol. 315, pp. 46–57, 2017.
- [8] A. García-Peñas, C. Martínez, M. L. Cerrada, E. Pérez, and J. M. Gómez-Elvira, "NMR study of the comonomer effect in metallocene poly(propylene-co-1-pentene) copolymers synthesized at low temperature," *J. Polym. Sci. Part A Polym. Chem.*, vol. 55, no. 5, pp. 843–854, 2017.
- [9] T. Fu, Z. Liu, R. Cheng, X. He, Z. Tian, and B. Liu, "Ethylene Polymerization over $MgCl_2/SiO_2Bi$ -Supported Ziegler–Natta Hybrid Titanium/Vanadium Catalysts," *Macromol. Chem. Phys.*, vol. 218, no. 13, pp. 1–12, 2017.

- [10] A. Munoz-Escalona, H. Garcia, and A. Albornoz, "Homo and Copolymerization of Ethylene with Highly Active Catalysts Based on TiCl₄ and Grignard Compounds," vol. 34, pp. 977–988, 1987.
- [11] M. Smit, X. Zheng, R. Brüll, J. Loos, J. C. Chadwick, and C. E. Koning, "Effect of 1-hexene comonomer on polyethylene particle growth and copolymer chemical composition distribution," *J. Polym. Sci. Part A Polym. Chem.*, vol. 44, no. 9, pp. 2883–2890, May 2006.
- [12] K. Soga, H. Yanagihara, and D. Lee, "Effect of monomer diffusion in the polymerization of olefins over Ziegler-Natta catalysts," *Die Makromol. Chemie*, vol. 190, no. 5, pp. 995–1006, 1989.
- [13] R. Van Grieken, A. Carrero, I. Suarez, and B. Paredes, "Effect of 1-hexene comonomer on polyethylene particle growth and kinetic profiles," *Macromol. Symp.*, vol. 259, no. Ccd, pp. 243–252, 2007.
- [14] M. Vakili, H. Arabi, and H. Salehi Mobarakeh, "The effect of SiO₂ porosity on activity profiles and comonomer incorporation in slurry ethylene/butene-1 polymerization by (SiO₂/MgCl₂/TEOS/TiCl₄) catalyst system," *J. Appl. Polym. Sci.*, vol. 5, no. 4, p. n/a-n/a, 2011.
- [15] L. Binder, C. Foster, and J. L. Binder, "The Effect of Comonomer on the Microstructure of Butadiene Copolymers," pp. 2910–2913.
- [16] M. I. Nikolaeva, M. A. Matsko, T. B. Mikenas, L. G. Echevskaya, and V. A. Zakharov, "Copolymerization of ethylene with α -olefins over supported titanium-magnesium catalysts. II. Comonomer as a chain transfer agent," *J. Appl. Polym. Sci.*, vol. 125, no. 3, pp. 2042–2049, Aug. 2012.
- [17] M. Ystenes, "The trigger mechanism for polymerization of α -olefins with Ziegler-Natta catalysts: A new model based on interaction of two monomers at the transition state and monomer activation of the catalytic centers," *J. Catal.*, vol. 129, no. 2, pp. 383–401, 1991.
- [18] M. P. McDaniel, E. D. Schwerdtfeger, and M. D. Jensen, "The 'comonomer effect' on chromium polymerization catalysts," *J. Catal.*, vol. 314, pp. 109–116, 2014.
- [19] I. A. Jaber and W. H. Ray, "Polymerization of olefins through heterogeneous catalysis. XIV. The influence of temperature in the solution copolymerization of ethylene," *J. Appl. Polym. Sci.*, vol. 50, no. 2, pp. 201–215, 1993.
- [20] P. Kumkaew, L. Wu, P. Praserttham, and S. E. Wanke, "Rates and product properties of polyethylene produced by copolymerization of 1-hexene and ethylene in the gas phase with (n-

BuCp)₂ZrCl₂ on supports with different pore sizes,” *Polymer (Guildf.)*, vol. 44, no. 17, pp. 4791–4803, 2003.

[21] T. Xu, H. Yang, Z. Fu, and Z. Fan, “Effects of comonomer on active center distribution of TiCl₄/MgCl₂-AlEt₃ catalyst in ethylene/1-hexene copolymerization,” *J. Organomet. Chem.*, vol. 798, pp. 328–334, 2015.

[22] A. K. C. Chan and M. Radosz, “Fluid-liquid and fluid-solid phase behavior of poly(ethylene-co-hexene-1) solutions in sub- and supercritical propane, ethylene, and ethylene+hexene-1,” *Macromolecules*, vol. 33, no. 18, pp. 6800–6807, 2000.

[23] A. Novak et al., “Ethylene and 1-hexene sorption in LLDPE under typical gas-phase reactor conditions: Experiments,” *J. Appl. Polym. Sci.*, vol. 100, no. 2, pp. 1124–1136, 2006.

[24] C. Wohlfarth, U. Finck, R. Schultz, and T. Heuer, “Investigation of phase equilibria in mixtures composed of ethene, 1-butene, 4-methyl-1-pentene and a polyethylene wax,” *Die Angew. Makromol. Chemie*, vol. 198, no. 1, pp. 91–110, 1992.

[25] S. J. Moore and S. E. Wanke, “Solubility of ethylene, 1-butene and 1-hexene in polyethylenes,” *Chem. Eng. Sci.*, vol. 56, no. 13, pp. 4121–4129, 2001.

[26] S. K. Nath, B. J. Banaszak, and J. J. De Pablo, “Simulation of ternary mixtures of ethylene, 1-hexene, and polyethylene,” *Macromolecules*, vol. 34, no. 22, pp. 7841–7848, 2001.

[27] J. Chmelař, K. Haškovcová, M. Podivinská, and J. Kosek, “Equilibrium Sorption of Propane and 1-Hexene in Polyethylene: Experiments and Perturbed-Chain Statistical Associating Fluid Theory Simulations,” *Ind. Eng. Chem. Res.*, vol. 56, no. 23, pp. 6820–6826, 2017.

[28] J. Sun, H. Wang, M. Chen, J. Ye, B. Jiang, J. Wang, Y. Yang, C. Ren, “Solubility measurement of hydrogen, ethylene, and 1-hexene in polyethylene films through an intelligent gravimetric analyzer,” *J. Appl. Polym. Sci.*, vol. 134, no. 8, pp. 1–7, 2017.

[29] M. Namkajorn, A. Alizadeh, D. Romano, S. Rastogi, and T. F. L. McKenna, “Condensed Mode Cooling for Ethylene Polymerization: Part III. The Impact of Induced Condensing Agents on Particle Morphology and Polymer Properties,” *Macromol. Chem. Phys.*, vol. 217, no. 13, pp. 1521–1528, 2016.

[30] H. Kocian, D. Rebhan, J. Parrish, T. Pilgram, “Control of gas phase polymerization reactions,” EP1000097B1, 2002.

[31] A.M.A.L. Duarte Bragança, A.L. Ribeiro de Castro Morschbaker, E. Rubbo, N. Cid Miro, T. Barlem, “Process for gas phase polymerization and copolymerization of olefin monomers,” EP001246853B1, 2004.

- [32] J.-C. Chinh, M. C. H. Filippelli, D. Newton, and M. B. Power, “Polymerisation process,” EP 0 699 213 B1, 1998.
- [33] G. Weickert and R. Gustafsson, Bill, Benjamin, “Process for the catalytic polymerization of olefins, a reactor system and its use in the process,” EP 1 633 466 B2, 2013.
- [34] J. M. F. Robert O. Hagerty, Kevin B. Stavens, Marc L. DeChellis, D. Brett Fischbuch, “Polymerization Process,” US 7300987 B2, 2006.
- [35] W. Yao, X. Hu, and Y. Yang, “Modeling the solubility of ternary mixtures of ethylene, iso-pentane, n-hexane in semicrystalline polyethylene,” *J. Appl. Polym. Sci.*, vol. 104, no. 6, pp. 3654–3662, Jun. 2007.
- [36] A. Alizadeh, M. Namkajorn, E. Somsook, and T. F. L. McKenna, “Condensed Mode Cooling for Ethylene Polymerization: Part II. From Cosolubility to Comonomer and Hydrogen Effects,” *Macromol. Chem. Phys.*, no. 216, pp. 985–995, 2015.

Chapter 5

Reduction of crystallization rate in the presence of Induced Condensing Agents

Abstract: The crystallization of high-density polyethylene (HDPE) alone, and in the presence of Induced Condensing Agents (ICA) was studied using Differential Scanning Calorimetry (DSC). DSC analyses showed that the equilibrium melting temperature (T_m°) of HDPE decreased in the presence of ICA. The presence of a non-crystallizable ICA which is partially soluble in the amorphous phase of HDPE reduces the capacity of the polymer to crystallize. This was observed in the DSC analyses by a shifting of the crystallization and melting peaks of HDPE to lower temperatures when the ICA concentration in the medium increases. It is also observed that the rate of crystallization of HDPE can be very slow when the ratio of ICA:HDPE increases from zero. This behavior is important for a better understanding of the physical effects that occur at the beginning of the gas phase polymerization of ethylene, and suggests that the crystallization of the nascent polymer, and thus the properties of the polymer in the reactor will be quite different from the powder at a later stage of the reaction when running in condensed mode.

5. INTRODUCTION

High density polyethylene (HDPE) can be produced on an industrial scale using different processes; the two most important being in a diluent slurry or a gas phase process. In a gas phase process, the polymerization takes place in a continuous fluidized bed reactor (FBR) where a gas mixture is brought into contact with a supported catalyst. The mixture typically is composed of ethylene, hydrogen, variable amounts of comonomers such as 1-butene or 1-hexene, inert gases to regulate partial pressures, and eventually alkanes to help with heat transfer. These last compounds are often referred to as induced condensing agents (ICA) and are often isomers of butane, pentane, and hexane [1– 3].

The monomer(s) are polymerized in the pores of the solid catalyst particles. As polymer builds up in the pores of the catalyst support, it creates hydraulic tensions that provoke the rupture or fragmentation of the original support [4 – 6]. The morphology of the final particles will depend

strongly on this fragmentation step since the way in which the particles rupture will represent a trade-off between the rate of generation of stress caused by the polymerization on the one hand, and the ability of the particle to dissipate the mechanical energy on the other [7 – 9]. Thus, the physical properties of the polymer during this part of the polymerization, and in particular the crystallinity [10] can have a strong influence on fragmentation. In addition, the crystallinity can influence monomer solubility [11], as well as the rates of diffusion [12] through the growing polymer particle [13 – 15]. These last two quantities (solubility and diffusivity of penetrants) will also be a function of the type and quantity of ICA added to the reactor. For instance, Alizadeh et al. have recently shown that adding up to 0.8 bars of n-hexane to a gas phase polymerization of ethylene can lead to a significant rate enhancement with respect to a polymerization of ethylene only through both an enhanced solubility of ethylene due to the cosolubility effect and an enhanced diffusion of ethylene [16]. A single particle model was developed, assuming constant crystallinity, to describe these effects with some success. The authors noted that the greatest deviation between experiment and model predictions was at the beginning of the reaction where the free-volume based model apparently underestimated the effective diffusivity of ethylene in the amorphous polymer in the presence of n-hexane. It is entirely possible that this is because the fraction of amorphous material is underestimated during this phase of the polymerization. This, in turn, begs the question about how fast the formation of crystals is with respect to the formation of polymer chains – in other words, can we assume that the crystallinity of the nascent polymer is similar to that of the final reactor powder?

Note also that ICA has been shown to have an influence on the crystallinity (of the reactor powder) and molecular weight distribution of HDPE produced in the presence of n-pentane and n-hexane [16]. While no explanation was found for the magnitude of the increase in the average molecular weights, the higher crystallinity in the presence of an ICA was mainly attributed to the mechanism of crystallization of polymer chains in the presence of solubilized ICA which can act to promote solvent vapor annealing [17].

The crystallization of the polymer is governed by the extent and type of branching, the comonomer composition, and external factors such as the presence of plasticizers like ICA. In general, the crystallization of polymers is a kinetic phenomenon: in the molten state, all the polymer chains are disordered (amorphous), and they need time to organize in ordered regions

(crystalline). This, of course, will also be true for chains as they are formed at the active sites; there will, therefore, be a characteristic time for chain crystallization, just as there is a characteristic time for chain formation.

All of these points suggest that it would be useful for us to understand what can influence the rate of crystallization during PE production – is it rapid with respect to the fraction of a second that the polymer chains grow? Or is it a slower process? In addition to the presence of monomer in the reactor, what else will impact the rate of crystallization?

Polymer crystallization theory

Whenever particles are formed by solution crystallization, two fundamental processes, nucleation, and crystal growth, are involved. A good understanding of these phenomena is essential to align the evaluation of the impact of alkanes adsorbed on the crystallization of polyethylene. A unified theory of crystallization does not exist, but a set of complementary theories have been developed. Morphological theories generally calculate an equilibrium morphology based on calculating the energetic interactions of the different faces of the crystal to estimate its final form and thus do not take into consideration the nucleation phase [18 – 20].

In all theories, there are two mechanisms: one considering the thermodynamic barrier to include a crystalline stem on the growing lamella, and another considering the diffusion of a molecule towards the lamella. The former mechanism is enhanced by decreasing temperatures whereas the latter is enhanced for increasing temperatures. The purpose here is not to discuss the differences between the theories but rather to understand the points they have in common to assess what affects the rate of crystallization. Moreover, for temperatures far above the glass transition temperature (T_g), which is the case in the present work, the polymer diffusion is so fast that it is not the limiting mechanism. Therefore, only the crystalline stem deposit mechanism has to be considered.

In that case, the crystallization rate is controlled by the free energy difference between the liquid and the solid phases. This difference is commonly considered proportional to the supercooling that is the difference between the equilibrium melting temperature (T_m^0) and the temperature at which we are observing the system. T_m^0 is the temperature at which the crystal would melt if it

was of infinite dimensions, [21] and it is thus the limiting temperature for the crystallization process. More rarely, a “zero growth” temperature instead of T_m^0 is considered as the limit [22]. Regardless of the definition chosen, the crystallization kinetics are governed by the temperature difference between this limiting temperature and the actual crystallization temperature and this supercooling is in the denominator of a negative exponential function. This means that a small variation of the supercooling drastically modifies the crystallization kinetics. In addition to the crystallization temperature, the crystallization kinetics can be alternatively modified by the concentration of the diluent [23] which alter the equilibrium melting temperature.

This last point can be seen by the Flory-Huggins theory, which can be used to calculate the free energy of the fringed micelle model, in which the crystallization processes occur only when the system is supersaturated. In general, supersaturation can be imposed on a system by cooling, solvent evaporation, the addition of an anti-solvent or by chemical reaction. [24] Crystallization is governed by two processes that occur spontaneously: nucleation and crystal growth. Supersaturation is the driving force of the crystallization process, meaning that crystallization occurs only if the system is supersaturated. This implies that in order for a crystallization process to occur spontaneously, there needs to be a decrease in the free energy, and the increase of entropy due to the presence of a diluent means that T_m^0 decreases, and this must be compensated for by a decrease in the crystallization temperature. The Flory-Huggins equation describes this dependence of the equilibrium melt temperature on the concentration of a diluent [25].

Figure 5.1 shows the relationship of the free energy with temperature, where it compares the effect of the presence of the diluent on the free energy. The equilibrium melt temperature will be lower for a diluted system, as observed in some studies of polyethylene with heavier alkanes [26], xylenes and o-dichlorobenzene [27 – 29], and other diluents [25], [30], [31]. Teymouri et al. [32] evaluated LDPE and n-hexane thermograms with different swelling times and observed that although there were no major changes in equilibrium melt temperature, there was a significant shift in the lowest melt peak in the presence of the solvent (from 90 °C for pure LDPE to 70 °C for LDPE swollen by hexane). The rate of crystallization decreases at temperatures near the melting point and is kinetically controlled under thermodynamic conditions far from equilibrium [33]. Some kinetic studies of polyethylene with xylene [34] and

o-dichlorobenzene [35], show that the rate of crystallization decreases as we approach the melting point.

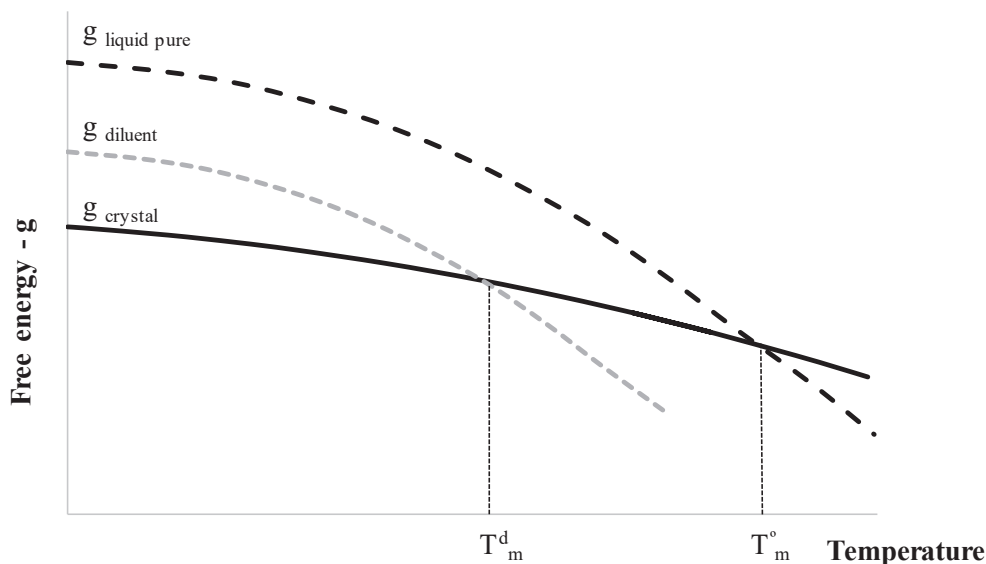


Figure 5.1 - Relation between free energy and temperature for pure polymer and diluted systems.

If one considers crystallization caused by cooling, it can be assumed that crystallization in the presence of diluent will occur for an equivalent degree supercooling with respect to the crystallization temperature of the pure polymer.

In conclusion, since the presence of alkanes in polyethylene causes a decrease in the equilibrium melting temperature, it must also lead to a depression of the crystallization temperature and rate. It is, therefore, possible that when polyethylene particles are formed at temperatures between 90 - 115 °C in a gas phase system with appreciable levels of ICA, it is possible that the crystallization rate is slowed down with respect to what one sees in the absence of ICA.

5.1. Experimental section

5.1.1. Materials

The high-density polyethylene (HDPE) used in this work was produced in gas phase polymerization experiments performed in the spherical stirred-bed semi-batch reactor, as

described in a previous publication [15]. Polymerizations were run at a pressure of 7 bars of ethylene at 70 without hydrogen and 80 °C in presence of 1 and 3 bar hydrogen. Molecular weights data are shown in Table 5.1. N-Hexane was used as the induced condensing agent (minimum purity 99%, from Sigma-Aldrich ICN - Germany). The ICA properties are shown in Table 5.2.

Table 5.1 HDPE types.

Samples ^{a)}	T _{reactor}	P _{Ethylene}	P _{Hydrogen}	Yield	M _n	M _w	M _z
	°C	bar g	bar g	g _{pol.} ·g _{cat} ⁻¹	kg·mol ⁻¹	kg·mol ⁻¹	kg·mol ⁻¹
HDPE70	70	7	0	1,575	114	751	2,936
HDPE-1H ₂	80	7	1	2,158	59	278	955
HDPE-3H ₂	80	7	3	1,312	33	145	448

a) The sample name is identified by HDPE + polymerization temperature [°C]

Table 5.2 ICA proprieties.

ICA	P ^{vap}	BP	MW
	bar	°C	g·g mol ⁻¹
	70 – 120 °C	at 1 atm	
<i>n</i> -Hexane	1.034 – 3.987	69	86.18

5.1.2. Preparation of sample blends

In order to evaluate the impact of ICA on the crystallization process, HDPE and blends of HDPE plus different levels of ICA were placed in 120 µL medium pressure steel capsules, and analyzed by DSC. In the case of the blends, a given mass (5-20 mg) of HDPE was weighed and placed in the medium pressure capsule. Then a specific volume (varying from 10-60 µL) of *n*-hexane (ICA) was added to the capsule using a micropipette. Due to the volatile nature of *n*-hexane, the amount of ICA finally enclosed in the capsule was determined gravimetrically. To determine the ICA mass within the capsule, the mass of the capsule and its contents was noted after weighing the polymer, and again after the addition of ICA and capsule closure. The mass

measurements before and after the DSC analysis were taken to verify if any solvent had evaporated during the procedure, thus correcting the ICA mass. These limits of polymer weight plus ICA concentration were chosen to represent different moments in the semi-batch, lab scale polymerization process. Note that in a semi-batch reactor the ratio of ICA to polymer is actually quite high during the very early stages of polymerization, and decreases as more and more polymer are formed.

5.1.3. Differential Scanning Calorimetry (DSC)

The DSC analyses were carried out using a Mettler Toledo DSC 3+ model in two different ways: i) a non-isothermal evaluation of the impact of different compositions (HDPE:ICA) on the range of crystallization temperatures and degree of crystallinity of the polymer samples; ii) a study of the isothermal crystallization kinetics to assess the crystallization times at different values of T_c . The ICA concentration in the blends for each study phase is shown in Table 5.3.

Table 5.3 ICA:HDPE blends (weight percent ICA:HDPE).

Samples	Non-isothermal	Isothermal
HDPE70	0 – 22 – 87 – 99 – 99.8 %	0 – 17 – 25 – 85 %
HDPE-1H ₂	-	0 – 15 – 28 – 86 %
HDPE-3H ₂	-	0 – 15 – 28 – 86 %

In the non-isothermal analyses were performed under a nitrogen atmosphere - 30 mL/min, with the following analysis procedure performed in six sequential steps:

- (i) Cooling of the sample from room temperature to -20 °C at a rate of 10 °C / min;
- (ii) Heating from -20 °C to 180 °C at a rate of 2 °C / min;
- (iii) Isothermal hold at 180 °C for 120 min;
- (iv) Cooling from 180 °C to -20 °C with rates of 2 °C / min;
- (v) Isothermal hold at -20 °C for 120 min;
- (vi) Heating from -20 °C to 180 °C at a rate of 2 °C / min.

The parameters of interest in the first non-isothermal studies are the range of crystallization temperatures (T_c), melting temperatures (T_m - corresponding to the second heating), total heat of crystallization (Q_c - measurement of the area under the endotherm divided by the polymer mass in the blend), total heat of fusion (Q_m - measurement of the area under the exotherm also divided by the polymer mass in the blend), and degree of crystallinity (w_c - calculated in relation to 100% crystalline HDPE).

In the isothermal analyses, the capsules were kept under a nitrogen atmosphere flowing at 30 mL/min. The isothermal crystallization of the ICA:HDPE mixtures was at different crystallization temperatures (T_c). The procedure starts with sample cooling from room temperature to -20 °C at a rate of 10 °C / min and continues with a cycle of five sequential steps:

- (i) Heating from -20 °C to 180 °C at a rate of 2 °C / min;
- (ii) Cooling from 180 °C to T_c at rates of 50 °C / min;
- (iii) Isothermal hold at T_c for 120 min;
- (iv) T_c cooling to -20 °C with rates of 10 °C / min;
- (v) Heating from -20 °C to 180 °C at a rate of 2 °C / min.

T_c values of 91, 94, 97, 100 and 115 °C have studied her. The thermograms were analyzed to obtain the time and degree of crystallization for a given T_c isotherm, and the melting temperature.

All values obtained in the analysis were from the thermograms treated using STARe Software Evaluation, version 14.00. The enthalpy of 100% crystalline polymer was taken as $\Delta H^\circ = 293$ J / g [36]. For validation, the method was repeated for different concentrations of the blend, such as HDPE70-85% for the non-isothermal and HDPE70-1%, HDPE70-80% for the isothermal. All runs showed a standard deviation of less than 10%.

5.2. Results and discussion

5.2.1. Non-isothermal analyses

In the first series of experiments, the non-isothermal evolution of the crystallization and melting points of the different mixtures of HDPE and ICA are shown in Figure 5.2, and a summary of the properties of these same runs are presented in Table 5.4. If one considers the thermograms in Figure 5.2, it is immediately (and perhaps intuitively) obvious that the crystallization temperature of mixtures of HDPE and ICA decrease as the relative concentration of the latter increases. As pointed out by Yamamoto [33], the rate of crystallization decreases as the system approaches its melting point. In other words, one might suspect from these results that the characteristic time for crystallization would be very different in the samples with high ICA:HDPE ratios – i.e., the same conditions that one would find in a semi-batch reactor at the start of a polymerization in the presence of an alkane.

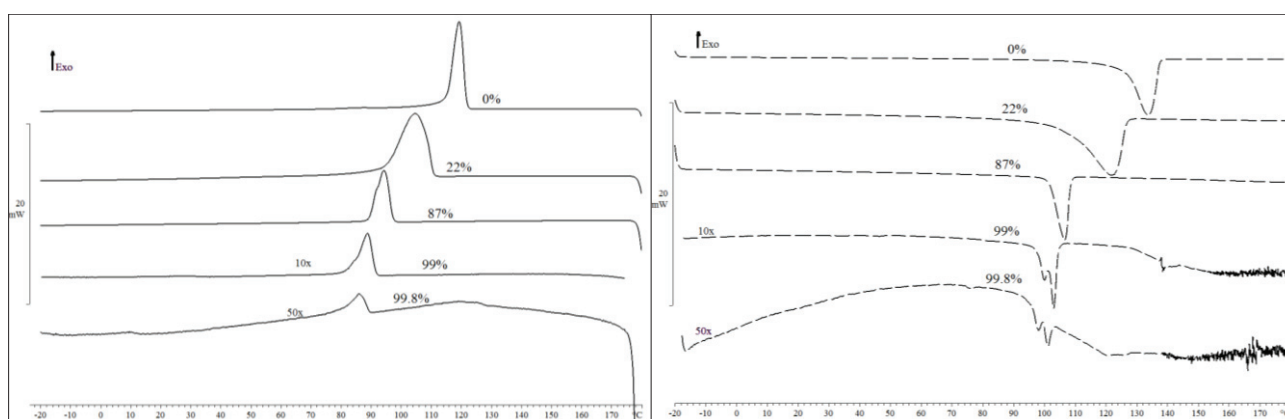


Figure 5.2 – Non-isothermal thermograms from HDPE70 samples: — Peaks of the exothermic – crystallization curves (T_c) and ---- Peaks of the endothermic – melting curves (2a heating – (T_m)). The curve size of the 99% blend is multiplied by ten, and for the blend, 99.8% is multiplied by fifty.

In addition, and as shown in Table 5.4, all the samples show the same (expected) tendencies with the increase of ICA concentration in the blends:

- T_c and T_m , estimated by the peak of the endothermic and exothermic curves respectively, decrease. The T_m decreases by 33 °C over the range of compositions studied, and T_c by 34°C in the case of HDPE70;
- There is an increase in the total heat of crystallization (Q_c), of melting (Q_m), and of the degree of crystallinity (w_c). At high ICA to polymer ratios, the polymer is almost entirely crystalline at the end of the cooling step.

The difference between Q_c and Q_m remained approximately invariant, which shows that the presence of ICA has a very strong influence on the total amount of crystalline phase in the polymer, the HDPE that recrystallizes from dilute solutions having higher overall crystallinity than those recrystallizing from solutions more concentrated in the polymer.

Table 5.4 Parameters obtained from the thermograms.

Samples	Parameters	ICA:HDPE blends				
		0%	22%	87%	99%	99.8%
HDPE70	y_{ICA}	0%	22%	87%	99%	99.8%
	$y_{polymer}$	100%	78%	13%	1%	0.2%
	w_c (%)	55.7	56.2	67.5	86.3	97.3
	w_c (%)	122	111	97	92	90
	T_c on (°C)	120	105	95	89	86
	T_c peak (°C)	115	95	90	84	82
	T_c end (°C)	134	122	106	103	101
	T_m (°C)	163	165	198	253	285
	Q_c (J / g)	-165	-165	-197	-250	-282
	Q_m (J / g)	1.2%	0.3%	0.5%	1.1%	1.1%

Figure 5.3a shows that the melting point depression is more pronounced when there more ICA in the capsule, which agrees with the literature [37]. Figure 5.3b shows the peak of the crystallization temperature and the crystallization range. It can be seen from this figure that 20% ICA:HDPE crystallization can be seen at temperatures below 100 °C. For levels of less than 20% ICA by weight, the range is around 115 - 122 °C.

These initial observations support the idea that when ICA are present during the nascent stage of polymerization in a semi-batch reactor, they can promote a decrease in rate of crystallization during the first instants of the polymerization before significant levels of polymer begin to accumulate, and the equilibrium melt temperature can eventually approach the temperature of the reactor.

In order to better understand the behavior of the crystallization rate, the isotherms were evaluated in the range 90 - 115 °C for comparison in the different blends. Isotherm at 130 °C

was also measured and used to subtract any imperfections from the curves analyzed. This guarantees that we will have a curve that will not crystallize the polymer.

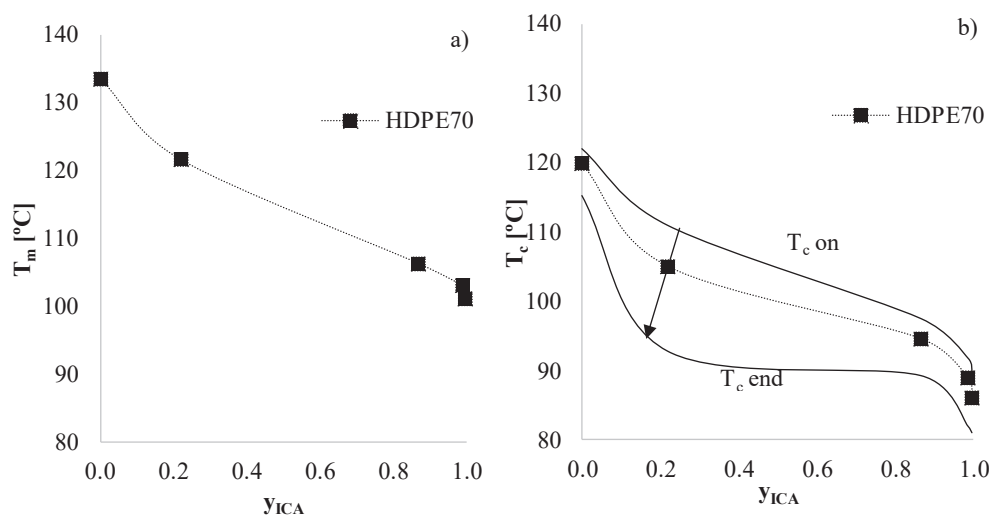


Figure 5.3 a) Melt temperature and b) Crystallization temperature as a function of the mass fraction of ICA in an ICA-HDPE mixture.

5.2.2. Isothermal analyses

The isotherms used in this part of the study began after abrupt cooling. According to Zhang et al. [36] in the cooling is rapid enough under the right conditions, there is not sufficient time for crystal nucleation and growth. We, therefore, considered that the quantity of crystallization that occurred during the cooling phase was negligible and that the vast majority crystallization occurred during the isothermal phase. Nevertheless, when the degree of supercooling is high enough, as the crystallization can be quite rapid. Even though we used the cooling rate of 50 °C / min, a preliminary study showed that some of the samples could be to crystallize during the phase cooling before the isotherm temperature is stabilized. Thus we will only present results for the pure polymer and 17% ICA:HDPE at $T_c = 115$ °C, 25% ICA:HDPE at $T_c = 100$ °C and 85% ICA:HDPE at $T_c = 94$ °C, and for samples of polymers with hydrogen (lower molecular weight) at $T_c = 115$ °C. The ICA in each blend can be solubilized in the amorphous phase of the available polymer mass and present as a vapor. If enough ICA is present, it can also be present as a separate liquid phase.

From these data obtained by DSC, the study of **crystallization kinetics** was carried out using the classical model of Avrami [38, 39] and an evaluation of the **equilibrium melt temperature** (T_m^0) with the procedure of Hoffman and Weeks [40].

The Avrami approach aims at calculating the volume of material that crystallizes as a function of time. The model states that the crystallinity developed by a heated isothermal material for a time t can be correlated with the type and kinetics of nucleation and crystalline growth. Thus, when the assumptions of the theory are satisfied, i.e., infinitely large sample, spatially random nucleation, and time independent nucleation and growth rates. This model, described by equation 5.1, provides parameters for the kinetics of total crystallization under isothermal conditions [36], [41].

$$\alpha(t) = 1 - \exp(-kt^n) \quad (5.1)$$

Where: $\alpha(t)$ is the relative crystallinity as a function of time, and n e k is the Avrami parameters. n is related to the type of nucleation, morphology, and size of crystals developed during crystallization, depends on the crystal sizing, and k is related to the nucleation rate and growth of the crystalline phase. The evaluation of the relative crystallinity as a function of time is carried out from the ratio between the partial (at time t) and total areas of the crystallization isotherm (in relation to the baseline, which represents the zero-heat flux), generating a typical sigmoidal curve. By plotting equation 5.1 in double log form, we obtain a straight line whose slope gives the values of n , and the intercept (at $\log(t) = 0$) gives the values of k .

All analyzed isotherms have a sigmoid shape characterizing a phase transformation process, as shown in Figures 5.4 and 5.5. In the analyzed samples an increase of T_c promoted a shift to longer times, indicating a decrease in the rate of crystallization for all of the blends studied. This is a consequence of reducing the supercooling, thus reducing the driving force of the crystallization process. Analyzing the specific behavior of the mixtures (Figure 5.4) at 0 and 17% of ICA at $T_c = 115$ °C (all ICA absorbed in the polymer), and as the ICA concentration in the capsule increases (liquid phase presence) it was found that the presence of ICA affects the crystallization behavior of the polymer, both in terms of the temperature and the time of crystallization. It is clear that the blends have a much slower crystallization relative to the pure polymer. The hexane molecules act as a diluent, slowing down the crystallization process by modifying the liquid free energy (see Figure 5.1). We can observe time it takes to reach 50% of the total crystallization (the half crystallization time, $t_{1/2}$), that is, the time from the beginning

of the crystallization so that there is relative crystallinity equal to 0.5, and which is directly connected to the rate of crystallization. Table 6 shows a significant increase in the $t_{1/2}$ values in the presence of ICA.

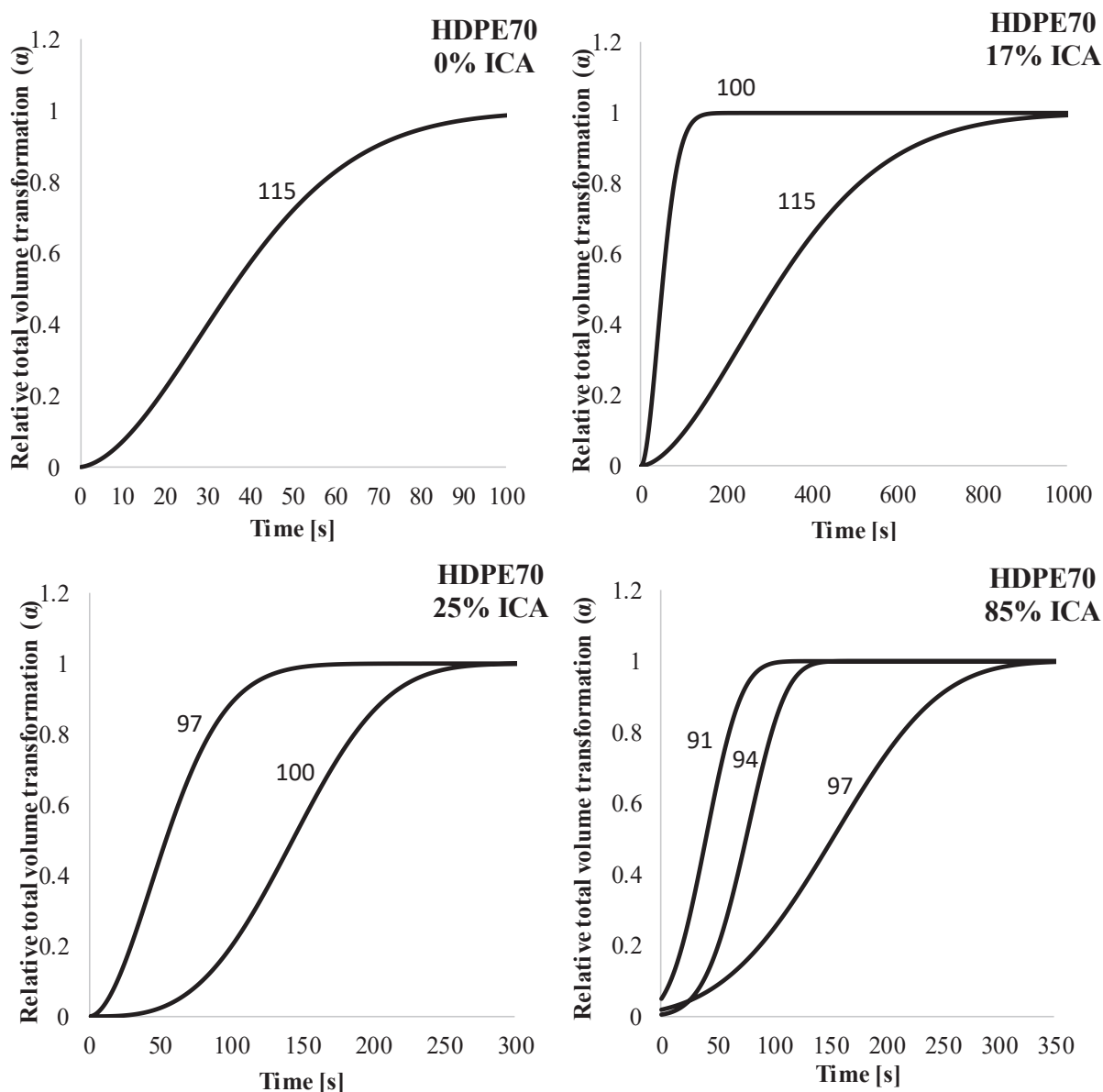


Figure 5.4 Relative crystallinity curves for HDPE70 blends samples at different T_c [°C]

When we evaluate the impact of the molecular weight on the rate of crystallization, we see that the crystallization time increases with the increase of the molecular weight [19]. HDPE-1H₂ (278 kDa) and HDPE-3H₂ (145 kDa) pure, 15% ICA:HDPE-H₂ and 86% ICA:HDPE-H₂, the crystallization time is faster for the lower molecular weight polymer. However, 28% ICA:HDPE-H₂ exhibit almost the same behavior (Figure 5.5). Indeed, for such dilution, the

decrease in molecular mobility caused by an increase of molecular weight is negligible. In Table 6 the $t_{1/2}$ change, with different molecular weight is displayed.

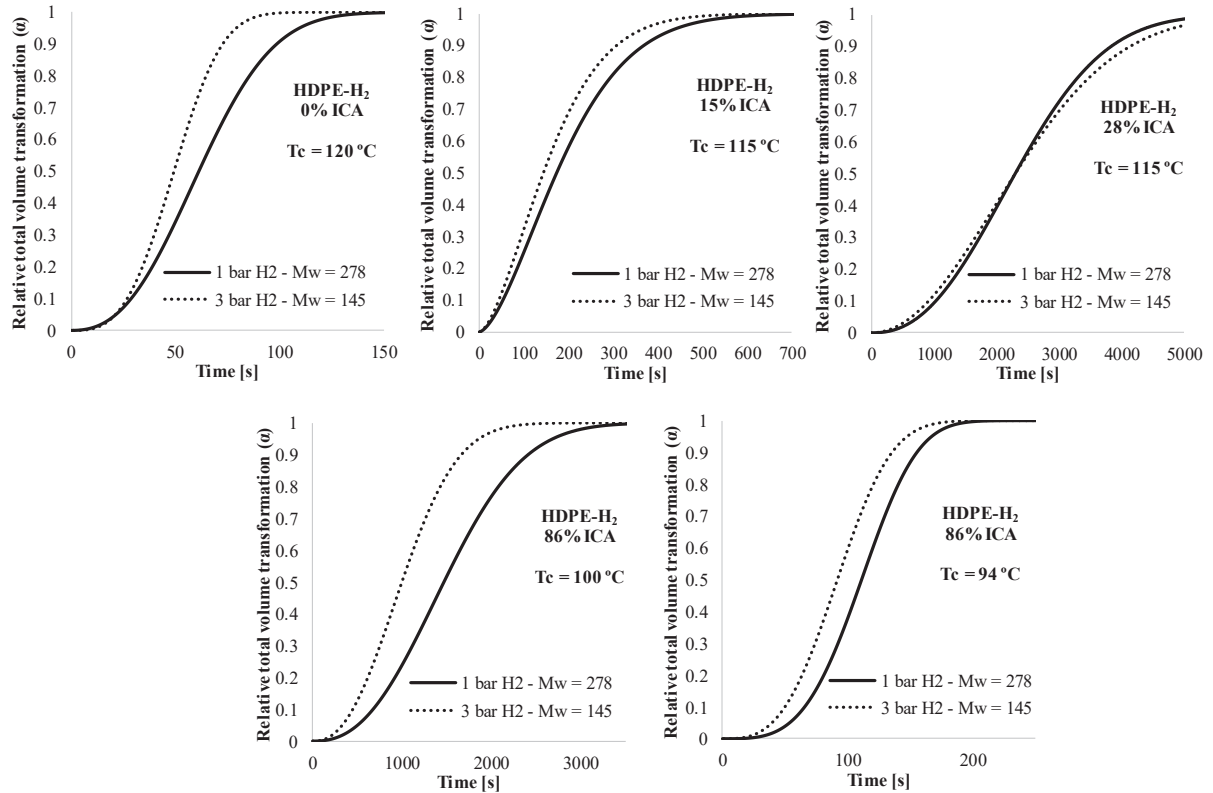


Figure 5.5 Relative crystallinity curves for HDPE-H₂ blends samples at different T_c [°C].

A study of the melting behavior of the samples in the presence of ICA was then performed on the samples that were isothermally crystallized at different temperatures. The melting occurs over a wide range of temperatures because of different sizes and degrees of perfection of the crystals present, if T_m is defined as the peak of the curve, its value does not truly represent an intrinsic property of the material. For this reason, T_m^o , which represents the melting temperature of infinitely large crystals, constitutes a more appropriate parameter for evaluating the differences in thermal stability of the various compositions [39].

The calculation of T_m^o was performed according to the Hoffman-Weeks procedure, in which the measured melting temperature T_m (obtained in the last step of the thermal characterization procedure) of each isothermally crystallized sample is plotted against its T_c . The line of equation $T_m = T_c$ is also plotted and the intersection of the two lines gives the value of T_m^o .

Table 5.5 Half Crystallization Time - $t^{1/2}$ [s].

T_c [°C]	HDPE70				HDPE-1H ₂				HDPE-3H ₂			
	0%	17%	25%	85%	0%	15%	28%	86%	0%	15%	28%	86%
91				73								
94				108				112				92
97			54	240				322				212
100		49	143					1470				998
115	36	313				174	2.303			143	2.303	
120					62					49		

The evaluation of T_m^0 according to the Hoffman-Weeks method (Figure 5.6), allows one to compare T_m^0 of the pure HDPE with that of the blends. For pure HDPE average value of T_m^0 is approximately 135.5 °C. While this value is lower than the theoretical melting point for HDPE ($T_m^0 \approx 142$ °C [40]), this value lies within the range 133 - 138 °C for HDPE [42]. These differences are due to possible experimental errors, all points present errors of less than 5%. T_m^0 for blends of ICA and HDPE is lower than pure HDPE, typically near 130 °C for 15-17% ICA:HDPE, and 110 °C for 85% ICA:HDPE. A decrease in the equilibrium melting temperature is observed for both two samples. This shows that there is miscibility between HDPE and ICA.

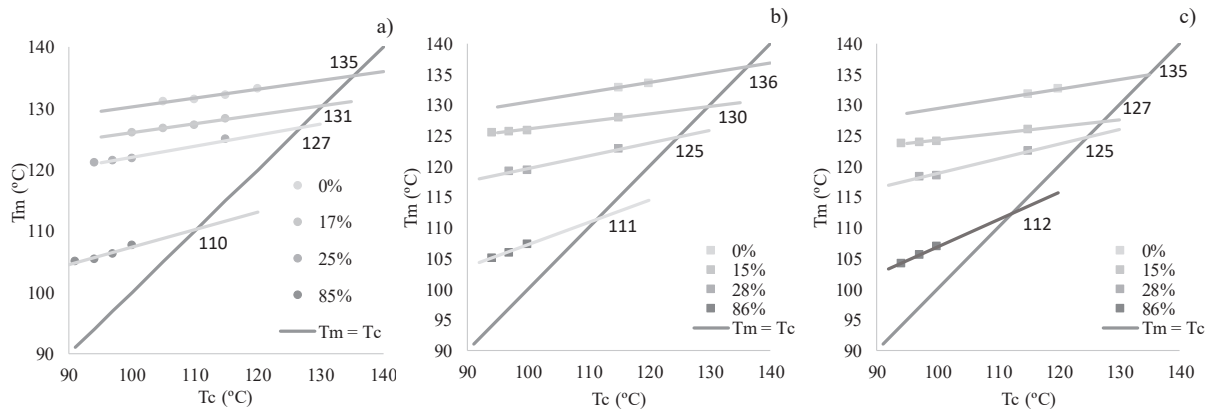


Figure 5.6 Determination of T_m^0 by the Hoffman-Weeks method. a) HDPE70 - fraction ICA. b) HDPE-1H₂ - fraction ICA. c) HDPE-3H₂ - fraction ICA.

Considering the Flory-Huggins theory, the equilibrium melting temperature variation with the diluent concentration can be expressed by:

$$\frac{1}{T_m^0} - \frac{1}{T_{m,melt}^0} = \frac{RV_u}{\Delta h_u V_d} (\phi_d - \chi \phi_d^2) \quad (5.2)$$

where T_m^0 and $T_{m, melt}^0$ are the equilibrium melting temperatures of respectively the polymer in solution and the bulk polymer $T_{m, melt}^0 = 414.6$ K and V_d is the molar volume of the diluent (for hexane this is 113 \AA^3), V_u is the molar volume of the repeat unit (for ethylene 38 \AA^3) [43], ΔH_u is the heat of fusion of the repeat unit ($4,096 \text{ J.mol}^{-1}$), ϕ_d is the volume fraction of the diluent in the blend and χ is the Flory-Huggins interaction parameter. An interaction parameter value lower than 0.5 indicates total miscibility while the miscibility is only partial for χ greater than 0.5. The experimental equilibrium melting temperature was considered in the equation.

Figure 5.7, the obtained values of T_m^0 are plotted against the volume fraction of ICA. Clearly (especially for HDPE 70), a value of χ lower than 0.5 leads to a well theoretical description of the equilibrium melting temperature for all ICA fractions. This leads to the conclusion that, in the investigated range of ICA fractions, the miscibility of the PE is total.

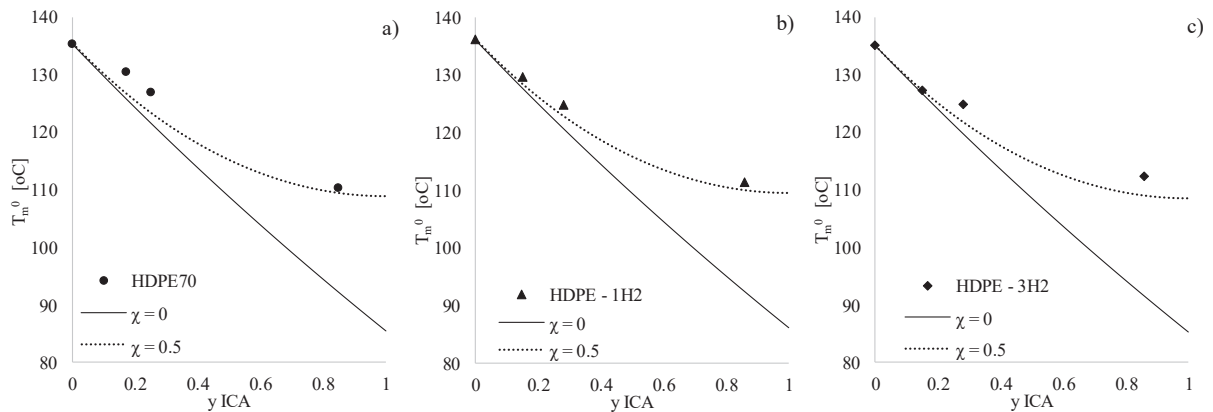


Figure 5.7 Evaluation Flory equation. a) HDPE70 - fraction ICA. b) HDPE-1H₂ - fraction ICA. c) HDPE-3H₂ - fraction ICA.

5.3. Conclusion

In the current study, the isothermal crystallization kinetics of blends of n-hexane and HDPE were analyzed by differential scanning calorimetry. The main conclusions are summarized below:

- ICA:HDPE ratios form blends, and an equilibrium melt temperature depression and an increase in the crystallinity of HDPE were observed with the presence of ICA;
- The impact of ICA on the crystallization rate: the crystallization time is significantly higher for the blends compared to the pure polymer.

The results obtained with the kinetic study showed that the presence of n-hexane, at the concentrations employed, leads to an equilibrium melting temperature depression and thus a decrease of the crystallization rate for a given temperature. Moreover, an analysis on the basis of the Flory Huggins equation showed that in the melted state, the polymer is entirely miscible in ICA.

Reference

- [1] D. N. T. John R. Parrish, Glenn A. Lambert, "Gas Phase Polymerization and Method Of Controlling Same," US 7625987 B2, 2009.
- [2] A. K. M. Yahya Banat, Fahad Al-Obaidi, "Olefin Gas Phase Polymerisation," US 2013/0066027 A1, 2013.
- [3] F. A. O. Yahya Banat, A. K. Malek, "Olefin Gas Phase Polymerisation," US 2014/0148563 A1, 2014.
- [4] R. J. T. Carrick, Wayne L., George L. Karapinka, "Polymerization Process," 3324095, 1967.
- [5] Howard B. Irvin; Fred T. Sherk, "Polyolefin Reactor System," 4121029, 1978.
- [6] A. R. Miller, "Fluidized Bed Reactor," 4003712, 1977.
- [7] T. F. L. McKenna, A. Di Martino, G. Weickert, J. B. P. Soares, "Particle growth during the polymerization of olefins on supported catalysts, 1 - Nascent polymer structures," *Macromol. React. Eng.*, vol. 4, no. 1, pp. 40–64, 2010.

- [8] A. Di Martino, G. Weickert, F. Sidoroff, T. F. L. McKenna, "Modelling Induced Tension in a Growing Catalyst/Polyolefin Particle: A Multi-Scale Approach for Simplified Morphology Modelling," *Macromol. React. Eng.*, vol. 1, no. 3, pp. 338–352, 2007.
- [9] B. Horáčková, Z. Grof, J. Kosek, "Dynamics of fragmentation of catalyst carriers in catalytic polymerization of olefins," *Chem. Eng. Sci.*, vol. 62, no. 18–20, pp. 5264–5270, 2007.
- [10] A. Alizadeh, T. F. L. McKenna, "Particle Growth during the Polymerization of Olefins on Supported Catalysts. Part 2: Current Experimental Understanding and Modeling Progresses on Particle Fragmentation, Growth, and Morphology Development," *Macromol. React. Eng.*, vol. 12, no. 1, 2018.
- [11] V. Kanellopoulos, D. Mouratides, P. Pladis, C. Kiparissides, "Prediction of solubility of α -olefins in polyolefins using a combined equation of state - Molecular dynamics approach," *Ind. Eng. Chem. Res.*, vol. 45, no. 17, pp. 5870–5878, 2006.
- [12] A. G. Fisch, J. H. Z. dos Santos, N. S. M. Cardozo, A. R. Secchi, "Mass transfer in olefin polymerization: estimative of macro- and microscale diffusion coefficients through the swollen polymer," *Chem. Eng. Sci.*, vol. 63, no. 14, pp. 3727–3739, Jul. 2008.
- [13] M. Namkajorn, A. Alizadeh, E. Somsook, T. F. L. McKenna, "Condensed Mode Cooling for Ethylene Polymerisation : The Influence of Inert Condensing Agent on the Polymerisation Rate," *Macromol. Chem. Phys.*, vol. 2014, no. 215, pp. 873–878, 1918.
- [14] A. Alizadeh, M. Namkajorn, E. Somsook, T. F. L. McKenna, "Condensed Mode Cooling for Ethylene Polymerization: Part II. From Cosolubility to Comonomer and Hydrogen Effects," *Macromol. Chem. Phys.*, no. 216, pp. 985–995, 2015.
- [15] F. N. Andrade, T. F. L. McKenna, "Condensed Mode Cooling for Ethylene Polymerization: Part IV. The Effect of Temperature in the Presence of Induced Condensing Agents," *Macromol. Chem. Phys.*, vol. 218, no. 20, pp. 1–8, 2017.
- [16] M. Namkajorn, A. Alizadeh, D. Romano, S. Rastogi, T. F. L. McKenna, "Condensed Mode Cooling for Ethylene Polymerization: Part III. The Impact of Induced Condensing Agents on Particle Morphology and Polymer Properties," *Macromol. Chem. Phys.*, vol. 217, no. 13, pp. 1521–1528, 2016.
- [17] J. K. and G. James Mark, Kia Ngai, William Graessley, Leo Mandelkern, Edward Samulski, *Physical properties of polymers*, Third. 2003.
- [18] R. Boistelle, J. P. Astier, "Crystallization mechanisms in solution," *J. Cryst. Growth*, vol. 90, no. 1–3, pp. 14–30, 1988.

- [19] R. J. Kirkpatrick, "Crystal growth from the melt: a review," *Am. Miner.*, vol. 60, pp. 798–814, 1975.
- [20] M. Zhang, B.-H. Guo, J. Xu, *A Review on Polymer Crystallization Theories*, vol. 7, no. 1. 2016.
- [21] J. D. Hoffman, R. L. Miller, "Kinetic of crystallization from the melt and chain folding in polyethylene fractions revisited: theory and experiment," *Polymer (Guildf.)*, vol. 38, no. 13, pp. 3151–3212, Jan. 1997.
- [22] G. Strobl, T. Y. Cho, "Growth kinetics of polymer crystals in bulk," *Eur. Phys. J. E*, vol. 23, no. 1, pp. 55–65, 2007.
- [23] B. Wunderlich, *Macromolecular physics*. Academic Press, 1973.
- [24] A. G. Jones, "Crystallization Process Systems," *Cryst. Process Syst.*, p. 341, 2002.
- [25] F. Toquet, L. Guy, B. Schlegel, P. Cassagnau, R. Fulchiron, "Effect of the naphthenic oil and precipitated silica on the crystallization of ultrahigh-molecular-weight polyethylene," *Polym. (United Kingdom)*, vol. 97, pp. 63–68, 2016.
- [26] S. B. Mitchell, W. L. Hunter, R. Hosemann, "Estimation of Thermodynamic Interactions between Polyethylene and n-Alkanes by Means of Melting Point Measurements By Alcio Nalcajima and Fumiyuci Hamada," vol. 82, no. Bochum 1964, 1965.
- [27] G. Valdecasas, "The Crystallization of Polymer-Diluent Mixtures," vol. 13, pp. 2103–2115, 1975.
- [28] E. Riande, J. M. G. Fatou, "Effect of solvent on the crystallization from dilute polyethylene solutions," *Polymer (Guildf.)*, vol. 17, no. 9, pp. 795–801, 1976.
- [29] E. Riande, J. M. G. Fatou, "Crystallization of Dilute Polyethylene Solutions: Influence of Molecular Weight," *Polymer (Guildf.)*, vol. 17, pp. 99–104, 1976.
- [30] E. Riande, J. G. Fatou, "Crystallization kinetics of polyethylene paraffin mixtures," vol. 19, pp. 1295–1299, 1978.
- [31] W. Cobbs Jr, R. Burton, "Crystallization of polyethylene terephthalate," *J. Polym. Sci.*, vol. 10, no. 3, pp. 275–290, 1953.
- [32] Y. Teymouri, A. Adams, B. Blümich, "Compact low-field NMR: Unmasking morphological changes from solvent-induced crystallization in polyethylene," *Eur. Polym. J.*, vol. 80, pp. 48–57, 2016.
- [33] T. Yamamoto, "Computer modeling of polymer crystallization - Toward computer-assisted materials' design," *Polymer (Guildf.)*, vol. 50, no. 9, pp. 1975–1985, 2009.

- [34] A. J. McHugh, W. R. Burghardt, D. A. Holland, "The kinetics and morphology of polyethylene solution crystallization," *Polymer (Guildf)*., vol. 27, no. 10, pp. 1585–1594, 1986.
- [35] S. Chew, J. R. Griffiths, Z. H. Starchurski, "The crystallization kinetics of polyethylene under isothermal and non-isothermal conditions," *Polymer (Guildf)*., vol. 30, no. 5, pp. 874–881, 1989.
- [36] J. Zhang, S. Chen, J. Su, X. Shi, J. Jin, X. Wang, Z. Xu, "Non-isothermal crystallization kinetics and melting behavior of EAA with different acrylic acid content," *J. Therm. Anal. Calorim.*, vol. 97, no. 3, pp. 959–967, 2009.
- [37] T. F. L. McKenna, "Condensed Mode Cooling of Ethylene Polymerization in Fluidized Bed Reactors," *Macromol. React. Eng.*, vol. 1800026, 2018.
- [38] Z. Zhang, F. Yu, H. Zhang, "Isothermal and non-isothermal crystallization studies of long chain branched polypropylene containing poly(ethylene-co-octene) under quiescent and shear conditions," *Polymers (Basel)*., vol. 9, no. 6, 2017.
- [39] H. Marand, J. Xu, S. Srinivas, "Determination of the equilibrium melting temperature of polymer crystals: Linear and nonlinear Hoffman-Weeks extrapolations," *Macromolecules*, vol. 31, no. 23, pp. 8219–8229, 1998.
- [40] J. D. Hoffman, J. J. Weeks, "Melting process and the equilibrium melting temperature of polychlorotrifluoroethylene," *J. Res. Natl. Bur. Stand. Sect. A Phys. Chem.*, vol. 66A, no. 1, pp. 13–28, 1962.
- [41] E. Koscher, R. Fulchiron, "Influence of shear on polypropylene crystallization: morphology development and kinetics," *Polymer (Guildf)*., vol. 43, no. 25, pp. 6931–6942, Jan. 2002.
- [42] E. Benham and M. McDaniel, "Polyethylene, high density," 2004.
- [43] "Anesthetic Structure Database | Ethene (Ethylene)." [Online]. Available: http://asd.molfield.org/php/view_details.php?id=45&java=false. [Accessed: 23-Nov-2018].
- [45] A. Alizadeh, T. F. L. Mckenna, "Condensed Mode Cooling for Ethylene Polymerization: The Influence of the Heat of Sorption," *Macromol. React. Eng.*, vol. 8, no. 5, pp. 419–433, 2014.

Chapter 6

Conclusion & Perspectives

1. CONCLUSION & PERSPECTIVES

1.1. Conclusion

An experimental study of the gas phase ethylene polymerization process using a supported catalyst was developed in this thesis. The focus was placed on the analysis of the impact of adding induced condensing agents (ICA) on the polymerization rates and final properties of the polymers. In particular, the presence of ICA impacts the process when: we change the temperature of the reactor; we have different concentrations of hydrogen; we have different concentrations of comonomer in copolymerizations; and finally, an experimental investigation of the impact of ICA on the crystallization rate in the formation of polyethylene, presented in Chapter 5, suggests that ICA can significantly slow down the crystallization process.

The behavior of the catalytic activity of the homopolymerization of ethylene in the presence of ICA at different temperatures was evaluated at 70 °C, 80 °C and 90 °C. The results obtained show that the evolution of the reaction rate as a function of temperature is not what one might expect in the presence of ICAs, with the rate decreasing as the temperature increases when either hexane or pentane is present in the gas phase. This observation is attributed to tradeoffs between the competing effects caused by increasing the reaction temperature. While increasing temperature increases the value of the propagation rate constant, it also decreases the solubility of the gas phase species in the amorphous phase of the reaction. When this occurs in the presence of an ICA, the ICA concentration is lower, and therefore the cosolubility effect has a much lower impact on the overall rate. In addition, the presence of ICA in the gas phase also increases the heat capacity. This can lead to a lower particle temperature, which, in certain circumstances, can also slow down the polymerization.

Experimental design and statistical analysis techniques were used to evaluate the effects and interactions of hydrogen and *n*-pentane concentrations, on ethylene polymerizations, as well as on copolymerization of ethylene with 1-butene in the presence of *n*-pentane. The behavior of copolymer formation in the presence of lighter ICA with heavier copolymer was also evaluated.

Homopolymerization rate of ethylene decreases as the hydrogen concentration increases (as expected). The experiments revealed that high concentrations of ICA cause high activity at the beginning of the reaction and that for an ICA/C₂ ratio much larger than the H₂/C₂ ratio, the effect of ICA may counteract the hydrogen effect on the ethylene polymerizations.

Results of the copolymerizations showed that the comonomer effect is more intense in the presence of ICA. It is observed that the comonomer / ICA combination is more important in the initial stages, quite a possibly due to the fact that the comonomer is consumed during the reaction. Different systems were analyzed by varying the concentration of light ICA combined with the heavier comonomer. There it is observed that a light ICA causes influence even when combined with a higher comonomer in the copolymerization rates that presented higher productivities in the presence of propane and pentane.

The presence of ICA increases the ethylene concentration in the amorphous polymer over the active sites. Consequently, there is an increase in molecular weight for homopolymerization. However, when we evaluated different combinations between ICA and hydrogen, the molecular weight is affected only by hydrogen. However, a trend is identified, it showed that only the minimum region of hydrogen observed the effect of any ICA concentration on the increase of Mw. A statistical study on copolymerization identified that for molecular weight, there is an increase of Mn in the presence of ICA independent of the amount of comonomer. Differently, the increase of Mw is observed when there is a minimum of comonomer. In addition, by evaluating the relationship between the light ICA and the heavier comonomer, ICA impacted the increase of Mw.

The results obtained for the impact on the incorporation of the comonomer, represented by CH₃/1000C, show that high concentrations of ICA lead to decreasing the number of methyls. Propane and *n*-pentane decreases CH₃/1000C for poly (ethylene-co-1-butene), in contrast *n*-pentane increased slightly CH₃/1000C for poly (ethylene-co-1-hexene). Again, we can

hypothesize that this is due to different (co)solubility effects, but a lack of experimental (and thus modeling) information in this area makes it difficult to formalize this explanation.

The crystalline content of the final polymers was also evaluated. In the homopolymerizations, it observed that, when annealing the polymer made without hydrogen for a sufficiently long time, the ICA did not influence the final degree of crystallinity. This was attributed to the long relaxation times of high MW PE. When H₂ was present, the chains were shorter, and again, no impact of ICA on total crystallinity was evident, regardless of the annealing times chosen. However, at first, glance, increasing the quantity of ICA appears to increase the crystallinity of the copolymers. However, care must be taken in interpreting these results, and we believe that this increase in crystallinity can be attributed to a cosolubility effect. When the concentration of ICA increase, it is likely that the concentration of ethylene rises faster in the amorphous phase than does that of the comonomer. This means that the C₂/C₄ ratio at the active sites increases, so we have fewer CH₃ per 1000 C, and the density of the final product increases.

It was postulated that since the ratio of ICA to polymer is very high at the beginning of the polymerizations carried out in our semi-batch reactor, we might see a greater than expected chain mobility and a slower rate of crystallization during the nascent phase of the reaction. Given that this might have a significant impact on the laboratory scale kinetic studies presented here (and elsewhere for that matter), a study on the kinetics of crystallization under isothermal conditions was carried out by differential scanning calorimetry. Blends of n-hexane and HDPE were studied in dynamic and isothermal experiments, and it was demonstrated that for certain combinations of ICA and HDPE, the crystallization time is significantly higher for the blends compared to the pure polymer.

The presence of ICA appears to have its highest impact on the rate of polymerization during the initial moments of the reaction, and clearly, the enhancement in the rate cannot be explained by the cosolubility effect alone. We postulate that the ICA can promote greater mobility of the polymer chains, thus slowing down the crystallization process, and increasing both the solubility of monomer(s) and the diffusion process for small molecules. This behavior is important for a better understanding of the physical phenomena since the size and spatial arrangement of the crystals influence the mechanical and thermal regions of the polymer until they reach equilibrium.

1.2. Perspectives

The current thesis covered a wide range of industrially pertinent topics, and this clearly leads to a certain number of open questions. Here below there are some suggestions for follow up of the studies to this work:

1) *Further of new experimental evaluation of polymerization kinetics.*

While it is unlikely that *ethylene + ethane systems* will show any significant co-solubility effects because of their similar physical make-up, ethane's higher heat capacity might translate into cooler particles that lead to different rates and molecular weight distributions through a thermal effect and might help us to better separate co-solubility effects and thermal effects in homopolymerizations carried out in the presence of butane or propane.

Additionally, it would be interesting to see if the thermal effect in the presence of *n*-pentane and *n*-hexane (decreasing rate with increasing temperature) would be the same with lighter ICA.

In addition, we should evaluate the behavior of the productivity and properties of the polymers formed with more complex mixtures of ICA, in order to better understand and to predict more realistic conditions in the reactor in the gas phase.

In the copolymerization experiments carried out here, the reaction time is important to interpret the effect of ICA on the properties of the copolymer (it is possible that we undergo non-negligible composition drift). A re-evaluation of the experimental copolymerization protocol is necessary. In other words, one needs to evaluate the best way of injecting the comonomer into the reactor: a continuous or semi-continuous feed of the comonomer together with ethylene; this trade-off will play a role on the reaction time. Perhaps for longer times, continuous feeding of the comonomer is necessary, so it is possible to better evaluate the effect of ICA on the incorporation of the comonomer. If it is not possible to retrofit the lab reactors for this purpose, shorter experimental times and continuous evaluation of the headspace composition would be useful.

Once the experimental ethylene copolymerization process has been defined, it is suggested evaluating reactions containing mixtures of alkanes and alkenes with greater differences in carbon numbers than was carried out here (e.g. *propane* and *1-hexene* rather than *pentane* and *1-hexene*, and vice versa *hexane* and *propylene*).

2) *Realization of new experimental measurements of gas-polymer equilibrium for multicomponent systems.*

One of the main observed difficulties is the lack of experimental data available in the literature for the systems of interest, which greatly limits the possibility of validating cases for study. In addition, the existence of available reliable experimental data is essential for any modeling study of real systems with EoS. In this way, the realization of new experimental measurements with new systems is presently identified as being a higher priority task. Solubility data for at least ternary systems need to be carried out; ideally involving the measurement of hydrogen solubility even though that might be difficult because of the low solubility of this compound). A quick look at the patent literature tells us that mixtures of C2 through C6 alkanes and alkenes is badly needed. It goes without saying that if these studies could be extended to multicomponent systems, this would be ideal.

3) *Realization of new experimental measurements of crystallization rate.*

Since ICA promotes higher chain mobility due to the low rate of crystallization, we suggest that this study could be better explored by other components, especially lighter penetrants. For this, the optimization of the analysis process is interesting, since with a very rapid cooling rate the polymer may not crystallize, leading to a completely amorphous polymer, so the process, in this case, is kinetically controlled. Analysis with higher cooling rates can be evaluated for new ICA:PE systems, in particular, LLDPE systems. It is desirable a better understanding about the connection between free volume and glass transition temperature: this understanding may contribute to a better comprehension of the relationship between the crystallization process and the involved transport and equilibrium phenomena.

4) *Slurry polymerization.*

The gas phase polymerization process in a laboratory scale has technical limitations for operation in condensed mode or supercondensed mode, restricting it only to super dry mode. It is therefore convenient to evaluate the solubility effects on slurry process polymerization with solvent mixtures which act as antisolvent.

5) *Modeling.*

Clearly, we wish to develop working models of fluidized bed reactors in the presence of vaporized alkanes. The results of this study point to the need for more detailed thermodynamic studies that allow us to develop models of solubility in multicomponent systems over a range of temperatures and pressures.

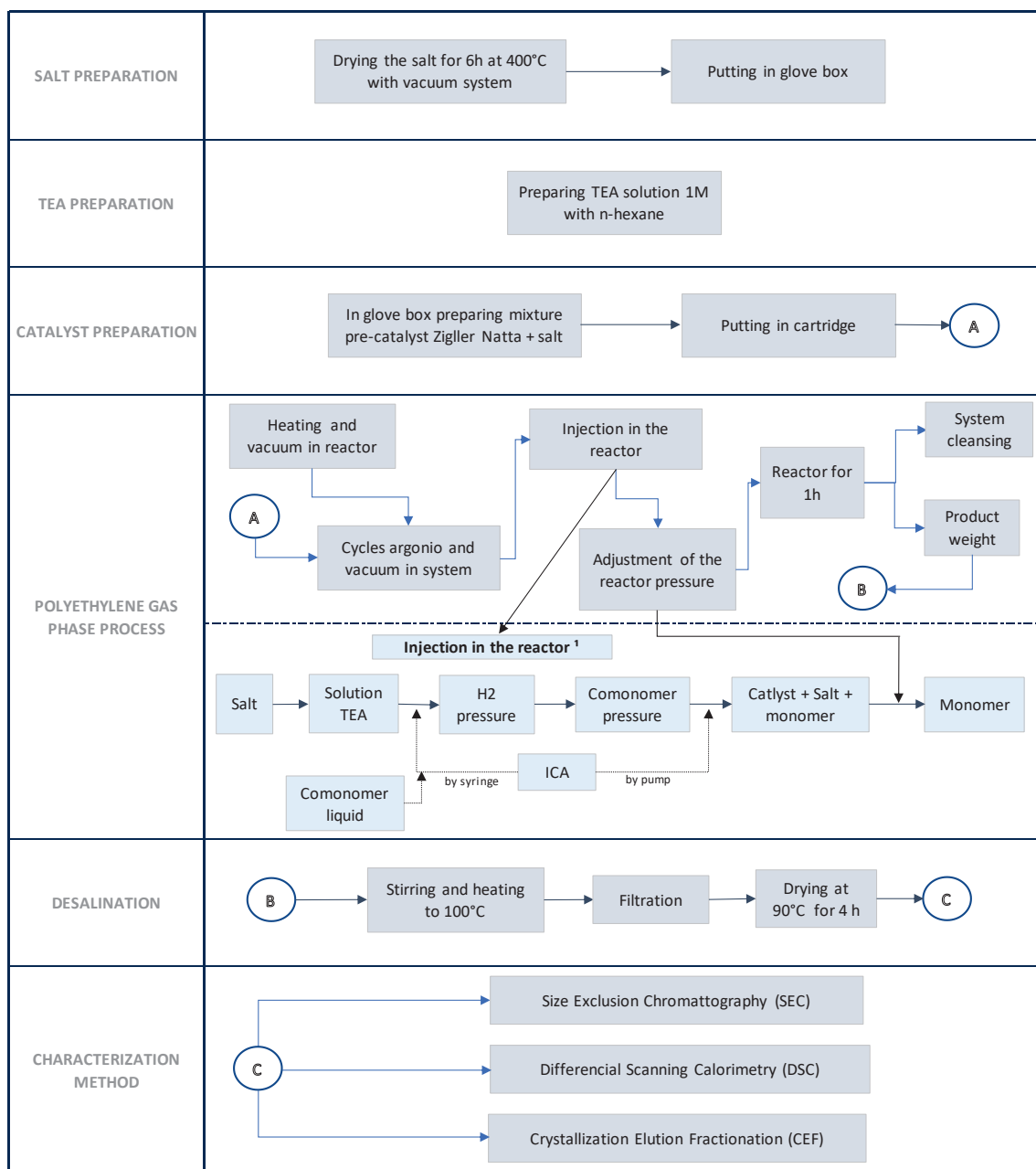
With respect to the physical phenomena aspects, a precise description of the solubility and diffusivity of the compounds present in the polymer is necessary. For complex systems, in order to identify the issue of selectivity among species in the polymer matrix, future researches may contribute to a better understanding and good estimation of the effects on the chemical phenomena.

Thinking on a model including the effect of crystallinity, because the crystallinity is not constant along the time. The adsorption of impurities (inerts) on the faces of polymer crystals appears to be specific and particularly determinant for particle growth. During the crystallization, stresses occur and, consequently, mechanical and thermal phenomena arise, among which the kinetic growth of the crystals, ignored by the model.

Appendix I

Reaction protocol and analyses

Appendix I contains the gas phase polyethylene reaction protocol and characterization analyzes of the studies described in Chapters 2, 3 and 4. The working method is summarized according to the diagram in Figure I.1.



1. The steps of the injection process depends on each procedural condition

Figure I.1: Reaction Protocol Diagram

1. POLYETHYLENE GAS PHASE PROCESS IN THE LABORATORY

The gas phase polymerization experiments are performed in the spherical stirred-bed semi-batch reactor shown in the diagram in Figure I.2. Gas-phase polymerization process of ethylene was developed using a stirred bed reactor (Figure I.3), operating below 25 bar and temperatures from 70 to 90 °C, and using a helical stirrer to maintain uniform the reacting conditions. Heating of the reactor uses water jackets connected to the heat exchanger and when cooled the connection with water is changed at room temperature. Unlike the FBR reactor, where there is a constant supply of catalyst, make-up and recycle, ie continuous phase, the stirred-bed reactor operates in semi-batch mode. In this system, all components involved in the formation of the polymer are added to the reactor and only the ethylene reactant is added continuously until the desired reaction time is reached. The control system in the pilot plant is monitored by a computer where it reads the total pressure of the reactor and the pressure in the ballast acting on the consumed flow of ethylene during the reaction. Temperature control can also be monitored by controlling the thermal bath.

This system is composed of equipment and instruments:

Equipment:

B-1: ethylene cylinder
 C-1, 2 and 3: purification columns
 B-2: ethylene cylinder pure
 B-3: 1-butene cylinder
 B-4: Propane cylinder (with cylinder sleeve)
 VE-1: vacuum equipment
 P-1: injection pump
 M: electric motor
 R-1: reactor - spherical stirred-bed

AG-1: agitation controller
 E-1: exchanger water (heating)
 E-2: exchanger oil (cooling)
 Ct-1: cartridge

Instrument:

PT: pressure transmitter
 PI: pressure indicator
 TIT: temperature transmitter and indicator
 TI: temperature indicator

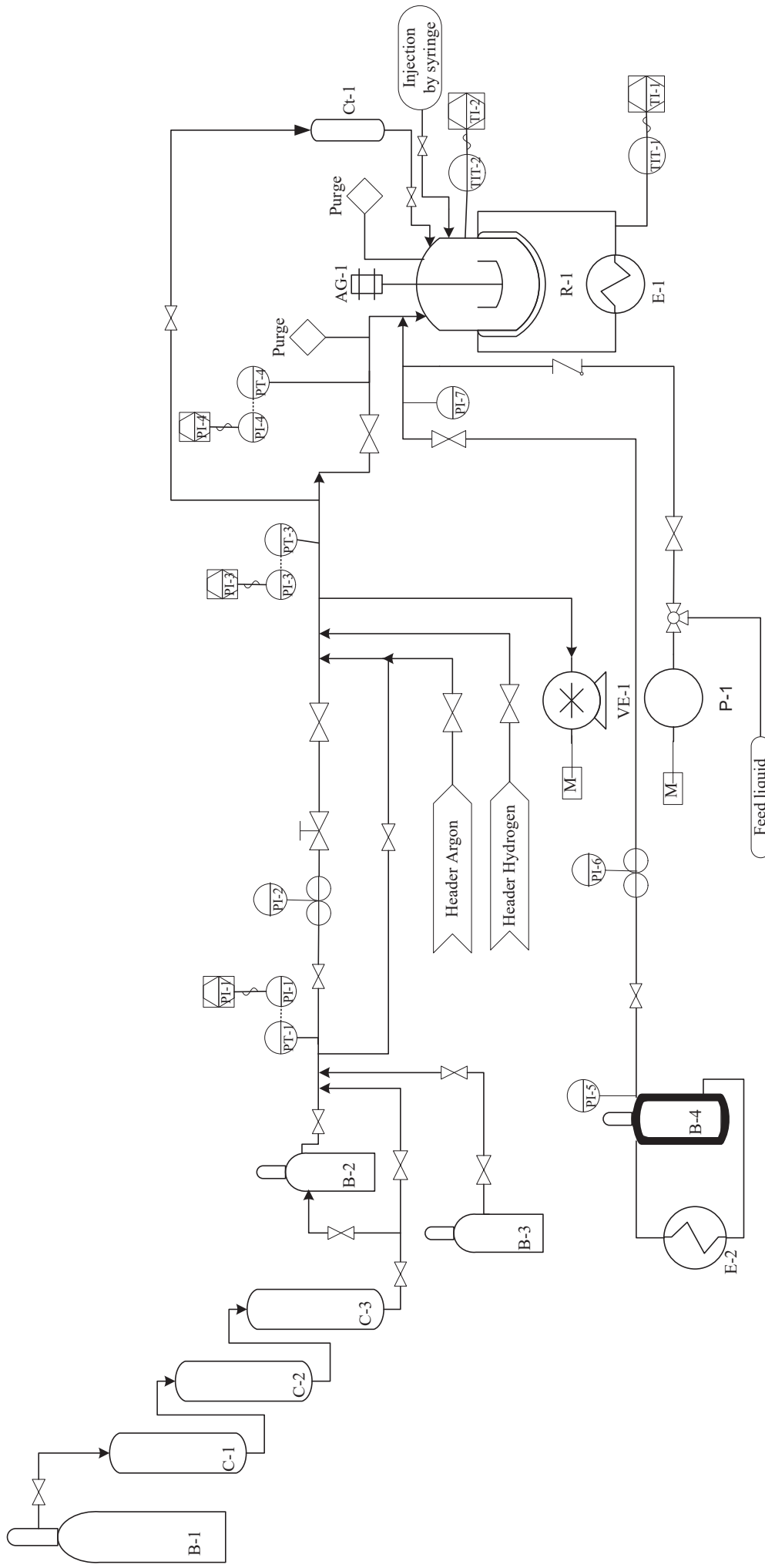


Figure I.2: PFDE polyethylene gas phase process in the laboratory C2P2.



Figure I.3: Stirred bed reactor of the laboratory C2P2

The system is still composed of a supply of hydrogen and argon and a three-column ethylene purification system supplied from ballast B-1, being stored in ballast B-2, which will be used in the reactions. The manual procedure performed in this study to make polyethylene in the C2P2 laboratory plant is described in the following steps:

- a) Heat (with equipment E-1) the reactor R-1 at the desired temperature for half an hour.
- b) Turn on the vacuum pump (VE-1) and let the reactor R-1 conditioned under vacuum and heated for one hour.
- c) This time is used to prepare the pre-catalyst mixture in the glove box. This process varies for each chapter, that is, process condition.

Before entering the glove box compartment, collect the materials and follow the glovebox operating procedures.

Chapter 2: prepare a mixture with pre-catalyst mass (10 wt%) and salt in the glove box which is stored in Schlenk flasks for later injection into the reactor. Mass of catalyst is $12 \pm 0,5$ mg.

Chapter 3 and 4: prepare a mixture with pre-catalyst mass (10 wt%) and salt which is stored in the cartridge for connecting in the reactor. The mass of the catalyst is 10 ± 5

mg, depending on the condition to obtain more or less product. Preparer in a Schlenk flask additional 40 g of salt. The total salt mass is 50 g in the reactor. When leaving the glove box, immediately connect the cartridge to the reactor and vacuum the connections with the line and reactor.

- d) The reactor is purged with cycles argon/vacuum five times to eliminate any trace of oxygen in the system.
- e) The process of injection of catalyst and gases in the R-1 reactor. This process varies for each chapter, that is, process condition.

Chapter 2: 50% total volume of a solution of TEA in n-hexane was introduced into the reactor for five minutes and after put the rest of the solution volume. It remained inside the reactor at a stirring speed of 300 rpm. In the experiments using ICA, the desired volume of liquid is injected into the reactor at this point at room temperature by syringe at argon atmospheric. The amount of alkane used in each experiment was limited by the temperature of the reactor to be sure that the entire volume was completely vaporized. The mixture of catalyst and salt was then injected into the reactor under argon atmosphere. The catalyst was left to contact the TEA in the reactor for two minutes. The reaction then began upon injection of ethylene at a constant pressure.

Chapter 3: Cool the reactor to 30 °C. Under argon connect the Schlenk flask with salt the cap with a hose connection to the reactor. Turn on the reactor agitation at 200 rpm. Feed the reactor with argon and wait to stabilize the pressure. Open the valve and inject the salt into the Schlenk flasks an argon atmosphere. Add the whole volume of the TEA solution to the n-hexane. This volume varies between 0.3 - 0.8 mL, which is a function of the measured pre-catalyst mass. In the reactions in the presence of ICA, we inject the volume corresponding to the desired ICA pressure (at the reactor operating temperature). Using a syringe, the ICA is collected from the Schlenk flasks and injected into the reactor in an argon atmosphere. This procedure must be done prior to the injection of gases into the reactor and the agitation off to minimize the loss of TEA in the reactor. The reactor is again heated to the desired reaction temperature. When the temperature is stable we inject the desired pressure of hydrogen. At this point the reactor is ready for injection of the pre-catalyst with high ethylene pressure, using the line for Ct-1 cartridge. When closing the valves after feeding the pre-catalyst. Open the pure

ethylene feed valve (line connected to B-2) to the reactor and adjust the total reactor pressure by starting the reaction.

Chapter 4: Under argon connect the Schlenk flask contained salt the cap with a hose connection to the reactor. Turn on the reactor agitation at 200 rpm. Feed the reactor with argon and wait to stabilize the pressure. Open the valve and inject the salt into the schlenk flasks under an argon atmosphere at the reaction temperature. Add the volume of the TEA solution to the n-hexane. This volume varies between 0.3 - 0.8 mL, which is as a function of the mass of pre-catalyst measured. Inject the desired pressure of comonomer¹. Inject one bar of hydrogen. In the reactions in the presence of ICA, we inject the volume corresponding to the desired ICA pressure (at the reactor operating temperature) through the injection pump P-1 if n-pentane and to injection propane through ballast B4, controlled by pressure regulator PI-7. At this point, the reactor is ready for injection of the pre-catalyst with high ethylene pressure using the Ct-1 cartridge. When closing the valves after feeding the pre-catalyst. Open the pure ethylene feed valve (line connected to B-2) to the reactor and adjust the total reactor pressure by starting the reaction.

- f) A pressure gauge records the rate of consumption of ethylene ballast. The reaction lasts one hour, the ethylene consumption time and pressure data on the B-2 ballast are collected through the PI-1 pressure gauge. The temperature of the reactor (TI-2) and the stability of the reactor pressure (PI-4) are monitored. The control system maintained the pressure and the polymerization temperature within ± 0.1 bar and ± 0.5 °C of the reference value.
- g) At the end of the polymerization the reactor was cooled and depressurized, then filled with argon and opened at room temperature.
- h) The polymer was weighed, the salt was then removed.
- i) The salt removal process consisted of the immersion of the polymer in water at 100 °C in a beaker with a magnetic stirrer turning at 800 rpm for 4 hours.
- j) Then the polymer was filtered and finally dried at 90 °C using a cooling trap for 3 hours.
- k) Treatment of the collected data: consists in the calculation of a profile of polymerization activity, that is, the amount of mass of polymer formed by the mass of pre-catalyst used

¹ If 1-butene uses the line connected to B-3. In the case of 1-hexene the injection is given via the syringe under argon. Procedure identical to ICA injection in Chapter 2.

by the time. For this, the pressure drop profile in the ethylene reservoir (B-2) is used in the Soave-Redlich-Kwong cubic equation (SRK) to translate into a mass flow rate. The catalytic activity of the present study is the result of the arithmetic mean of three experiments for chapter 2 and of chapters 4 and 5 we used the experimental planning matrix.

2. SIZE EXCLUSION CHROMATOGRAPHY (SEC)

SEC analysis based on size exclusion high-temperature chromatography was performed by a triple detection set in Viscotek 350A HT-GPC - Malvern Instrument. The system is equipped with a refractometric detector, static light scattering RALS (90°) and LALS (7°) and a viscometer detector. The set is thermostat at 150 °C. The set of columns used comprises a pre-column, followed by three high-temperature columns in series (Waters Styragel HT6E) having a mass range of 500 – 4,200,000 g/g mol (equivalent to Polystyrene - PDI = 1.01). The mobile phase is trichlorobenzene (TCB) at 150 °C with a flow rate of 0.6 ml.min⁻¹. The solvent is stabilized by Butylhydroxytoluol at 0.2 g.L⁻¹. Samples are injected through a 200 µL loop and filtered in-line prior to separation in the columns. The samples are approximately 30 mg and diluted in TCB as a solvent. For samples without hydrogen, the dilution was done by heating (at 150 °C) and cooling (at room temperature) the sample every 30 minutes for seven hours. A triple detection calibration curve was used for better curve fitting using Malvern Instruments "OmniSEC" version 5.2 software. The main parameters determined were: Mw - molar mass weight average; Mn - number average molecular weight and Mw/Mn - molar mass distribution or polydispersity (PDI). A data that allows us to obtain is the amount of insoluble, which is the ratio between the concentration calculated by equipment and the input concentration of the experiment (measured mass / volume of solvent added).

3. DIFFERENTIAL SCANNING CALORIMETRY (DSC)

DSC analysis was performed using Mettler Toledo DSC 3+ model. To measure and plot the heat supplied from the samples, as a function of temperature. They called thermograms, show the peaks associated the latent heat (of fusion or solidification) at the temperature (melt point

or crystallization temperature). The most common method is used for the analysis of semi-crystalline polymers. 5-10 mg polyethylene was weighed from each sample and placed in an aluminum capsule 40 μ L. The sample was first cooled to $-20\text{ }^{\circ}\text{C}$, giving start the analysis being heated to $180\text{ }^{\circ}\text{C}$ at a rate of $10\text{ }^{\circ}\text{C}/\text{min}$, kept for 10 min and then cooled up $-20\text{ }^{\circ}\text{C}$ at a rate of $10\text{ }^{\circ}\text{C}/\text{min}$. This temperature was maintained for 10 minutes, and the sample was reheated to $10\text{ }^{\circ}\text{C}/\text{min}$ to $180\text{ }^{\circ}\text{C}$.

The melting behavior of the samples was studied in the second heating run from room temperature up to $180\text{ }^{\circ}\text{C}$ at the same rate of cooling to detect the melting point (T_m) and the determination of the melting enthalpy (ΔH_f) of the samples. The degree of crystallinity (χ_c) of the samples was calculated by considering the percentage by weight of the crystalline phase obtained from the polyethylene fraction and the heat of melting from $293\text{ J}\cdot\text{g}^{-1}$ to 100% crystalline polyethylene. The crystallization temperature (T_c) is obtained in the cooling run.

4. CRYSTALLIZATION ELUTION FRACTIONATION (CEF)

CEF analysis was performed using Agilent Technologies 7890B Gas Chromatograph. During the sample preparation stage, a sample of 4 mg of polymer is dissolved in 8 mL of 1,2,4-trichlorobenzene (TCB) in a vial at $160\text{ }^{\circ}\text{C}$ in the automatic sampler. Dilution proceeds for 60 min. The polymer solution is stabilized at $95\text{ }^{\circ}\text{C}$ before being injected into the CEF column. The dynamic crystallization step starts by lowering the column temperature from 95 to $35\text{ }^{\circ}\text{C}$ under a cooling rate of $2\text{ }^{\circ}\text{C}\cdot\text{min}^{-1}$ and a solvent flow of $0.065\text{ mL}\cdot\text{min}^{-1}$. This flow allows the polymer to not crystallize early, as it has a thin column. The polymer chains are crystallized and fractionated along the CEF column in this step. After the crystallization cycle is complete, the column temperature is maintained at $35\text{ }^{\circ}\text{C}$ for a few minutes under fresh solvent flow at a constant elution flow rate of $1\text{ mL}\cdot\text{min}^{-1}$. The dynamic elution step begins when the temperature begins to increase at a constant heating rate of $4\text{ }^{\circ}\text{C}\cdot\text{min}^{-1}$, from 35 to $130\text{ }^{\circ}\text{C}$. The concentration of the polymer fractions in the eluent is monitored by an infrared detector placed at the outlet of the CEF column.

The behavior of dynamic crystallization allows the evaluation of the peak temperature and the dynamic elution of the amount of methyl (-CH₃) per thousand carbon atoms, which is considered the comonomer content of the analyzed polymer.

Appendix II

Sanchez Lacombe model

Appendix II has the objective to deal with the theory involved in the thermodynamic model adopted, as well as to explain the calculation procedure developed by Arash Alizadeh and Rita Alves, who also executed the program in MatLab.

1. INTRODUCTION

The lattice fluid theory for liquid and gaseous mixtures developed by Sanchez and Lacombe, empty cells are introduced into the structure to describe the extra change in entropy of the system as a function of volume and temperature. Explain variations in compressibility and density, i.e., the density of the blend may vary by increasing the fraction of holes in the framework. The size of the structure is fixed so that the volume variations can only occur by the appearance of new voids on the structure [1], [2]. As in the cell models, the Sanchez-Lacombe equation (EOS-SL) the lattice is occupied by mere and empty cell sites (Figure II.1), where hexamers are distributed along the lattice but do not have all the sites occupied.

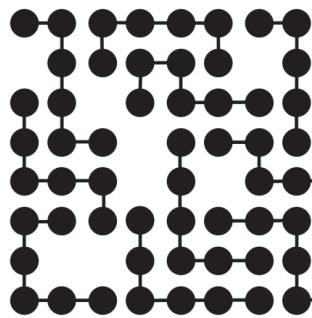


Figure II.1 A two-dimensional example of a pure fluid based on the network model. The fraction of occupied sites is denoted by $\tilde{\rho}$.

The energy of the structure depends only on the interactions of the nearest neighbors. For a pure component, the only non-zero interaction energy is the mer-mer interaction energy (ϵ). The empty-mer and empty-empty interaction energy is zero. The lattice model assumes random blending of voids and mers. Random mixing means that the composition everywhere in the

solution is equal to the total composition, ie there are no composition effects. In this way, EOS-SL is represented by:

$$\bar{\rho}^2 + \bar{P} + \bar{T} \left[\ln(1 - \bar{\rho}) + \left(1 - \frac{1}{r}\right) \bar{\rho} \right] = 0 \quad (1)$$

Where,

$$\bar{T} = \frac{T}{T^*} \quad \bar{P} = \frac{P}{P^*} \quad \bar{\rho} = \frac{\rho}{\rho^*} = \frac{1}{\bar{V}} = \frac{V^*}{V} \quad (2)$$

$$T^* = \frac{\varepsilon^*}{R} \quad P^* = \frac{\varepsilon^*}{v^*} \quad \rho^* = \frac{MW}{rv^*} \quad V^* = Nr v^* \quad (3)$$

$\bar{T}, \bar{P}, \bar{V}$ and $\bar{\rho}$ are the reduced temperature, pressure, volume and density respectively. T is the absolute temperature, P is the pressure, ρ is the density, MW is the molecular weight, R is the ideal gas constant. T^*, P^*, V^* and ρ^* are the characteristic temperature, pressure, volume, and density, respectively. Where r is the number of network sites occupied by mers, ε^* and v^* are characteristics parameters related the mer-mer interaction energy and molar volume.

Conventional mixing rules are employed to determine the parameters for a different pair of segments depending on the composition.

$$v_{mix}^* = \sum_i \sum_j \phi_i \phi_j v_{ij}^* \quad (4)$$

$$\varepsilon_{mix}^* = \frac{1}{v_{mix}^*} \sum_i \sum_j \phi_i \phi_j v_{ij}^* \varepsilon_{ij}^* \quad (5)$$

$$\frac{1}{r_{mix}^*} = \sum_j \frac{\phi_j}{r_j} \quad (6)$$

The volumetric fraction of component i at the zero temperature limit or incompressible state, ϕ_i , is calculated as a function of the weight fraction w_i , given by:

$$\phi_i = \frac{\frac{w_i}{\rho_i^* v_i^*}}{\sum_j \frac{w_j}{\rho_j^* v_j^*}} \quad (6)$$

The cross parameters are:

$$v_{ij}^* = \frac{v_{ii}^* v_{jj}^*}{2} (1 - l_{ij}) \quad (7)$$

$$\varepsilon_{ij}^* = (\varepsilon_{ii}^* \varepsilon_{jj}^*)^{0.5} (1 - k_{ij}) \quad (8)$$

Where, l_{ij} corrects the deviation from the arithmetic mean and subscripts i and j are the components in the solution. k_{ij} is a mixture parameter that accounts for specific interactions between components i and j . Assumptions of these parameters for all calculations is that $l_{ij} = 0$, while k_{ij} will be adjusted with data obtained in the literature.

The sorption equilibrium for the polymer-solvent system is defined when the chemical potential for a μ_i component indicates that only the quantity n_i of the i^{th} component changes, and the quantities of all other components $n_j, j \neq i$ remain constant as well as pressure and temperature. The chemical potential can be written generically by the following expression:

$$\mu_i = R_g T \left[\ln \phi_i + \left(1 - \frac{r_i}{r} \right) \right] + r_i \left\{ -\bar{\rho} \left[\frac{2}{v^*} (\sum_j \phi_j v_{ij}^* \varepsilon_{ij}^* - \varepsilon^* \sum_j \phi_j v_{ij}^*) + \varepsilon^* \right] + \frac{R_g T}{\bar{\rho}} \left[(1 - \bar{\rho}) \ln(1 - \bar{\rho}) + \frac{\bar{\rho}}{r_i} \ln \bar{\rho} \right] + \frac{P}{\bar{\rho}} (2 \sum_j \phi_j v_{ij}^* - v^*) \right\} \quad (9)$$

Where ϕ_i is closed packed volume fraction of components defined for each desired phase.

2. MODELING POLYMERIC SYSTEMS

The modeling of polymer systems involved in the study can be binary (polymer – solvent) or ternary (polymer - solvent 1 - solvent 2) system. The calculation procedure will be described through the flowchart of subroutines for the ternary system, the procedure for the reduced binary system only two components [3]. Some concepts and fundamental terms for the application of the procedure are presented:

Component 1: solvent with a lighter molecular weight in the system, which can penetrate the polymer, being in the polymer phase or in the gaseous state.

Component 2: solvent with a heavier molecular weight in the system, which can penetrate the polymer, being in the polymer phase or in the gaseous state.

Component 3: Polyethylene which is the solid phase of the system.

Gas phase: involved components that are in the gaseous state.

Polymer phase: a solvent that is inside the polymer matrix

The calculation aims to define the solubility of component 1 and 2 in the polymer and to determine the interaction constant between the solvents and polymer (k_{13}, k_{23}), from the premise that there is no interaction between the solvents, so $k_{12} = 0$. Sorption of solute species is assumed only in the amorphous phase of the polymer, while the crystalline phase is considered impenetrable for solute species.

Figure II.2 shows the flowchart of subroutines comprising the pre-calculation, calculations in the gas phase and the polymer phase. All equations involved are expressed in Table II.2. The

pre-calculation defines the system input data and characteristic parameters for each component found in the literature. Table II.1 can be found the parameters used in this study. There are also predefined constants that will be used in the gas phase and the polymer. Then the subroutines in the gas phase, where the reduced condition is defined for each component by interactive calculation. Also, in the gas phase the closed packed volume fraction of each component is resolute, thus determining the reduced density of the gas mixture and then the chemical potential in the gas phase is defined for each component. This value will define the equilibrium condition, in which the chemical potential of each component is equal in all phases, therefore, $\mu_1^{gas} = \mu_1^{pol}$ and $\mu_2^{gas} = \mu_2^{pol}$. In the equilibrium condition the reduced density and closed packed volume fraction of each component in the polymer phase is defined by the method of interaction and interdependence (solving equation). Once the closed packed volume fraction of each component in the polymer phase is known, the mass fraction of each component is defined and thus the solubility of the penetrant in the amorphous phase of the polymer is calculated. For all binary systems investigated, the difference in the calculations is that there will be no gas mixing, only being reduced to a calculated component for gas and polymer phase.

The interaction parameter depends on the penetrating molecule as well as the experimental temperature conditions. The adjustment of these parameters between polymers and solvents were adjusted by minimizing the following objective function:

$$FO = \frac{S_{exp} - S_{calc}}{S_{exp}} \quad (10)$$

The calculated theoretical solubility showed excellent agreement with measurements and demonstrated the ability of SL-EOS to predict the solubility of olefins in semicrystalline polyolefins.

Table II.1 Characteristic parameters

Component	T*	P*	ρ^*	Reference
	K	bar	kg.m ⁻³	
ethylene	283	3395	680	[1]
propane	371	3090	690	[1]
1-butene	410	3350	770	[4]
n-pentane	445	3060	755	[1]
n-hexane	476	2979	775	[1]
1-hexene	450	3252	814	[1]
hydrogen	46	1000	152	[5]
LLDPE – 1-hexene	653	4360	903	[4]
HDPE	653	4360	903	[4]

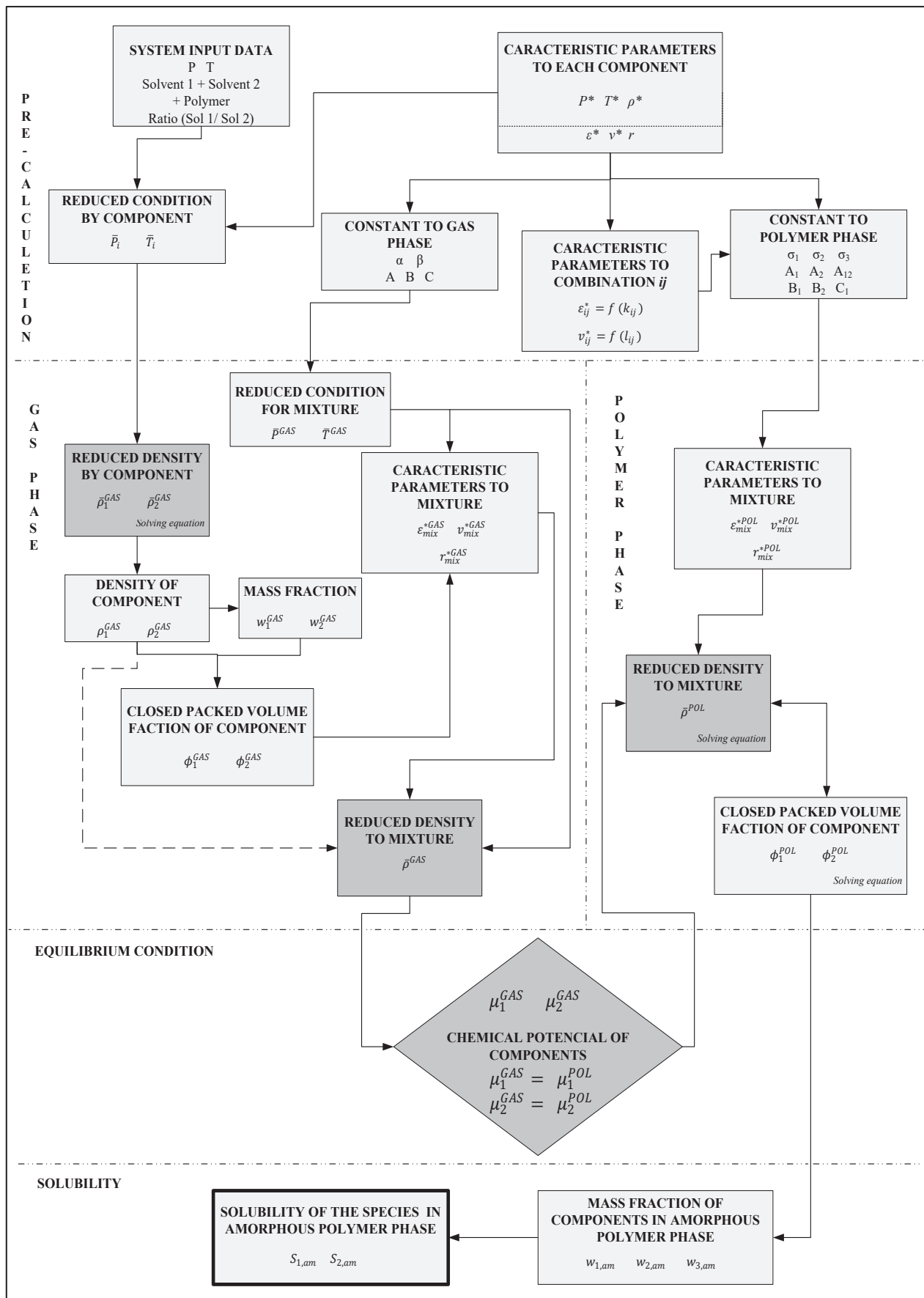


Figure II.2 Flowchart of subroutines for the ternary system

Table II.2 Equations used in subroutines

Sub-routine	Description	Equation
Pré-calculation	Condition reduced for each component i	$\bar{T}_1 = \frac{T}{T^*_{1}} \quad \bar{T}_2 = \frac{T}{T^*_{2}} \quad \bar{T}_3 = \frac{T}{T^*_{3}} \quad (K)$ $\bar{P}_1 = \frac{P}{P^*_{1}} \quad \bar{P}_2 = \frac{P}{P^*_{2}} \quad \bar{P}_3 = \frac{P}{P^*_{3}} \quad (bar)$
	Characteristic parameters for each component i	$\varepsilon^*_i = T^*_i R \quad (m^3 barkmol^{-1}) \text{ and } v_i^* = \frac{\varepsilon_i^*}{P_i^*} \quad (m^3 kmol^{-1})$ $r_i = \frac{MW}{\rho_i^* v_i^*}$
	Pre-defined constants to gas phase	$\alpha = v_1^* - v_2^* \quad \beta = v_2^*$ $A = \varepsilon_1^* v_1^* + \varepsilon_2^* v_2^* - \varepsilon_{12}^* (v_1^* + v_2^*)$ $B = \varepsilon_{12}^* (v_1^* + v_2^*) - 2\varepsilon_2^* v_2^*$ $C = \varepsilon_2^* v_2^*$
	Characteristic parameters for combination $ij = 12, 13$ and 23	$\varepsilon_{ij}^* = (\varepsilon_{ii}^* \varepsilon_{jj}^*)^{0.5} (1 - k_{ij})$ $v_{ij}^* = \frac{v_{ii}^* + v_{jj}^*}{2} (1 - l_{ij})$
	Pre-defined constants to polymeric phase	$\sigma_1 = v_1^* - v_3^* \quad \sigma_2 = v_2^* - v_3^* \quad \sigma_3 = v_3^*$ $A_1 = \varepsilon_1^* v_1^* + \varepsilon_3^* v_3^* - 2\varepsilon_{13}^* v_{13}^*$ $A_2 = \varepsilon_2^* v_2^* + \varepsilon_3^* v_3^* - 2\varepsilon_{23}^* v_{23}^*$ $A_{12} = 2(\varepsilon_{12}^* v_{12}^* - \varepsilon_{13}^* v_{13}^* - \varepsilon_{23}^* v_{23}^* + \varepsilon_3^* v_3^*)$ $B_1 = 2\varepsilon_{13}^* v_{13}^* - 2\varepsilon_3^* v_3^*$ $B_2 = 2\varepsilon_{23}^* v_{23}^* - 2\varepsilon_3^* v_3^*$ $C_1 = \varepsilon_3^* v_3^*$
Gas phase	Reduced density of component 1 and 2 (SL- EOS)	$\bar{\rho}_1^{gas} = 1 - \exp\left(-\frac{(\bar{\rho}_1^{gas})^2}{\bar{T}_1} - \frac{\bar{P}_1}{\bar{T}_1} - \left(1 - \frac{1}{r_1}\right)\bar{\rho}_1^{gas}\right)$ $\bar{\rho}_2^{gas} = 1 - \exp\left(-\frac{(\bar{\rho}_2^{gas})^2}{\bar{T}_2} - \frac{\bar{P}_2}{\bar{T}_2} - \left(1 - \frac{1}{r_2}\right)\bar{\rho}_2^{gas}\right)$ (kgm^{-3})

Density of component 1 and 2	$\rho_1^{gas} = \rho_1^* \bar{\rho}_1^{gas}$ $\rho_2^{gas} = \rho_2^* \bar{\rho}_2^{gas}$ (kgm^{-3})
Mass fraction of component 1 and 2	$\omega_1^{gas} = \frac{\rho_1^{gas}}{\rho_1^{gas} + \rho_2^{gas}}$ $\omega_2^{gas} = \frac{\rho_2^{gas}}{\rho_1^{gas} + \rho_2^{gas}}$
Closed packed volume fraction of component 1 and 2	$\phi_1^{gas} = \frac{\frac{(\rho_1^{gas}/\rho_1^{gas} + \rho_2^{gas})}{\rho_1^* v_1^*}}{\frac{(\rho_1^{gas}/\rho_1^{gas} + \rho_2^{gas})}{\rho_1^* v_1^*} + \frac{(\rho_2^{gas}/\rho_1^{gas} + \rho_2^{gas})}{\rho_2^* v_2^*}}$ <p>Assuming no polymer molecules in the gas phase</p> $\phi_2^{gas} = 1 - \phi_1^{gas}.$
Condition reduced for a mixture	$\bar{T}^{gas} = R_g T \frac{\alpha \phi_1^{gas} + \beta}{A \phi_1^{gas^2} + B \phi_1^{gas} + C}$ $\bar{p}^{gas} = p \frac{(\alpha \phi_1^{gas} + \beta)^2}{A \phi_1^{gas^2} + B \phi_1^{gas} + C}$
Characteristic parameters for a mixture	$\varepsilon^{*gas}_{mix} = \frac{A \phi_1^{gas^2} + B \phi_1^{gas} + C}{\alpha \phi_1^{gas} + \beta}$ $v^{*gas}_{mix} = \alpha \phi_1^{gas} + \beta$ $\frac{1}{r^{gas}_{mix}} = \frac{\phi_1^{gas}}{r_1} + \frac{(1 - \phi_1^{gas})}{r_2}$
Reduced density of the mixture (SL- EOS)	$\bar{\rho}^{gas} = 1 - \exp\left(-\frac{\bar{\rho}^{gas^2}}{\bar{T}^{gas}} - \frac{\bar{p}^{gas}}{\bar{T}^{gas}} - \left(1 - \frac{1}{r^{gas}_{mix}}\right) \bar{\rho}^{gas}\right)$ (kgm^{-3})

	Chemical potential of components 1 and 2	$\mu_1^{gas} = R_g T \left[\ln \phi_1^{gas} + 1 - \frac{r_1}{r^{gas}_{mix}} \right]$ $+ r_1 \left\{ -\bar{\rho}^{gas} \left[\frac{2}{v^{*gas}_{mix}} \left((\phi_1^{gas} v_1^* \varepsilon_1^* + \phi_2^{gas} v_{12}^* \varepsilon_{12}^*) - \varepsilon^{*gas}_{mix} (\phi_1^{gas} v_1^* + \phi_2^{gas} v_{12}^*) \right) + \varepsilon^{*gas}_{mix} \right] \right.$ $+ \frac{R_g T}{\bar{\rho}^{gas}} \left[(1 - \bar{\rho}^{gas}) \ln(1 - \bar{\rho}^{gas}) + \frac{\bar{\rho}^{gas}}{r_1} \ln \bar{\rho}^{gas} \right]$ $\left. + \frac{P}{\bar{\rho}^{gas}} [2(\phi_1^{gas} v_1^* + \phi_2^{gas} v_{12}^*) - v^{*gas}_{mix}] \right\}$ $\mu_2^{gas} = R_g T \left[\ln \phi_2^{gas} + 1 - \frac{r_2}{r^{gas}_{mix}} \right]$ $+ r_2 \left\{ -\bar{\rho}^{gas} \left[\frac{2}{v^{*gas}_{mix}} \left((\phi_1^{gas} v_{12}^* \varepsilon_{12}^* + \phi_2^{gas} v_2^* \varepsilon_2^*) - \varepsilon^{*gas}_{mix} (\phi_1^{gas} v_{12}^* + \phi_2^{gas} v_2^*) \right) + \varepsilon^{*gas}_{mix} \right] \right.$ $+ \frac{R_g T}{\bar{\rho}^{gas}} \left[(1 - \bar{\rho}^{gas}) \ln(1 - \bar{\rho}^{gas}) + \frac{\bar{\rho}^{gas}}{r_2} \ln \bar{\rho}^{gas} \right]$ $\left. + \frac{P}{\bar{\rho}^{gas}} [2(\phi_1^{gas} v_{12}^* + \phi_2^{gas} v_2^*) - v^{*gas}_{mix}] \right\}$ Equilibrium condition: $\mu_1^{gas} = \mu_1^{pol}$ and $\mu_2^{gas} = \mu_2^{pol}$
Polymer phase	Closed-packed molar volume of “mer” of a polymer phase mixture	Condition to characteristic parameters: $\phi_1^{pol} + \phi_2^{pol} + \phi_3^{pol} = 1$

	Characteristic parameters for a mixture	$\varepsilon_{mix}^{* pol} = \frac{A_1 \phi_1^{pol^2} + A_2 \phi_2^{pol^2} + A_{12} \phi_1^{pol} \phi_2^{pol} + B_1 \phi_1^{pol} + B_2 \phi_2^{pol} + C_1}{\sigma_1 \phi_1^{pol} + \sigma_2 \phi_2^{pol} + \sigma_3}$ $v_{mix}^{* pol} = \sigma_1 \phi_1^{pol} + \sigma_2 \phi_2^{pol} + \sigma_3$ $\frac{1}{r_{mix}^{pol}} = \frac{\phi_1^{pol}}{r_1} + \frac{\phi_2^{pol}}{r_2}$
	Reduced density of the mixture (SL- EOS)	$\bar{\rho}^{pol^2} + P \frac{(\sigma_1 \phi_1^{pol} + \sigma_2 \phi_2^{pol} + \sigma_3)^2}{A_1 \phi_1^{pol^2} + A_2 \phi_2^{pol^2} + A_{12} \phi_1^{pol} \phi_2^{pol} + B_1 \phi_1^{pol} + B_2 \phi_2^{pol} + C_1} +$ $R_g T \frac{\sigma_1 \phi_1^{pol} + \sigma_2 \phi_2^{pol} + \sigma_3}{A_1 \phi_1^{pol^2} + A_2 \phi_2^{pol^2} + A_{12} \phi_1^{pol} \phi_2^{pol} + B_1 \phi_1^{pol} + B_2 \phi_2^{pol} + C_1} \left[\ln(1 - \bar{\rho}^{pol}) + \left(1 - \frac{\phi_1^{pol}}{r_1} - \frac{\phi_2^{pol}}{r_2}\right) \bar{\rho}^{pol} \right] = 0 \quad (kgm^{-3})$

Closed packed volume fraction of component 1 and 2		$ \begin{aligned} & R_g T \left[\ln \phi_1^{pol} + 1 - r_1 \left(\frac{\phi_1^{pol}}{r_1} + \frac{\phi_2^{pol}}{r_2} \right) \right] \\ & + r_1 \left\{ -\bar{\rho}^{pol} \left[\frac{2}{\sigma_1 \phi_1^{pol} + \sigma_2 \phi_2^{pol} + \sigma_3} \left((v_1^* \varepsilon_1^* - v_{13}^* \varepsilon_{13}^*) \phi_1^{pol} + (v_{12}^* \varepsilon_{12}^* - v_{13}^* \varepsilon_{13}^*) \phi_2^{pol} + v_{13}^* \varepsilon_{13}^* \right) - \right. \right. \\ & \left. \left(\frac{A_1 \phi_1^{pol^2} + A_2 \phi_2^{pol^2} + A_{12} \phi_1^{pol} \phi_2^{pol} + B_1 \phi_1^{pol} + B_2 \phi_2^{pol} + C_1}{\sigma_1 \phi_1^{pol} + \sigma_2 \phi_2^{pol} + \sigma_3} \right) \left((v_1^* - v_{13}^*) \phi_1^{pol} + (v_{12}^* - v_{13}^*) \phi_2^{pol} + v_{13}^* \right) \right] + \\ & \left. \left(\frac{A_1 \phi_1^{pol^2} + A_2 \phi_2^{pol^2} + A_{12} \phi_1^{pol} \phi_2^{pol} + B_1 \phi_1^{pol} + B_2 \phi_2^{pol} + C_1}{\sigma_1 \phi_1^{pol} + \sigma_2 \phi_2^{pol} + \sigma_3} \right) \right] + \frac{R_g T}{\bar{\rho}^{pol}} \left[(1 - \bar{\rho}^{pol}) \ln(1 - \bar{\rho}^{pol}) + \frac{\bar{\rho}^{pol}}{r_1} \ln \bar{\rho}^{pol} \right] + \frac{P}{\bar{\rho}^{pol}} \left[2 \left((v_1^* - v_{13}^*) \phi_1^{pol} + (v_{12}^* - v_{13}^*) \phi_2^{pol} + v_{13}^* \right) - (\sigma_1 \phi_1^{pol} + \sigma_2 \phi_2^{pol} + \sigma_3) \right] \left. \right\} - \mu_1^{gas} = 0 \\ \\ & R_g T \left[\ln \phi_2^{pol} + 1 - r_2 \left(\frac{\phi_1^{pol}}{r_1} + \frac{\phi_2^{pol}}{r_2} \right) \right] \\ & + r_2 \left\{ -\bar{\rho}^{pol} \left[\frac{2}{\sigma_1 \phi_1^{pol} + \sigma_2 \phi_2^{pol} + \sigma_3} \left((v_{12}^* \varepsilon_{12}^* - v_{23}^* \varepsilon_{23}^*) \phi_1^{pol} + (v_2^* \varepsilon_2^* - v_{23}^* \varepsilon_{23}^*) \phi_2^{pol} + v_{23}^* \varepsilon_{23}^* \right) - \right. \right. \\ & \left. \left(\frac{A_1 \phi_1^{pol^2} + A_2 \phi_2^{pol^2} + A_{12} \phi_1^{pol} \phi_2^{pol} + B_1 \phi_1^{pol} + B_2 \phi_2^{pol} + C_1}{\sigma_1 \phi_1^{pol} + \sigma_2 \phi_2^{pol} + \sigma_3} \right) \left((v_{12}^* - v_{23}^*) \phi_1^{pol} + (v_2^* - v_{23}^*) \phi_2^{pol} + v_{23}^* \right) \right] + \\ & \left. \left(\frac{A_1 \phi_1^{pol^2} + A_2 \phi_2^{pol^2} + A_{12} \phi_1^{pol} \phi_2^{pol} + B_1 \phi_1^{pol} + B_2 \phi_2^{pol} + C_1}{\sigma_1 \phi_1^{pol} + \sigma_2 \phi_2^{pol} + \sigma_3} \right) \right] + \frac{R_g T}{\bar{\rho}^{pol}} \left[(1 - \bar{\rho}^{pol}) \ln(1 - \bar{\rho}^{pol}) + \frac{\bar{\rho}^{pol}}{r_2} \ln \bar{\rho}^{pol} \right] + \frac{P}{\bar{\rho}^{pol}} \left[2 \left((v_{12}^* - v_{23}^*) \phi_1^{pol} + (v_2^* - v_{23}^*) \phi_2^{pol} + v_{23}^* \right) - (\sigma_1 \phi_1^{pol} + \sigma_2 \phi_2^{pol} + \sigma_3) \right] \left. \right\} - \mu_2^{gas} = 0 \end{aligned} $
--	--	---

Solubility	Mass fraction of solute 1 and 2 in the amorphous phase of the polymer	$\omega_{1,am} = \frac{1}{1 + \left(\frac{\rho_2^* v_2^*}{\rho_1^* v_1^*}\right) \left(\frac{\phi_2^{pol}}{\phi_1^{pol}}\right) + \left(\frac{\rho_3^* v_3^*}{\rho_1^* v_1^*}\right) \left(\frac{1 - \phi_1^{pol} - \phi_2^{pol}}{\phi_1^{pol}}\right)} \left(\frac{gr \text{ sol. 1}}{gr \text{ (sol. 1 + sol. 2 + am. pol)}}\right)$ $\omega_{2,am} = \left[\left(\frac{\rho_2^* v_2^*}{\rho_1^* v_1^*}\right) \left(\frac{\phi_2^{pol}}{\phi_1^{pol}}\right)\right] \omega_{1,am} \left(\frac{gr \text{ sol. 2}}{gr \text{ (sol. 1 + sol. 2 + am. pol)}}\right)$ $\omega_{3,am} = 1 - \omega_{1,am} - \omega_{2,am} \left(\frac{gr \text{ am. pol}}{gr \text{ (sol. 1 + sol. 2 + am. pol)}}\right)$
	Solubility of the species	$S_{1,am} = \frac{\omega_{1,am}}{\omega_{3,am}} \left(\frac{gr \text{ sol. 1}}{gr \text{ am. pol}}\right)$ $S_{2,am} = \frac{\omega_{2,am}}{\omega_{3,am}} \left(\frac{gr \text{ sol. 2}}{gr \text{ am. pol}}\right)$ $S_{12,am} = \frac{\omega_{1,am} + \omega_{2,am}}{\omega_{3,am}} \left(\frac{gr \text{ (sol. 1 + sol. 2)}}{gr \text{ am. pol}}\right)$

Reference

- [1] I. C. Sanchez and R. H. Lacombe, "An Elementary Molecular Theory of Classical Fluids. Pure Fluids," J. Phys. Chem., vol. 80, p. 21, 1976.
- [2] I. C. Sanchez and R. H. Lacombe, "Statistical Thermodynamics of Polymer Solutions," Macromolecules, vol. 11, no. 6, pp. 1145–1156, 1978.
- [3] A. Alizadeh, "Study of Sorption, Heat and Mass Transfer During Condensed Mode Operation of Gas Phase Ethylene Polymerization on Supported Catalyst," 2014.
- [4] M. A. Bashir, M. Al-haj Ali, V. Kanellopoulos, and J. Seppälä, "Modelling of multicomponent olefins solubility in polyolefins using Sanchez-Lacombe equation of state," Fluid Phase Equilib., vol. 358, pp. 83–90, 2013.
- [5] Yampolskii Yu., I. (Ingo) Pinnau, and B. D. (Benny D. Freeman), Materials science of membranes for gas and vapor separation. John Wiley & Sons, 2006.

Appendix III

Statistical analysis

Statistical analysis is used to identify the factors that contribute to or influence the occurrence of a phenomenon or to determine through reason the basis of things [1]. Several methods are used as scientific means to validate or reject the hypotheses formulated. The experimental research method consists of "... determining a study object, selecting the variables that would be able to influence it, defining the ways of controlling and observing the effects that the variable produces on the object" (Gil, 2010) [1].

Factorial projects a technique of information collection used with two or more independent variables [2]. In this case, experiments are performed to determine the main effects and possible interactions between variables or control factors, in the natural environment or in the field of experimentation. When evaluating only the effect of a factor on the responses of the product or manufacturing process, it is recommended to use the completely randomized experiment planning technique or the randomized block experimentation technique [3]. On the other hand, when it becomes important to investigate the effect on the responses of the experiments by two or more control factors, and each with two or more levels of regulation, Juran et al [3] recommends the use of classic planning techniques, such as full factorial planning technique, fractional factorial or central point experiments.

Some concepts and fundamental terms for the application of the factorial project are presented:

Response variables: dependent variables that have some effect on the tests, when stimuli are introduced purposively into the factors that regulate or adjust the processes. In the experiments, there may be one or more response variables (y) that are important to evaluate.

Control Factors: these are the factors deliberately altered in the experiment (k). The main objective of introducing stimuli in the control factors is to evaluate the effect produced in the response variables and, with this, to determine the main factors of the process.

Noise factors: are the factors, known or unknown, that influence the response variables of the experiment. Special care should be taken when testing for these factors because it is important to avoid that the effects produced by the control factors are mixed or masked by the effects caused by the noise factors.

Levels of factors: are the operating conditions of the control factors investigated in the experiments. Levels (q) are identified by low level (-1) and high level (+1).

Treatments: it is the combination of levels of control factors, this means that each of the races of the experiment will represent a treatment.

Main effect: is the average difference observed in the response when the level of the control factor investigated changes.

Interaction effect: it is half the difference between the main effects of a factor on the levels of another factor.

Matrix of experiments: it is the formal plan built to conduct the experiments. In this matrix are included control factors, levels, and treatments of the experiment.

Random: it is the process of defining the order of the treatments of the experimental matrix, through sweepstakes or through specific limitations of the tests. Randomization in the experiments is performed to balance the effects produced by the non-controllable factors on the analyzed responses and to meet the requirements of the statistical methods, which require that the components of the experimental error be independent random variables [4].

Repetition: is the process of repeating each of the combinations (lines) of the experimental matrix under the same experimental conditions. This concept allows us to find an estimate of the experimental error, which is used to determine if the observed differences between the data are statistically significant [4].

According to Box and Wilson [5] statistical analysis of an orthogonal factorial design is based on the following sequence:

- i) Statement of the problem with the formulation of hypotheses;
- ii) Choice of factors (independent variables);
- iii) Choice of the experimental setup and analytical techniques to provide information on the response;
- iv) determination of the rules and procedures by which the different treatments (combination of factor levels) are assigned to the experimental procedure;
- v) Statistical analysis of results.

The regression coefficients β_i are estimated according to the least square method, considering the least square function (\mathfrak{S}) to be minimized as expressed by Equation 3.2:

$$\mathfrak{S} = \sum_{i=1}^n \varepsilon^2 = \sum_{i=1}^n \left[Y - \left(\beta_0 + \sum_{i=1}^k \beta_i x_i + \sum_{i=1}^k \sum_{j=1, i \leq j}^k \beta_{ij} x_i x_j \right) \right]^2 \quad (2)$$

For an experimental matrix of 3^2 is given by the following equation:

$$\varphi = \beta_0 + \beta_1 x_1 + \beta_2 x_2 + \beta_{11} x_1^2 + \beta_{22} x_2^2 + \beta_{12} x_1 x_2 + \epsilon \quad (3)$$

where:

		Chapter 3	Chapter 4
β_0	medium of results		
$\beta_1 x_1$	main linear effect of factor A	H2(L)	1-C4(L)
$\beta_2 x_2$	main linear effect of factor B	nC5(L)	nC5(L)
$\beta_{11} x_1^2$	main quadratic effect of factor A	H2(Q)	1-C4(Q)
$\beta_{22} x_2^2$	main quadratic effect of factor B	nC5(Q)	nC5(Q)
$\beta_{12} x_1 x_2$	interaction effect between factors A and B		1Lby2L
ϵ	experimental error		

The main effects corresponding to the change in the average response when the level of a factor is changed, keeping the other factors constant. To determine the interaction effect, the columns of the planning matrix interactions must first be constructed. These columns are formed by multiplying the columns of the main effects. To represent and interpret graphically the main and interaction effects we can observe through the *Pareto diagram*, where parameters with p values less than 0.05 will not have significant statistical value. The Pareto diagram shows the frequency of occurrence of items and the organization from the most frequent to the less frequent. The evaluation of the model can also be done by observing the graph of the *predicted values versus values observed* with a confidence interval of $\pm 95\%$. Where the observed value is the dependent variable and the predicted value given the current regression equation.

Factor	Effect	Std.Err.	t(3)	p	-95,% Cnf.Limt	+95,% Cnf.Limt	Coeff.	Std.Err. Coeff.	-95,% Cnf.Limt	+95,% Cnf.Limt
Mean/Interc.	7575.33	305.5203	24.79486	0.000144	6603.03	8547.635	7575.333	305.5203	6603.03	8547.635
(1)1-C4(L)	7445.33	748.3689	9.94875	0.002161	5063.69	9826.977	3722.667	374.1845	2531.84	4913.489
1-C4(Q)	-1754.00	648.1065	-2.70635	0.073391	-3816.56	308.564	-877.000	324.0533	-1908.28	154.282
(2)nC5 (L)	3415.00	748.3689	4.56326	0.019735	1033.36	5796.644	1707.500	374.1845	516.68	2898.322
nC5 (Q)	69.50	648.1065	0.10724	0.921371	-1993.06	2132.064	34.750	324.0533	-996.53	1066.032
1L by 2L	-1.00	916.5610	-0.00109	0.999198	-2917.91	2915.906	-0.500	458.2805	-1458.95	1457.953

Figure III.2 Example results in effects estimates by *Statistica*.

The authors recommend that it is necessary to apply variance analysis techniques (ANOVA) to conclude about the main and interaction effects of the factors. The analysis of variance is used to accept or reject, statistically, the hypotheses investigated. The objective of this technique is to analyze the mean variation of the test results and to demonstrate which are the factors that actually produce significant effects (main and interaction) on the responses of a system.

Factor	SS	df	MS	F	p
(1)1-C4(L)	83149483	1	83149483	98.97757	0.002161
1-C4(Q)	6153032	1	6153032	7.32430	0.073391
(2)nC5 (L)	17493338	1	17493338	20.82332	0.019735
nC5 (Q)	9660	1	9660	0.01150	0.921371
1L by 2L	1	1	1	0.00000	0.999198
Error	2520252	3	840084		
Total SS	109325766	8			

Figure III.3 Example results in ANOVA by *Statistica*.

Figure III.2 and III.3 show results that represent the effects of estimates and ANOVA analysis of the factorial experiment with two factors, each with three levels. The columns in this table include the sources of variation, the sum of squares ($SS_A, SS_B, \dots, SS_{AB}$), degrees of freedom (df is the property by which any of the observations in one sample completely determine the other observation), the mean squares (MS), or the parameter variance, and the F test statistic. In addition to this advantage, the p value is included. With this statistical parameter it is possible to conclude on the null hypotheses without having to resort to a table of critical values of the distribution F . That is, if the value p is smaller than the level of significance chosen α , the null hypothesis is rejected. The reason for variation explained is represented by R^2 , the coefficient of determination of the variation from 0 to 1. The value of R^2 represents a fraction of the variation that is explained by the regression or by the coefficients of the model.

Response Surface methodology (RSM) is a set of planning and analysis techniques used in the mathematical modeling of responses to determine and simultaneously solve multivariate equations. According to Box & Hunter [5] the main reasons for studying the problems of a system with RSM are interested in:

- i) describe how the variables under test affect the responses;
- ii) identify the relationship that exists between the parameters (which can be represented by quantitative variables);
- iii) describe the combined effects of all test variables on the response.

Algebraic polynomials are widely used to approximate the response region. The authors state that the degree of approximation depends essentially on the degree of the polynomial (defined by the product of k factors) and the range of the considered interval. Generally, the first function that is used to approximate the result set is the first-order polynomials, represented by equation III.1. The most important aspects considered by the models in the optimization procedure are the mean and the variance of the repetitions of each experimental run.

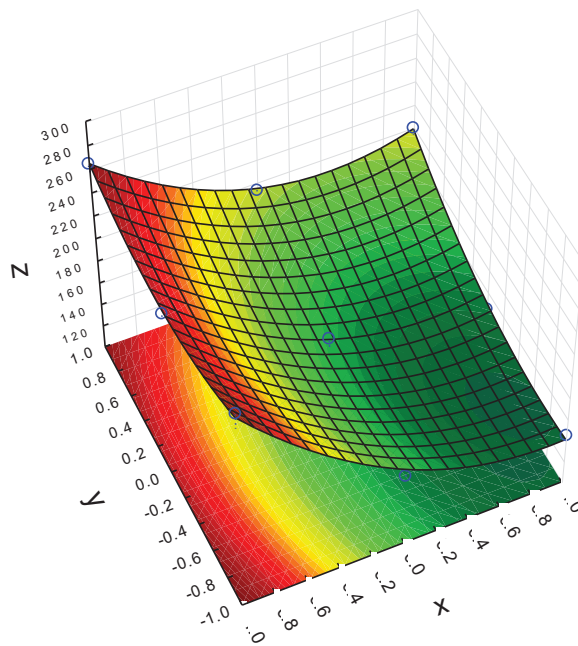


Figure III.2 Example of the response surface.

In a surface chart, the values of the two factors are plotted on the x and y axes, while the response values are plotted on the z axis (Figure III.2). This graphic provides a three-

dimensional view that can display a clearer drawing of the response surface. Where the red region presents a greater statistical significance of the factor, while the green region is less significant. The model applied in this study has polynomials with quadratic terms, applying the Box-Behnken planning, with variables of three levels: minimum cubic, central and maximum cubic. Each experimental point crosses the extreme level of the two or three variables of the project with the average values of the others. In addition, it also includes an intermediate point.

Reference

- [1] A. C. Gil, Como Elaborar Projetos de Pesquisa. Atlas, 1996.
- [2] F. C. Dane, Research methods. Brooks/Cole Pub. Co, 1990.
- [3] J. M. Juran et al., "Juran's Quality Handbook A. Blanton Godfrey Co-Editor-in-Chief," 1999.
- [4] W. Navidi, Statistics for engineers and scientists, vol. 53, no. 9. 2011.
- [5] G. E. P. Box, W. G. Hunter, and J. S. Hunter, Statistics for experimenters : an introduction to design, data analysis, and model building. Wiley, 1978.

